THE UNIVERSITY OF
SYDNEY

Effect of Posttranslational Modification on the Na^+, K^+ ATPase Kinetics

by

Alvaro Garcia

A thesis submitted in fulfilment of the requirements for the degree of Doctor of Philosophy, University of Sydney

April 2015

DECLARATION

This work contained in this thesis is original research by the author, carried out in the North Shore Heart Research Laboratory of the Kolling Institute of Medical Research, University of Sydney, Sydney, Australia.

It has not been submitted to any other institution for a higher degree.

Alvaro Garcia BSc. (Hons)

ABSTRACT

The Na^+, K^+ ATPase is an essential membrane protein in eukaryotic cells, which transports Na^+ out of the cell in exchange for K^+ into the cell. For this transport it hydrolyses one molecule of ATP for each cycle. This 3 Na^+ : 2 K^+ ratio of positive charges creates a net outward current and maintains the electrochemical gradient for these cations across the membrane. This is important for the resting membrane potential of excitable cells and in addition the Na^+ gradient generated by the ATPase provides the electrochemical energy for several counter and co-transporters in cells that derive their energy from the ions gradients maintained by the ATPase.

A large body of work has been published on experiments performed with isolated Na^+, K^+ ATPase enriched membrane fragments from the kidney of several animals. This work has proven to be invaluable in elucidating the rate constants for the partial reactions of the Na^+, K^+ ATPase cycle. However, certain inherent difficulties are apparent with this method, such as an inability to control both the internal and external ionic concentrations and the inability to determine posttranslational regulation that occurs in situ. To understand the regulation of the Na^+, K^+ ATPase in situ whole-cell patch clamping has proven to be an excellent method. However, it has been very difficult to reconcile the results observed for the rate constants of the partial reactions with the effect of posttranslational modifications.

We have designed a simplified four-state mathematical model of the Na^+, K^+ ATPase using published results for the partial reactions. This model has been tested and refined with data garnered from whole-cell patch clamping under circumstances that didn't involve elucidation of a posttranslational modification. This allowed us to clarify

the difference between the kidney enzyme population and the heart enzyme population. We also described the allosteric site effect in the whole cell patch clamped cardiac myocyte and incorporated it into the model using previously reported results in the isolated Na^+, K^+ ATPase-enriched membrane fragments.

One of the critical difficulties in incorporating a posttranslational modification into a mathematical model of Na^+, K^+ ATPase function is that very little information on the effect that these alterations impart on specific partial reactions exist. For the last twenty years the K^+-activated transients reported using the whole-cell patch clamping technique have been attributed to the Na^+ diffusion restricted space. In this thesis we show that the transients are not due to restricted diffusion and propose an alternate hypothesis that suggests that transient changes to the level of β_1 subunit glutathionylation are the cause for these transient currents. These transient currents now offer us a measurable rate constant that can be incorporated into the mathematical model of the ATPase and with further refinement of the model to better reflect the experimental observations is clearly required.

This work offers the first mathematical model of the Na^+, K^+ ATPase that can simulate both steady state and transient currents. Attempts at reconciling the model with in situ whole-cell patch clamping experiments have offered insights into the kinetic differences between the kidney enzyme population and the heart enzyme population. Amalgamation of work performed on the kidney enzyme and whole-cell patch clamping have allowed us to incorporate the Na^+ allosteric site into the model. This has lead to the first ever kinetic model of the Na^+, K^+ ATPase to have a posttranslational regulatory effect incorporated with the ability to simulate what was once considered an effect derived from Na^+ loading of a restricted diffusion space within the cell.

ACKNOWLEDGEMENTS

The author was a recipient of a University of Sydney Postgraduate Award, Northern Clinical School/Ramsay Healthcare PhD Top-Up Scholarship and a Heart Research Australia PhD Scholarship. They are gratefully acknowledged.

I would like to thank my supervisor Prof. Helge Ramussen. His guidance, unerring support and enthusiasm throughout my candidature have been invaluable.

I would also like to thank Assoc. Prof. Ron Clarke for his patience and guidance with regards to understanding the Na^+, K^+ ATPase from a very different perspective.

To Ms Natasha Fry, Dr Chia-Chi Liu and Dr Elisha Hamilton without your friendship and constant encouragement this task would have been far more laborious.

Finally, I would like to thank my family and friends, particularly my wife, Hannah and my two young sons, Harry and Edward for understanding that Dad had to go to work on the weekends to “finish some experiments”.

TABLE OF CONTENTS

TABLE OF FIGURES AND TABLES

PUBLICATIONS ARISING FROM THIS THESIS

Garcia A, Rasmussen HH, Apell HJ, Clarke RJ. Kinetic comparisons of heart and kidney Na^+, K^+-ATPases. Biophys J. 2012 Aug 22;103(4):677-88.

Garcia A, Fry NA, Karimi K, Liu CC, Apell HJ, Rasmussen HH, Clarke RJ. Extracellular allosteric Na^+ binding to the Na^+, K^+-ATPase in cardiac myocytes. Biophys J. 2013 Dec 17;105(12):2695-705.

ABBREVIATIONS

[ATP]cyt	cytosolic adenosine triphosphate concentration
[K+]cyt	cytosolic potassium concentration
[K+]ext	extracellular potassium concentration
[Na+]cyt	cytosolic sodium concentration
[Na+]ext	extracellular sodium concentration
[Na+]o	superfusate sodium concentration
[Na+]pip	pipette sodium concentration
a	dielectric coefficient
ADP	Adenosine diphospate
AT1	Angiotensin II Receptor 1
ATP	Adenosine triphosphate
β1R	β-adrenergic receptor 1
β3R	β-adrenergic receptor 3
cAMP	cyclic adenosine monophosphate
cGMP	cyclic guanosine monophosphate
Cm	membrane capacitance
eNOS	endothelial nitric oxide synthase
F	faraday constant
Grx1	human glutaredoxin 1
HEPES	N-2-hydroxyethylpiperazine-N-2-ethanesulphonic acid
I_h	holding current
I_p	pump current
I_p-V	pump current vs voltage
I-V_m	current vs membrane voltage
$K_{0.5}$	substrate concentration for half-saturation

ms	milliseconds
mV	millivolt
$Na+_i$	intracellular sodium
NADPH	nicotinamide adenine dinucleotide phosphate hydrogen
NMG	N-methyl-D-glucamine
NO	nitric oxide
NPR-C	natriuretic peptide receptor C
$O_2^{\bullet-}$	superoxide
PKA	protein kinase A
PKC	protein kinase C
R	ideal gas constant
Ra	access resistance
SDS-PAGE	sodium dodecyl sulphate polyacrylamide gel electrophoresis
SOD	superoxide dismutase
SR	sarcoplasmic reticulum
T	absolute temperature
TMA-Cl	tetramethylammonium chloride
TTX	tetrodotoxin
Vm	membrane voltage

CHAPTER ONE

INTRODUCTION

The role of Na^+, K^+ ATPase.

First described in 1957 by Skou [1], the Na^+, K^+ ATPase is an essential membrane protein found in all eukaryotic cells. Its function is to transport Na^+ out of the cell and K^+ into the cell. For this transport it hydrolyses one molecule of ATP for each cycle. The complete cycle involves the exchange of three Na^+ with two K^+ and using one ATP molecule to pump against their respective ionic gradients. This 3 Na^+ : 2 K^+ ratio of positive charges creates a net outward current and maintains the electrochemical gradient for these cations across the membrane. This cation gradient is essential in maintaining the resting membrane potential of excitable cells [2]. The Na^+ gradient generated by the ATPase provides the electrochemical energy for several counter and co-transporters in cells, such as the Na^+/Ca^{2+} exchanger, Na^+/H^+ exchanger, Na^+-HCO co-transporter and sodium/glucose co-transporter (SGLT1) [3-5].

Na^+, K^+ ATPase structure.

The Na^+, K^+ ATPase was considered to be made up of predominantly two subunits, the alpha or catalytic subunit and the beta subunit. It was only confirmed in the early 1990's that a third gamma subunit coexisted in this complex [6]. It was subsequently realised that the gamma subunit belongs to a 7 member family of membrane proteins named after a conserved FXYD motif. The Na^+, K^+ ATPase is made up of an alpha:beta:gamma subunit ratio of 1:1:1 [7]. The α subunit has three different

cytoplasmic domains and ten membrane helices. The three cytoplasmic domains are; the actuator, the nucleotide binding site that binds ATP and the phosphorylation site that is phosphorylated by ATP and allows the transport of Na^+ from the cytoplasmic to extracellular side of the pump. Of the transmembrane helices M4-M6 and M8 coordinate the transported cations, M9 interacts with the FXYD protein and M10 has a close association with the transmembrane helix of the β subunit [8].

The β subunit has been shown to play a significant role in the chaperoning to and proper insertion of the α subunit into the plasma membrane [9,10]. The β subunit isn't limited to this role and has been associated with modulating the activity of the α subunit [9,11]. Structurally the β subunit consists of an N-terminal cytoplasmic domain, a single transmembrane domain and an extensive extracellular domain. The transmembrane helix of the β subunit runs closely to the M7 and M10 transmembrane domains of the α subunit and has significant contacts with these domains (see Figure 1.1) [8]. The extracellular surface of the β subunit has significant interactions with loop 7-8 of the α subunit [12]. These contacts have been implicated in the modulatory effects that the β subunit has on the catalytic activity of the α subunit [8].

Several early papers described low molecular weight proteins that ran on a gel with the purified preparations of the Na^+, K^+ ATPase [13-15]. Forbush *et al* established that they were related to the Na^+, K^+ ATPase through it's close association with a ouabain derivative [16]. Since these reports the FXYD family has been shown to be expressed in a variety of tissues with a specific-dependent manner and its association to the Na^+, K^+ ATPase has been confirmed in every tissue [17]. Even though the FXYD proteins are closely associated with the Na^+, K^+ ATPase they do not play an integral role in the basic function of the pump, however it has been

demonstrated that they can modulate pump function when co-expressed with the α/β heterodimer [18,19].

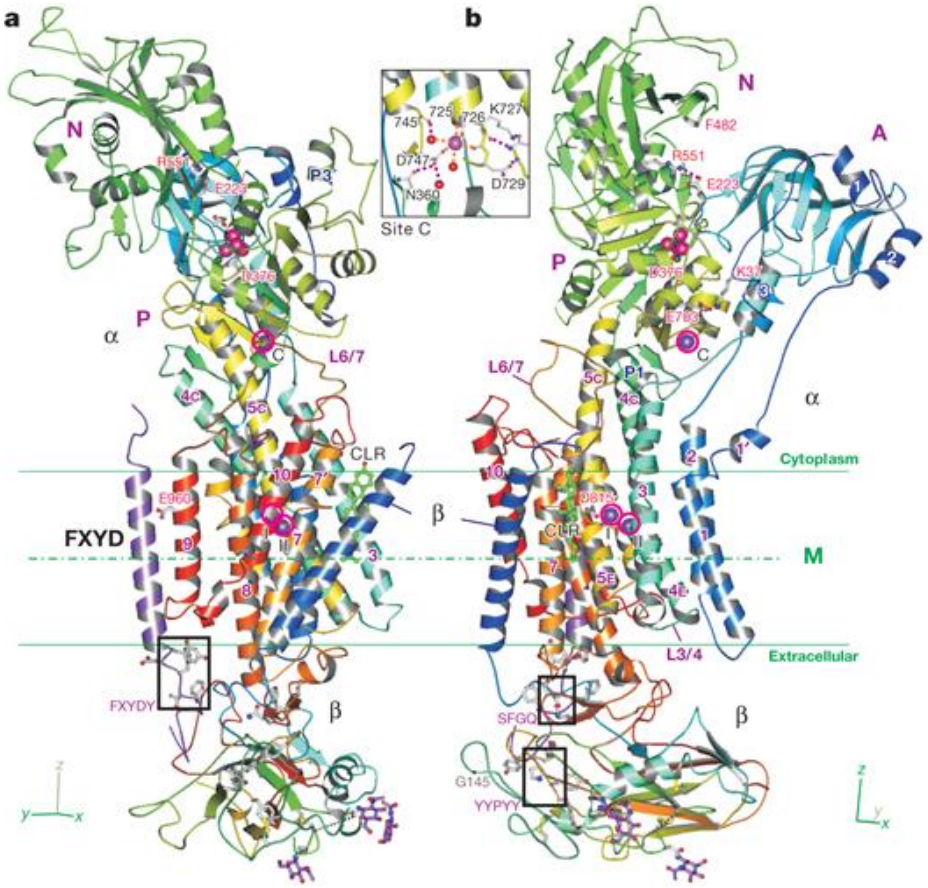

Figure 1.1. Architecture of Na^+, K^+ ATPase with bound MgF_4^{2-} and K^+. Taken from Shinoda *et al*. Crystal structure of the sodium–potassium pump at 2.4 Å resolution. Nature 459, 446-450 (21 May 2009).

The Na^+, K^+ ATPase cycle.

For the Na^+, K^+ ATPase to function effectively there are specific requirements that it must fulfil during its cycle. Firstly, it must be able to preferentially bind Na^+ and K^+ under unfavourable conditions with a low concentration of Na^+ and a high concentration of K^+ on the inside while it preferentially has to bind K^+ in an environment of low K^+ and high Na^+ concentrations on the outside. Therefore, there is a need for changing selectivity through subtle structural modifications to allow the pump to discriminate between these cations [20,21]. These structural conformations that define cation binding specificity have been termed E1 (High Na^+ affinity poise) and E2 (High K^+ affinity poise).

Secondly, it is a requirement that the transported cations are occluded within the enzyme to provide a gating style mechanism and hence prevent the more energetically favoured reverse flow of cations under physiological conditions [22].

The figure below shows a schematic of the Na^+, K^+ ATPase pumping cycle based on the Albers-Post scheme. Beginning at reaction 1 intracellular binding of Na^+ occurs to the α subunit at two sites in competition with K^+ and at a third Na^+ selective site. Once binding of Na^+ at all 3 sites is complete phosphorylation of an aspartate residue occurs and the 3 Na^+ ions are occluded within the pump molecule [23]. These Na^+ ions are subsequently deoccluded and then released to the extracellular side of the membrane in a sequential fashion [24]. This is followed by the binding of two K^+ ions at the competitive binding sites which has been described to occur in a sequential manner as well [25]. Occlusion of the two bound K^+ ions is preceded by dephosphorylation and subsequent release of the K^+ ions to the intracellular side of

the membrane. Another ATP molecule then binds and the cycle begins again through the binding of intracellular Na^+.

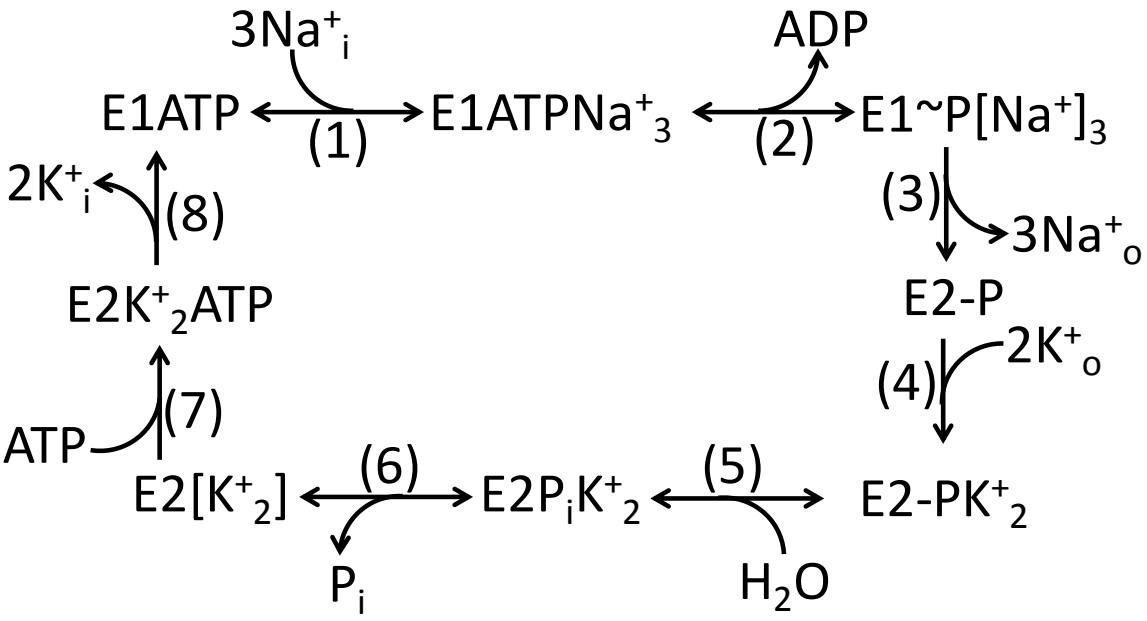

Figure 1.2. Albers-Post scheme for catalytic cycle of Na^+, K^+ ATPase.

Regulation of the Na+, K+ ATPase by intracellular cations.

Considering that there is competitive binding between Na^+ and K^+ at intracellular binding sites potential changes in concentrations of either would logically have an effect on overall turnover rate and in turn have a regulatory effect. In 1981 Eisner *et al* described that the activity of the Na^+, K^+ ATPase was a function of the concentration of intracellular sodium in experiments using voltage-clamped sheep cardiac Purkinje fibres and Na^+-sensitive microelectrodes. These experiments showed that when the Purkinje fibres were loaded with Na^+, in a K^+-free extracellular solution, upon reactivation with the K^+ congener Rb^+ an exponential decay in pump activity correlated well with an exponential decay in intracellular sodium concentration as measured by the Na^+-sensitive electrodes [26]. Subsequent experiments performed on guinea pig ventricular myocytes using the whole-cell patch clamp technique showed that pump activity was indeed dependent on intracellular Na^+ concentration (Figure 1.3). Nakao and Gadsby concluded that intracellular Na^+ activated pump activity had reached saturation with an intracellular Na^+ concentration of ~50 mM [27].

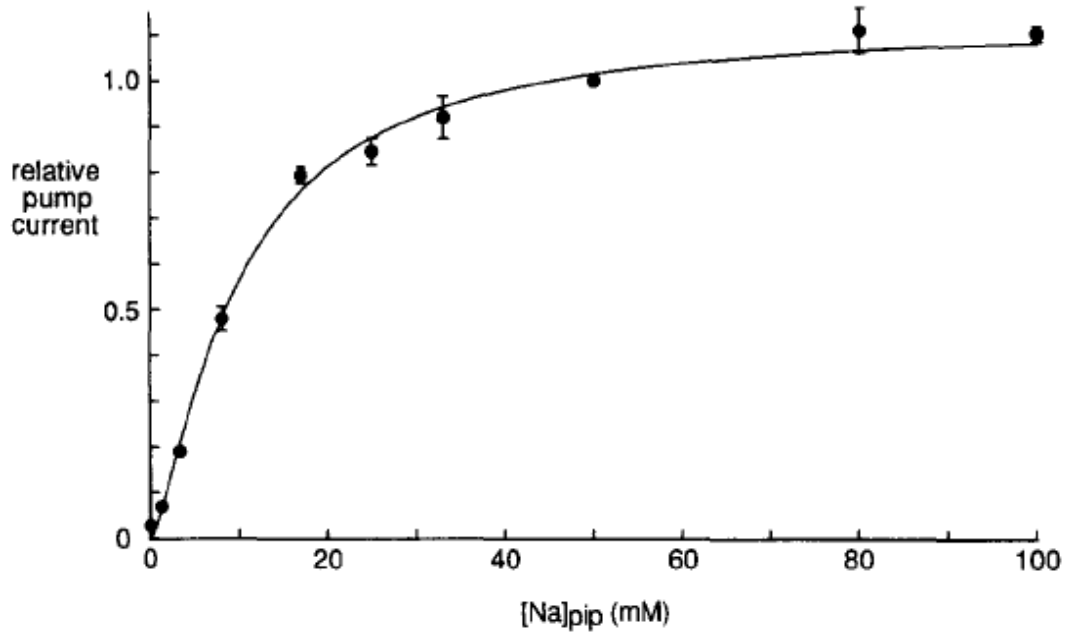

Figure 1.3. Saturable activation of Na^+, K^+ ATPase current at 0 mV by [Na]pip. Taken from Nakao & Gadsby. [Na] and [K] dependence of the Na/K pump current-voltage relationship in guinea pig ventricular myocytes. J Gen Physiol. 1989 Sep;94(3):539-65.

They obtained a $K_{0.5}$ value for activation by intracellular Na^+ of 10 ± 0.5 mM with Cs^+ as their K^+ conger in their patch pipette solutions [27]. Similar experiments performed by Shattock *et al* in rabbit ventricular myocytes found the $K_{0.5}$ for intracellular Na^+ activation to be ~19 mM under conditions with physiological intracellular K^+ concentrations [28].

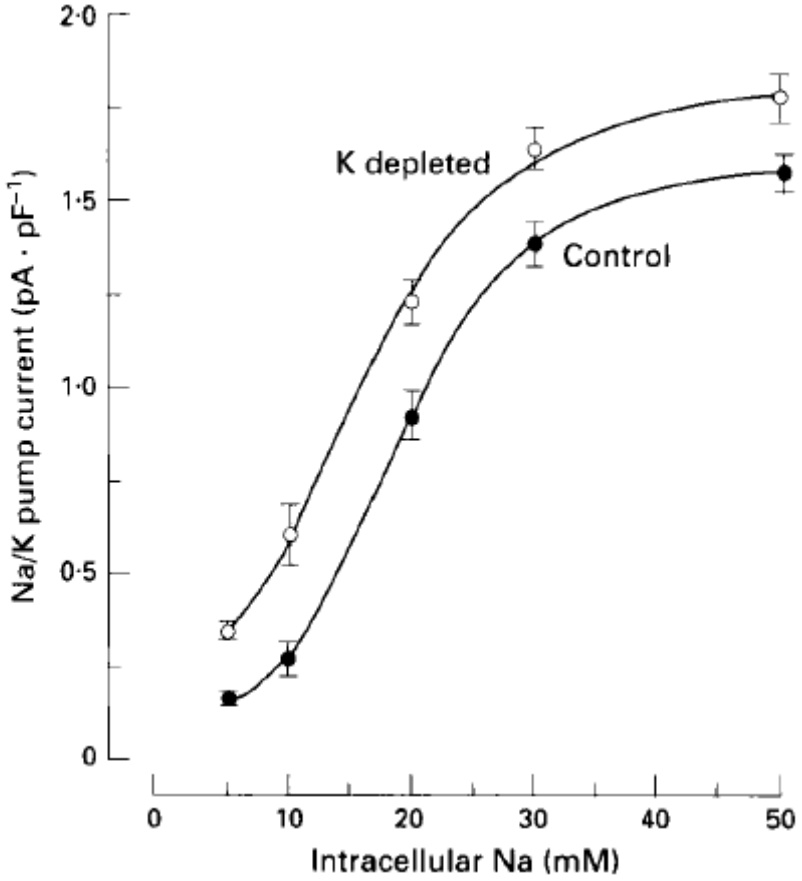

Figure 1.4. Relationship between extracellular [K^+] and sodium pump current in cells isolated from control (●) and potassium depleted (○) rabbits. Taken from Shattock *et al*. Sodium pump current measured in cardiac ventricular myocytes isolated from control and potassium depleted rabbits. Cardiovasc Res. 1994 Dec;28(12):1854-62.

As revealed in the above graph the intracellular Na^+ activation $K_{0.5}$ is dependent on the intracellular concentration of K^+, as was observed under conditions in which cells were K^+ depleted by placing rabbits on K^+ deficient diet for 25 days. In figure 1.4 K^+ depleted rabbit ventricular myocytes shift the activation curve to the left and a subsequent reduction in the $K_{0.5}$ of intracellular Na^+ to ~16mM is observed.

The idea that K^+ antagonises Na^+ activation creates a potential regulatory site that can be described by molecular modelling of the partial rate reactions of the Na^+, K^+

ATPase under physiological conditions. The competition at the intracellular binding sites at the E1 poise between Na^+ and K^+ causes an observable decrease in the overall forward rate constant in the model published by Kong and Clarke [29]. This competition was experimentally described in the isolated rabbit kidney enzyme preparation by Schulz and Apell [30] at the E1 poise using changes in the fluorescence of RH421 as a measure of ion binding and release. This is in agreement with several studies using the whole-cell patch clamping technique that reported that increasing K^+ concentrations in the patch pipette causes a significant decrease in the measured pump current, as seen in figure 1.5. This antagonism between Na^+ and K^+ ions is reflected in the regulation of the ATPase by extracellular cations.

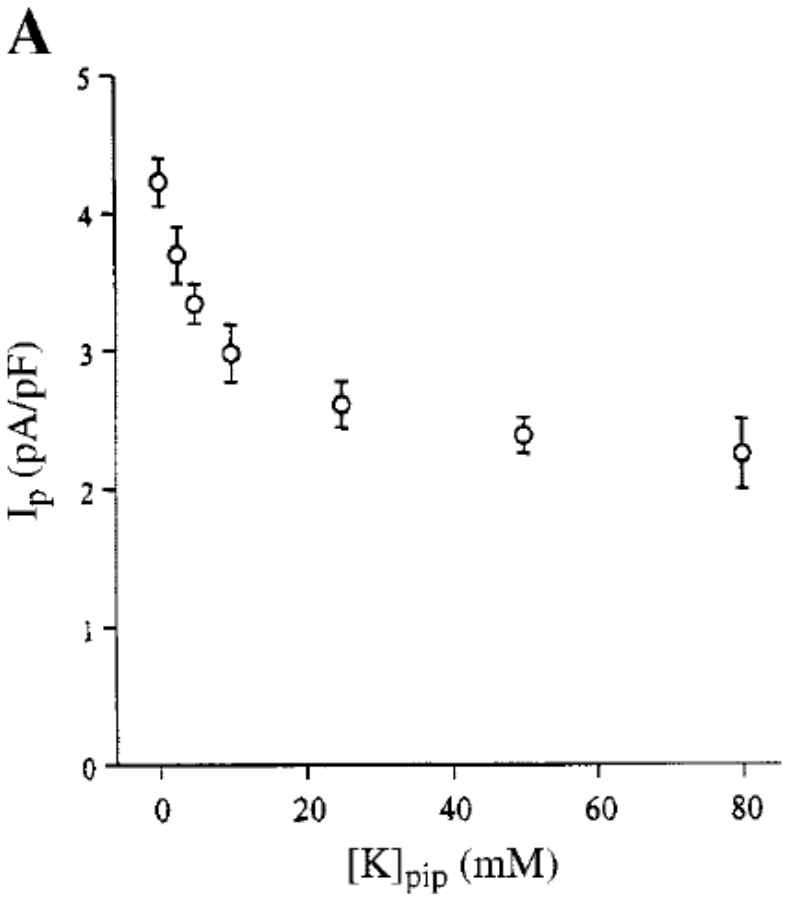

Figure 1.5. Pump current remaining after inhibition by $[K^+]$pip at 0 mV. Taken from Hansen *et al*. Dependence of Na^+-K^+ pump current-voltage relationship on intracellular Na^+, K^+, and Cs^+ in rabbit cardiac myocytes. Am J Physiol Cell Physiol. 2002 Nov;283(5):C1511-21.

Regulation of the Na^+, K^+ ATPase by extracellular cations.

Early studies in ghost red blood cells found that extracellular K^+ and its congeners had the ability to increase Na^+, K^+ ATPase activity in a concentration dependent manner [31] (Figure 1.6). It was also described that there was an antagonistic effect of Na^+ on the ability of K^+ to increase ATPase activity [31-34].

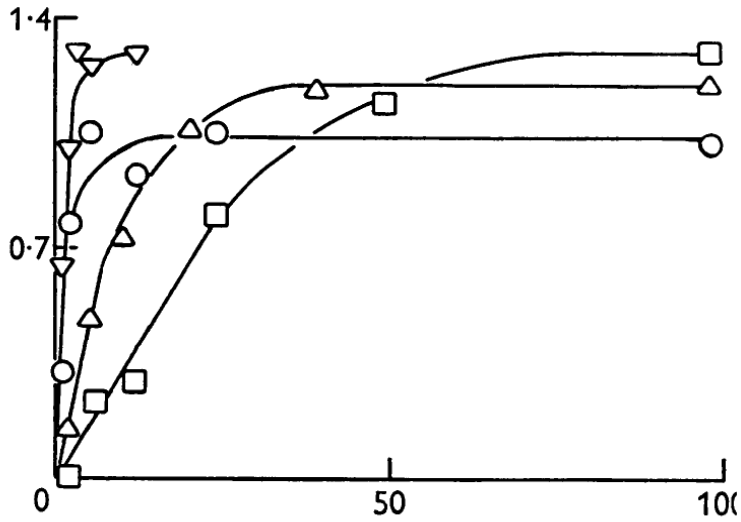

Figure 1.6. Stimulation of adenosine-triphosphatase activity by external Li^+ (□), K^+ (▽, Rb^+ (○) and Cs^+ (△) ions. Graph plots μmoles of orthophosphate liberated/ml of 'ghosts'/hr (Y-axis) against concentration of external cation (X-axis). Taken from Whittam & Ager. Vectorial aspects of adenosine-triphosphatase activity in erythrocyte membranes. Biochem J. 1964 Nov;93(2):337-48.

Under conditions where intracellular and extracellular ion concentrations can be separately controlled and membrane voltage fixed in voltage-clamped cardiac myocytes Nakao & Gadsby reported that extracellular Na^+ inhibits pump activity induced by activation through extracellular K^+ in a concentration dependent manner. They showed that the pump activity was also determined by extracellular K^+ and that

$K_{0.5}$ of K^+ activation was higher in Na^+ containing than Na^+-free extracellular solutions (Figure 1.7). These observations indicated that extracellular Na^+ and K^+ competed either for similar binding sites or for similar transport pathways through the pump [27].

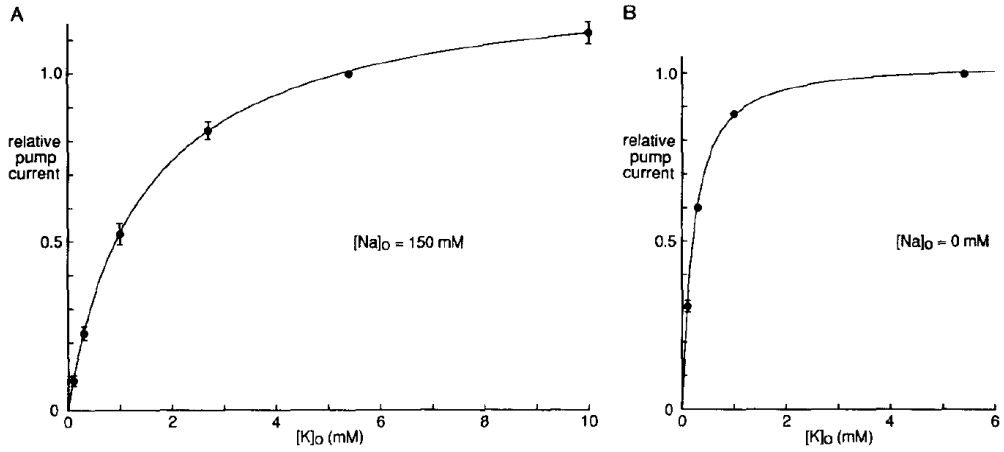

Figure 1.7. Activation of the Na/K pump current at 0 mV by $[K^+]o$, at 150 mM $[Na^+]o$ for (A) or at zero $[Na^+]$ for (B). Taken from Nakao & Gadsby. [Na] and [K] dependence of the Na/K pump current-voltage relationship in guinea pig ventricular myocytes. J Gen Physiol. 1989 Sep;94(3):539-65.

Voltage-dependence of the Na^+, K^+ ATPase.

The Na^+, K^+ ATPase generates an outward current through its exchange of 3 Na^+ with 2 K^+ ions. The extra Na^+ ion in the complete Na^+, K^+ ATPase cycle is electrogenic and the cycle is dependent on the membrane potential. Gadsby *et al* [35] were the first to investigate the effect of membrane potential on the Na^+, K^+ ATPase using the whole-cell patch clamping technique. This technique afforded them excellent control over not only the intracellular ionic concentration but also over the membrane potential. They measured pump currents between -140 mV and +60 mV, reporting a sigmoid shaped to the current-voltage (I_p-V) relationship which clearly demonstrated an effect of membrane potential on the pump current.

Considering the electrogenicity of the pump is derived from the third Na^+ ion transported it is of particular interest for understanding the steps in the pump cycle that depend on membrane potential. Nakao and Gadsby reported that changes in the extracellular Na^+ concentration altered the I_p-V relationship of the Na^+, K^+ ATPase [27]. They used several extracellular Na^+ concentrations as seen in figure 1.8 and observed that at very positive membrane potentials there was little effect of the concentration on pump current. However, the slope of the I_p-V relationship at negative membrane potentials was markedly dependent on the Na^+ concentration in the 50 to 150 mM range. When the external concentration of Na^+ was reduced to 1.5 mM the positive slope was almost abolished.

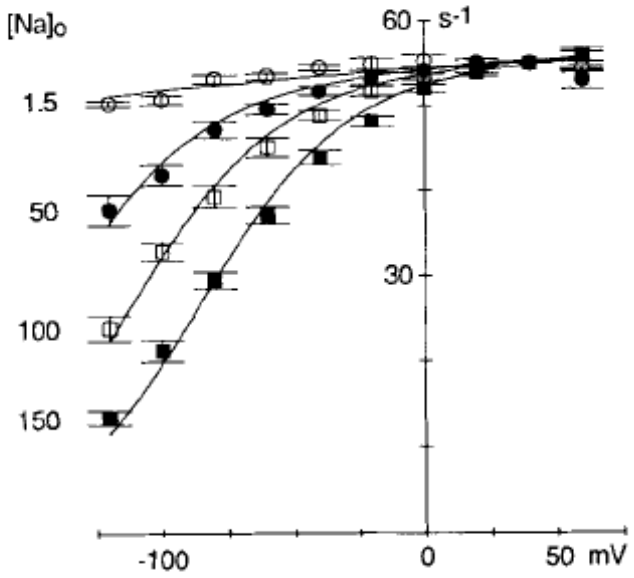

Figure 1.8. Graded influence of [Na^+]o on the shape of the Na/K pump I-V relationship at 50 mM [Na^+]pip and 5.4 mM [K^+]o. Taken from Nakao & Gadsby. [Na] and [K] dependence of the Na/K pump current-voltage relationship in guinea pig ventricular myocytes. J Gen Physiol. 1989 Sep;94(3):539-65.

The main voltage step in the Na^+ arm of the pump cycle has been attributed to the reverse rate constant of the Na^+ translocation step or what can be considered the rebinding of extracellular Na^+ [36].

K^+ translocation was thought to be voltage insensitive for many years. However, studies in voltage-clamped Xenopus oocytes by Lafaire and Schwarz suggested a possible second membrane potential sensitive step in the K^+ arm of the cycle [37]. Rakowski *et al* confirmed what others had shown that the pump is voltage-independent when extracellular Na^+ is eliminated and as long as extracellular K^+ concentrations are maintained at saturating levels (> 5 mM) [38]. However, as they reduced the concentration of extracellular K^+ to levels below saturating they

observed a distinct change in the I_p-V relationship consistent with a voltage dependence of extracellular K^+ binding. These results are in contrast to the earlier results obtained in cardiac myocytes by Nakao and Gadsby [27].

Peluffo and Berlin performed step changes in membrane potential in the presence of extracellular K^+ or the K^+ congener Tl^+ at concentrations below the levels that induced maximal steady state current [39]. They concluded that a small electrogenic step existed in the K^+ arm of the pump cycle and it was attributed to extracellular K^+ binding [39,40]. These results supported the earlier findings of Rakowski *et al* in Xenopus oocytes.

Hormonal regulation of the Na^+, K^+ ATPase.

Hormonal control of the Na^+, K^+ ATPase is an essential element in understanding the role and function of the pump in vivo and under pathophysiological conditions. A large variety of studies have established a clear role for hormonal regulation. However, the effect on both long term and short term pump activity and their interplay in vivo remains incompletely understood [41].

Corticosteroids, catecholamines and peptide hormones are some of the major hormonal regulators of the Na^+, K^+ ATPase [42-48]. Most of these hormones are reported to activate different protein kinases, phospholipases and phosphatases which in turn have been associated with the activation or inhibition of the Na^+, K^+ ATPase in a variety of different tissues and species (reviewed in Therien and Blostein, 2000) [41]. Recently reports have coupled the activation of these kinases/phospholipases and phosphatases to changes in the levels of glutathionylation of the β_1 subunit in cardiac myocytes and in turn changes to the pump activity (For summary see figure 1.9) [49].

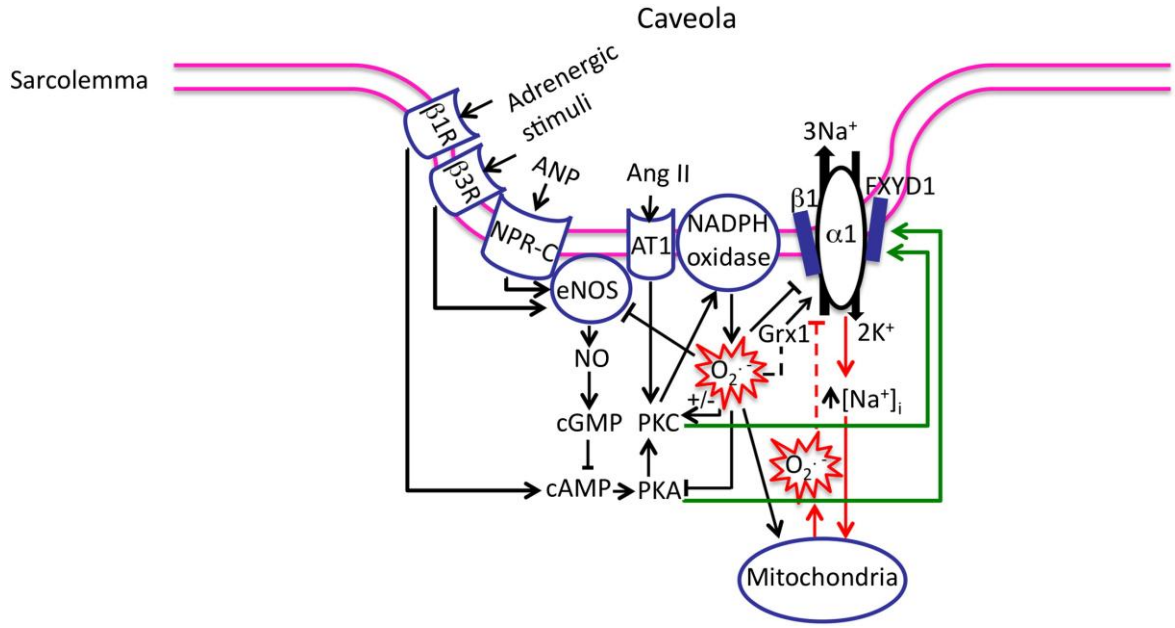

Figure 1.9. Schematic demonstrating redox regulation of Na^+, K^+ ATPase within the caveolae—the flask-shaped invaginations of plasma membrane that facilitate the spatiotemporal organization of the signaling complexes. Taken from Figtree *et al.* Oxidative regulation of the Na^+-K^+ pump in the cardiovascular system. Free Radic Biol Med. 2012 Dec 15;53(12):2263-8. The scheme represents the complex interplay of receptor coupled signaling currently reported. Activation of NADPH Oxidase by protein kinase C (PKC) can be derived from Ang II receptor type 1 activation or B1 adrenergic receptor activation via cAMP and protein kinase A (PKA). NADPH production of superoxide ($O_2^{\bullet-}$) can cause inhibition of the Na^+, K^+ ATPase via glutathionylation of the β_1 subunit. $O_2^{\bullet-}$ can also uncouple eNOS and exacerbate the effect by preventing cGMP pathway inhibition of cAMP. eNOS activation by β_3 adrenergic receptor (B3R) and Natriuretic Peptide receptor C (NPR-C) can cause increases in pump activity by reducing NADPH Oxidase activity through inhibition of cAMP. The green lines show the pathways reported that cause stimulation of the Na^+, K^+ ATPase via phosphorylation of the FXYD1 subunit.

Glutathionylation and the Na^+, K^+ ATPase.

Thiols are a class of organic sulphur derivatives that have been apportioned a variety of functions in biology. In biological systems sulphur derivatives are formed in two main groups, large complex proteins containing thiol groups and small simpler molecules such as the tripeptide glutathione. The reactive properties of these thiols play an important part in redox sensitive biochemical processes. Coupled with the reversibility of these reactions, mediated by the thiol-disulphide oxidoreductase superfamily, makes modifications of thiols good candidates for signal transduction.

Modifications of protein sulphur groups and the cysteinyl residues on proteins can modulate/regulate the function of many important proteins. The following table from Hill and Bhatnagar shows a sample of proteins from cardiovascular tissue that show significant changes in function when exposed to redox sensitive changes in their level of glutathionylation [50].

Glutathiolated proteins in cardiovascular tissues.

Protein	Function	Site	Condition	Cell or tissue	Response
Actin	Structure, polymerization	C10, C374	Acetycholine-induced relaxation, ischemia	Aorta, heart, VSMCs	Impaired polymerization
Aldose reductase	Glucose metabolism	C298	Reperfusion, L-arginine feeding	Heart, aorta	Inhibition of activity
ATP synthase α-subunit	ATP production	C163	iNOS overexpression	Heart	Inhibition of activity
ANT	Nucleotide transport; MPT	C57	iNOS overexpression	Heart	Facilitates ADP/ATP translocation; prevents MPT
SERCA	Ca^{2+} transport	C674	acetycholine-induced relaxation	Aorta, cardiac myocytes	Activation, Increased SR Ca^{2+} uptake
p21ras	Cell growth	C118	oxLDL, AngII	ECs, VSMCs, myocytes	ERK activation, insulin resistance, hypertrophy
Na^+/K^+ pump (β_1 subunit)	Membrane potential, excitation-contraction coupling, energy metabolism	C46	Present basally; increased by Ang II, forskolin, paraquat, uncoupled NOS	Heart, myocytes	Inhibition of pump activity
GAPDH	Glycolysis, mRNA stability	C149(152)	Ischemia–reperfusion	Heart, ECs	Inhibition of enzyme activity; enhanced ET-1 mRNA stability
Complex I –NQR	Electron transport, redox signaling	C206	Ischemia-reperfusion	Heart	Regulation of mitochondrial superoxide production
Complex II	Electron transport	C90	Present basally (removed upon reperfusion)	Heart	Enhanced electron transport activity; Protection from complex II nitration
eNOS	NO production	C689, C908	Hypertension	Aorta, ECs	Superoxide production
Caspase-3	Cell death	C184, C220	Present basally (removed with TNF-α treatment)	ECs	Protection from cleavage and cell death
Kir6.1	Vascular tone	C176	Oxidative stress	Vascular mesenteric rings	Channel inhibition, impairment of K_{ATP} channel-mediated vasodilation
RyR2	Ca^{2+} transport	C36, C822, C917, C1582, C2330, C3158, C3602*	Tachycardia, exercise	Heart	Increased Ca^{2+} release
Caspase-1	Initiation of inflammation	C362, C397	High superoxide production	Macrophages	Decreased cytokine production

* From human RyR2 sequence: Residues correspond to equivalent cysteines identified to be glutathiolated in RyR1.

Table 1.10. Glutathiolated proteins in cardiovascular tissues. Taken from Hill & Bhatnagar. Protein S-glutathiolation: Redox-sensitive regulation of protein function. J Mol Cell Cardiol. 2012 Mar;52(3):559-67.

As seen in the above table the Na^+, K^+ ATPase is susceptible to glutathionylation of the β_1 subunit at cysteine 46 in the transmembrane section. This was confirmed in a set of mutational studies were the α_1 and β_1 subunits were co-expressed in Xenopus oocytes and cysteine 46 was mutated to a tryptophan residue. In these experiments it was shown that peroxynitrite induced glutathionylation of the β_1 subunit inhibited pump turnover and that when the β_1 subunit was expressed with the mutated cysteine residue at position 46, exposure to peroxynitrite did not change pump activity [51].

Confirmation that glutathionylation of the β_1 subunit occurrs in a cellular system would confer it physiological relevance and it was shown that glutathionylation of the β_1 subunit occurred in cardiac myocytes of rabbits. Glutathionylation of the β_1 subunit has been shown to be regulated by several different receptor-coupled neurohormonal signals and that pump activity and levels of β_1 subunit glutathionylation are inversly corrolated [52].

A subsequent study described the poise dependence of the susceptibility of the β_1 subunit to glutathionylation. Differentiating between an E2 and E1 state using different compositions of solutions to suspend the ATPase in preferential conformational poises indicated that the E1 poise is highly susceptible to glutathionylation while the E2 poise is resistant to increases in peroxynitrite-induced glutathionylation of the β_1 subunit [53].

Na^+ Subsarcolemmal space and the Na^+, K^+ ATPase.

The concept of origin for the Na^+ subsarcolemmal space were instigated by experiments performed to understand the involvement of the Na^+/Ca^{2+} exchanger in Ca^{2+}-induced Ca^{2+}-release form the sarcoplasmic reticulum and whether voltage-dependent Na^+ channels modulated this interaction. LeBlanc and Hume studied the effect Na^+ channel conductance during the action potential of isolated guinea pig myocytes have on the Ca^{2+} transient. TTX, a specific Na^+ channel blocker, significantly reduced the Ca^{2+} transient as measured by the Ca^{2+} indicator Indo-1 [54]. They surmised that as TTX didn't change the action potential plateau or duration that a TTX-dependent reduction in Ca^{2+} transient observed was not due to changes in Ca^{2+} entry through the Ca^{2+} channels. To understand where this influx of Ca^{2+} originated from they used the Ca^{2+} channel blocker Nisoldipine. They activated the

voltage-sensitive Na^+ channels with voltage clamp pulses from -80 mV to -40 mV and described that a fast inward current that was associated with a Ca^{2+} transient was abolished by the application of TTX. They determined that the source of the Ca^{2+} transient was from the SR and they finally concluded that the Na^+ induced Ca^{2+}-release from the SR was dependent on extracellular Ca^{2+} and that the extracellular Ca^{2+} did not flow through sarcolemmal Ca^{2+} channels, thus implicating the Na^+/Ca^{2+} exchanger. They believed that the opening of the voltage-dependent Na^+ channels induced a localised increase in the Na^+ concentration around the Na^+/Ca^{2+} exchanger which induced the reverse mode of Na^+/Ca^{2+} exchanger. This was taken to account for the increase in the intracellular Ca^{2+} concentration and Ca^{2+}-induced release of Ca^{2+} from the SR.

An editorial by Lederer *et al* commenting on Leblanc and Hume's results, explicitly proposed the possible existence of a subsarcolemmal space with restricted diffusion for Na^+ as an explanation for the results reported [55]. To adequately explain the results presented by LeBlanc and Hume they discussed the fact that the activation of the Na^+ current cannot achieve a high enough concentration of Na^+ in the intracellular bulk phase to activate the reverse mode of the Na^+/Ca^{2+} exchanger [56]. The only probable explanation was that the Na^+ that travels through the channels enters a restricted diffusion space under the subsarcolemma and that this causes localised increases in the concentration of Na^+ that would activate the reverse mode of the Na^+/Ca^{2+} exchanger and subsequently cause enough Ca^{2+} entry to induce Ca^{2+} release from the SR. Since no real physical evidence existed at the time the phrase "fuzzy space" was coined to describe the area of restricted Na^+ diffusion [55].

A transient current in experiments using Rb^+ to activate the Na^+, K^+ ATPase had been reported in previous work on voltage clamped Purkinje fibres. The transient

current was associated with changes in the bulk cytosol Na^+ concentration [57]. Essentially these experiments were performed under conditions that could not control the intracellular cation concentrations. This problem could theoretically be overcome with whole-cell patch clamping. However experiments performed by Bielen *et al* reported that in whole-cell patch clamped single cardiac Purkinje cells or ventricular myocytes, re-activation of the Na^+, K^+ ATPase by extracellular K^+ also caused a transient current similar to the type previously reported under conditions where control of the bulk phase Na^+ concentration was not possible. This was unexpected since the whole-cell patch clamp technique was thought to control intracellular ionic concentrations and hence eliminate a transient pump current that was thought to be due to electrogenic pumping of Na^+ that had accumulated during pump inhibition in K^+-free extracellular solutions. The K^+-induced transient current was attributed to two different possible causes, a poor control of the bulk cytosol Na^+ concentration by the patch pipette when the Na^+, K^+ ATPase had been inhibited or an uncontrolled accumulation of Na^+ in a diffusion-restricted subsarcolemmal space that occurred when the Na^+, K^+ ATPase was inhibited [58].

Carmeliet attempted to consolidate the available observations and reviewed the potential existence of the Na^+ subsarcolemmal space. He put forward three different types of evidence for the existence Na^+ subsarcolemmal space, which include the Na^+, K^+ ATPase K^+-induced transients, the Na^+-activated K^+ channels that can be activated with low cytoplasmic Na^+ concentrations and the Na^+/Ca^{2+} exchanger derived Ca^{2+}-induced Ca^{2+} release reported by LeBlanc and Hume. Based on the data published by Bielen *et al* there are two explanations offered for the Na^+, K^+ ATPase K^+-induced transients, firstly that the transient is due to the accumulation of Na^+ in the subsarcolemmal space when the pump is deprived of extracellular K^+ or

that there is a build up of bulk phase Na^+ concentration in the cell through a diffusion-restricted interface with the patch pipette. Carmeliet deduced that it is not the accumulation of Na^+ by a suboptimal pipette/cell interface by describing a transient seen at very high Na^+ concentrations as a personal communication from Bielen and Verdonck. Therefore, Carmeliet believed there is no other explanation of the K^+-induced transients other than the existence of a subsarcolemmal space that restricts Na^+ diffusion relative to the bulk cytosol and that this space cannot be controlled by the patch pipette when the Na^+, K^+ ATPase is inactivated by K^+-free extracellular solutions [59].

Several efforts at describing the K^+-induced transient and how the inhibition of the Na^+, K^+ ATPase affected the function of the Na^+/Ca^{2+} exchanger in cardiac myocytes were made. Fujioka *et al* described that the Na^+, K^+ ATPase K^+-activated transients occurred with both 20 mM Na^+ and 100 mM Na^+ patch pipette solutions with Su *et al* producing similar results with a more comprehensive study of pipette Na^+ concentrations and its effect on the transient currents [60,61]. Fujioka *et al* reported that the reversal potential of the NCX hardly changed when the Na^+, K^+ ATPase was activated with extracellular K^+. This therefore contradicts the idea that the Na^+, K^+ ATPase can cause Na^+ depletion of the Na^+ subsarcolemmal space and subsequently cause the K^+-induced transients [60]. It's difficult to interpret the results presented by Fujioka *et al* as Cs^+ was included in the standard K^+-free external solution and Cs^+ is a known activator of the Na^+, K^+ ATPase [62,63]. Both Bielen *et al* and Su *et al* report the K^+-induced transients persist in Na^+-free extracellular solutions. However upon closer examination both display significant methodological issues as ascertained from close examination of their experimental solutions. The problem with Su *et al* and Bielen *et al* was that NaCl was replaced with Tris.HCl or

Choline chloride, in the case of Su *et al* no other base is mentioned in the methods to buffer the extracellular solution other than NaOH and Bielen *et al* used LiOH to buffer their Na^+-free extracellular solution. Li^+ can act as a K^+ conger causing activation of the Na^+, K^+ ATPase [31]. Experiments performed using these methods would introduce artefacts that make the results difficult to interpret.

Several reports have attempted to determine the diffusion coefficients for Na^+ in the restricted space. Despa *et al* reported that in experiments that were designed to measure intracellular diffusion rates, they exposed part of a myocyte to extracellular K^+ to activate the Na^+, K^+ ATPase and with SBFI measured a change in the intracellular Na^+ concentrations. With this method they were able to approximate a diffusion rate of Na^+ at 100-200 times slower than what is expected in water using a one dimensional diffusion model. They hypothesised that Na^+ might be taken up by the mitochondria or that the tortuosity of the cytosol may cause inhibition of free Na^+ diffusion through the cell [64]. Earlier Despa and Bers had attempted to determine the diffusion rate constants for Na^+ in the subsarcolemmal space using the whole-cell patch clamping method. They replicated transiently enhanced K^+-activated Na^+, K^+ ATPase currents previously shown by others at low pipette Na^+ concentrations. However, interestingly they showed that with a pipette solution containing 100 mM Na^+ they a transient peak pump current was abolished. Their explanation for this was that they had achieved a high enough concentration of Na^+ to overcome the restricted diffusion in the subsarcolemmal space and achieve saturation of intracellular Na^+ activation of the Na^+, K^+ ATPase. With such saturation Na^+, K^+ ATPase induced depletion of local Na^+ is not expected to be reflected in a transient peak current. These results were in contrast to the results reported by Su *et al* who

performed similar experiments and found that the transient persisted with high intracellular Na^+ [61].

Despa and Bers estimated from their radial diffusion model that the width of the "fuzzy space" was between 100 nm and 500 nm. This is much larger than that suggested by Lederer *et al* and would be impossible to reconcile with the necessary space that is required for the subsarcolemmal Na^+ concentration to cause the reverse mode in the Na^+/Ca^{2+} exchanger and subsequent Ca^{2+}-induced Ca^{2+} release by the SR. They also calculated that the diffusion coefficient required to adequately explain their results was 10^3 to 10^4 time lower then seen in the bulk cytosol and one to two orders of magnitude greater than what they observed in their experiments using SBFI two-photon fluorescent measurements [64]. Both reports describe potentially significant alterations to free Na^+ diffusion within cell. However there is very little direct evidence as to how this could occur.

Attempts to visually ascertain the structure of the Na^+ subsarcolemmal space through electron probe methods have yielded contradictory results. Wendt-Gallitelli *et al* showed through electron probe microanalysis that a subsarcolemmal gradient existed just below the cell membrane. They describe significant gradients in cells that were excited with paired voltage-clamp pulses and believed that the Na^+ gradient was coupled to constant electrical activity that is physiological for a cardiac myocyte. However, they found little evidence of a Na^+ gradient when the cell was at rest. Silvermann *et al*, using a similar method known as electron probe X-ray microanalysis, reported a gradient in cells at rest and that the gradient did not change during diastole and systole, at odds with what was reported by Wendt-Gallitelli *et al* [65]. Interestingly Wendt-Gallitelli *et al* observed a Na^+ gradient but they also observed microheterogeneity with patches of high, 60-80 mM Na^+ and low, 0-15

mM Na^+ concentrations together. They attributed this to microdomains containing a mixture of different ion channels and pumps in the membrane [66]. This idea of micropatches of high and low Na^+ concentrations together was recently discussed by Aronsen *et al* as potential hotspots/coldspots of Na^+ near the subsarcolemma as opposed to a large area of restricted Na^+ diffusion [67]. This conclusion of short-lived hotspots/coldspots occurring was supported by a recent study that reported Na^+ diffusion within the cell as being much faster than previously recognised [68].

Scope of Thesis.

A large amount of work has been published in the study of the Na^+, K^+ ATPase using two substantially different methods; isolated Na^+, K^+ ATPase-enriched membrane fragments, predominantly of the pig kidney and whole-cell patch clamping of cardiac myocytes. The studies on membrane fragments have been used to determine the kinetics of the pumping cycle. However, the extent to which this can be reconciled with kinetic properties of in situ pumps in cardiac myocytes is very poorly understood.

Typically, there is a disconnect between studies on membrane fragments and intact cells and the present study attempts to reconcile the work on isolated enzyme preparation from pig kidney and whole-cell patch clamping from cardiac myocytes and Xenopus Oocytes. The main aims of the study are:

1. With the large amount of data that has been gathered on the partial reactions of the kidney enzyme, we will attempt to reconstruct the kinetics of its entire reaction cycle in a mathematical model and make predictions from the kidney-based model to experimental results obtained on the Na^+, K^+ ATPase in heart muscle cells via the whole-cell patch clamp technique (Chapter 3).

2. We will investigate the effect of the Na^+ allosteric site on Na^+, K^+ ATPase activity in cardiac myocytes. In particular we aim to determine from which side of the protein the ions are acting using this cellular system and subsequently alter the kinetic model previously described to incorporate the allosteric site effect (Chapter 4).

3. We will examine the K^+-activated transient currents and the potential role that poise dependent glutathionylation may play in the widely reported peak transient K^+-activated pump currents that conventionally is attributed to a subsarcolemmal space with restricted Na^+ diffusion. We will incorporate results from these studies on glutathionylation into the kinetic model and compare this model to the experimental results (Chapter 5).

CHAPTER TWO

METHODS

Animals and Housing.

Male New Zealand white rabbits were used in all the experiments and weighed between 2.5 and 3.5 kgs when euthanased. Rabbits were sourced from two suppliers Merungora Rabbits suppliers. The rabbits were housed in the Kearns Animal Facility at the Kolling Institute of Medical Research, Royal North Shore Hospital. Rabbits were housed in individual cages and the environment was maintained at 22 degrees with a 12 hour light and dark cycle. Water and commercially sourced rabbit chow were offered ad libitum. All animals euthanased for the experimental protocols outlined below were approved by the local (RNSH/University of Technology Sydney) Animal Care and Ethics Committee.

Isolation of Cardiac Myocytes.

The method used for isolation was adapted from Haddad *et al* [69]. The rabbits were anaesthetised with 50mg/kg ketamine (Parnell Laboratories (Aust) PTY.Ltd.) and 20mg/kg xylazine (Troy Laboratories, PTY, Ltd, NSW, AU) intramuscularly. Heparin (1000U) was given intravenously via a marginal vein in the ear using a 23 G butterfly needle. Once deep anaesthesia was achieved, a left lateral intercostal incision at the level of the fifth intercostal space was made. This incision was extended using scissors across the midline and superiorly along the right ribs. The heart was exposed, freed from its attachments and the aorta transected rapidly.

The excised heart was rinsed three times in ice-cold (2-4 °C) Krebs solution containing (in mM): 130 NaCl, 2.8 KCl, 25.0 $NaHCO_3$, 1.2 KH_2PO_4, 1.2 $MgSO_4$, 10 glucose, 19.9 Taurine. The solution was preoxygenated using carbogen (95% O_2 - 5% CO_2) for one hour to achieve a pH of 7.4 at 35°C. Once free from any remaining blood and debris, the heart was attached to a Langendorff perfusion apparatus (Laboratory Supply Sydney, Australia) by securing the aorta to a glass cannula with a silk suture. The cannula tip was positioned 3-4 mm above the aortic valve to ensure adequate perfusion of the coronary arteries. The heart was perfused with cold Krebs solution for 6 minutes by attaching an intravenous infusion set to the side arm of the Langendorff perfusion apparatus. After 6mins, the perfusion solution was switched to a warm Krebs solution (35°C). It was warmed using a thermostatically controlled water bath (Julabo, Seelbach,Germany) and kept at a constant temperature using the recirculation circuit of heated distilled water surrounding the perfusion column. Perfusion of the warm Krebs solution was achieved using a rate adjustable peristaltic infusion pump (Cole-Palmer Instrument Co, Chicago, USA). A glass water jacket, also heated by the recirculation circuit was placed around the heart.

The suspended heart was perfused with warm Krebs solution for 6 minutes, and subsequently with a warmed Krebs solution containing ≈ 217 U/ml of type II collagenase (Worthington Biochemical Corp, Freehold, NJ, USA) and ≈ 874 U/ml of hyaluronidase (Worthington Biochemical Corp, Freehold, NJ, USA). (The ratio of collagenase to hyaluronidase depended on the season as rabbit hearts contain more collagen in the winter [70].The heart was perfused with the enzyme containing solution from 8-14 minutes. The enzymatic digestion of the heart was judged complete when it became enlarged and appeared glassy and translucent. It was cut down from the

apparatus using an incision separating the atria from the ventricles; only the ventricles were used in the subsequent experiments.

The ventricles were placed in a beaker containing a small amount (20 mls) of enzyme containing Krebs and coarsely shredded using scissors. The cell suspension was then strained through a plastic mesh (500 µM pores) to eliminate debris. The filtrate was transferred to test tubes, which were centrifuged for 1 minute 45 seconds at 350 rpm in a Krebs solution. The supernatant was then aspirated and the pellet was re-suspended in Krebs solution. This solution was centrifuged again using the same speed and time period as before. The resulting supernatant was then aspirated and the pellet re-suspended in a solution containing equal volumes of Ca^{2+} containing Krebs and non Ca^{2+} containing Krebs. This solution was centrifuged again for 1 minute and 45 seconds at 350 rpm. The resultant pellet formed was then stored in a solution of Ca^{2+} Krebs solution at room temperature until experimentation. Myocytes isolated were used for experimentation on the day of isolation only.

Detection of poise dependent Glutathionylation in purified pig kidney Na^+, K^+ ATPase.

The purified pig kidney enzyme was a generous gift from Prof. Flemming Cornelius, Department of Biomedicine, Aarhus University, Denmark. To induce the desired conformational states we incubated the enzyme in previously described metal fluoride solutions [71]. To stabilise the enzyme in an E2P-like state it was incubated in 5 mM NaF, 100 µM BeSO4 and 30 mM Histidine and for a Na+ occluded-like state the composition was 5 mM NaF, 200 uM AlCl3, 1 mM ADP and 30 mM Histidine. The enzyme was incubated at room temperature for 15 min to complete the transitions to metal fluoride stabilised poises. Glutathionylation was induced using

hydrogen peroxide at a nominal concentration of 0.5% and incubated at room temperature for 5 min. The samples were placed on ice and Laemmli buffer was added before the samples were incubated at 95° C for 5 mins.

Following SDS-PAGE, membranes were immunoblotted with an antibody for the β_1 Na^+, K^+ ATPase subunit (Millipore Bioscience) and an Anti-glutathione antibody (Virogen Corporation). Western blots were quantified by densitometry using a Las-4000 image reader and Multi Gauge 3.1 software (Fuji Photo Film Co., Ltd.). Exposure times were adjusted to ensure that the variation in signal intensity was in the linear dynamic range.

The Whole Cell Patch Clamping Technique.

The patch clamp technique allows the study of the electrophysiological properties of a cell or membrane. It allows control of both the intracellular and extracellular environment as well as control of the membrane potential V_m and measurement of membrane currents. A wide tipped glass pipette is placed on the surface of the cell membrane to form a seal with it. Gentle suction is then applied to rupture the membrane and allow perfusion of the intracellular compartment of the cell with the contents of the pipette. The pipette contains an Ag/AgCl electrode which acts as an interface between the pipette solution and the electronic circuitry. See figure 2.1.

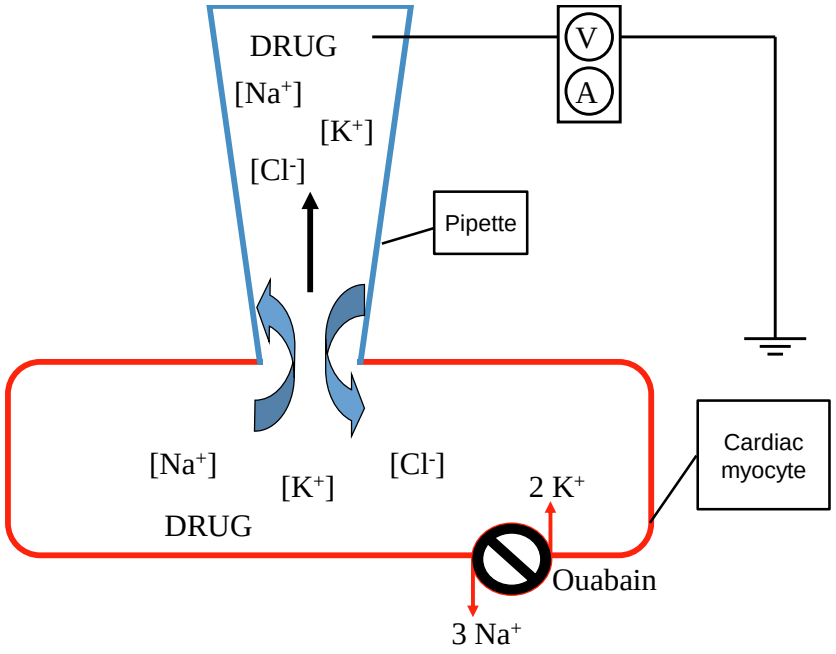

Figure 11. The whole-cell patch-clamp technique.

A wide-tipped (~5 μm) pipette is gently placed onto the surface membrane of a single ventricular myocyte. Gentle suction is then applied to the back of the pipette until the membrane under its tip is ruptured. This allows the patch pipette solution to perfuse the intracellular compartment and hence control of intracellular Na+, K+ ATPase ligand concentrations and membrane voltage. The technique also allows the measurement of membrane currents, including the electrogenic Na^+, K^+ ATPase current generated by pumps in the membrane.

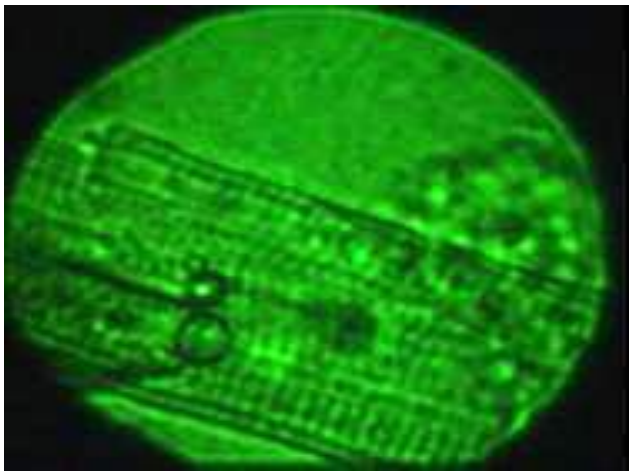

Figure 12.2. Cardiac myocyte as seen under high magnification using an inverted phase contrast microscope.

Tissue bath and experimental set up.

A 350 µL tissue bath was secured to the stage of an inverted phase contrast microscope (Nikon TE200, Nikon Corp, Tokyo, Japan), allowing direct visualisation of the isolated cardiac myocytes (see Figure 2.2. for an example). Two single in-line solution heater (Warner Instruments, Hamden, Connecticut, USA) with a dual temperature controller (Warner Instruments, Hamden, Connecticut, USA) maintained the temperature of the superfusate solutions before they entered the tissue bath. Temperatures were monitored using a telethermometer (Yellow Springs Instruments Co Inc, Yellow Springs, 0hio, USA).

The tissue bath was gravity fed; all superfusates were administered using intravenous infusion sets. Solutions were drained from the tissue bath, under continuous suction. The depth of the tissue bath was maintained at a constant level by the use of a Perspex cap bridge, which separated the tissue bath from a second reservoir. Rapid exchange of superfusate solutions were performed with fast-step perfusion equipment (Warner Instruments, Hamden, Connecticut, USA). The time

taken to exchange solutions over the complete membrane surface of the cardiac myocyte is restricted by the T-tubule system. All of the equipment was placed on a vibration isolation table (Technical Manufacturing Corp, MA, USA) located inside a Faraday cage. The bath solution was grounded via an Ag/AgCl electrode placed downstream in the tissue bath. Prior to experimentation, the ground electrode and tip of the filled patch pipette were lowered in to the tissue bath and the potential offset was reset to zero. All metallic equipment was grounded to a point within the Faraday cage to reduce electrical interference and noise.

Patch clamp equipment.

Wide tipped glass pipettes were prepared from unfilamented thin walled borosilicate glass tubing (Harvard apparatus, Kent, UK). Pipettes were pulled to a tip diameter of 4-5 µM using a Sutter P-87 puller (Sutter Instruments Co, Foster City, CA, USA) and fire polished using a Narishige microforge (Narishige Scientific Instrument Lab, Tokyo, Japan) to ensure a smooth tip. Patch pipettes were used within 8 hours of construction to ensure dust particles did not adhere to the glass and prevent seal formation between the pipette and the cell membrane. The pipettes were stored in a sealed electrode container (World Precision Instruments, Florida, USA) to prevent access of dust particles.

Patch pipettes were back filled with pipette solution, that was filtered using a 0.2 µm syringe filter (Pall Corporation, Ann Arbor, MI, USA) to minimize particle adhesion of the pipette tip, using suction before being placed in an electrode holder connected to a manipulator-mounted headstage (Axon Instruments, Foster City, California, USA). The headstage was connected to an Axoclamp 2B amplifier (Axon Instruments, Foster City, California, USA). The tip of the patch pipette was placed on the surface

of a cardiac myocyte using a Narishige Hydraulic Micromanipulator (Narishige Co. Ltd, Tokyo, Japan). An offset of 2-4 mV was typically observed due to the development of a liquid potential. Any offset larger than 4 mV, were corrected so as not to interfere with subsequent measurements.

Gentle suction was applied to the membrane directly under the membrane tip using the sidearm of the pipette holder. The cell was then lifted off the floor of the tissue bath. A 20 mV, 40 ms depolarising square wave pulse was passed from the voltage clamp amplifier through the pipette at an interval of 1500 ms. The process of seal formation was monitored by observing the current elicited during the plateau of the sealing pulse. Once a seal had formed, a small amount of suction was occasionally applied to rupture the membrane. Rupture of the membrane allowed low resistance access to the interior of the cell through the pipette tip and perfusion of the intracellular compartment with the contents of the patch pipette. This state is termed "whole cell configuration". A video microscopy camera (CCD-72S series, Dage-MTI Inc, Michigan City, IN, USA) and video monitor (Matsushita Electric Industrial Co Ltd, Osaka, Japan) connected to the microscope allowed continuous visual monitoring of the cell during the experiments.

Whole Cell Patch Clamping Experimental Solutions.

The myocytes suspended in the tissue bath were initially superfused with modified Tyrodes solution containing (in mM/L) 140 NaCl, 7 KCl, 2.16 $CaCl_2$, 10 glucose, 1.0 $MgCl_2$, and 10 N-2-hydroxyethylpiperazine-N-2-ethanesulphonic acid (HEPES). The solution was titrated to a pH of 7.4 at 25 °C with NaOH. After the whole cell configuration was established and membrane capacitance measured, the superfusates was switched to a modified Tyrodes solution similar to the one

described above except that it was nominally Ca^{2+} free and contained 0.2 mM $CdCl_2$. Cd^{2+} was included to block Ca^{2+} channel conductance and inhibit Na^+-Ca^{2+} exchange current[27]. The solution also contained 2 mM $BaCl_2$ to inhibit conductance through K^+ channels [72]. The composition of the pipette solution and the extracellular solutions were essentially designed to block any 'non-pump' currents leaving the Na^+, K^+ ATPase current as the dominant remaining current. A Tyrodes solution free of potassium was used to halt and hence identify pump activity.

In some experiments the superfusate used was Na^+ free. The Na^+-free modified Tyrodes superfusate contained (in mM/L) 140 NMG (D(-)-methylglucamine), 10 glucose, 10 HEPES, 1 $MgCl_2$, 0.2 $CdCl_2$, 2 $BaCl_2$, and 7 KCl. This solution is highly alkaline with a pH of ~10.4. It was titrated to a pH of 7.4 at 25 °C with concentrated HCl.

Whole Cell Patch Clamping Pipette filling solutions.

The pipettes were backed filled using suction with a solution containing (in mM) 20 Na^+ glutamate, 1 KH_2PO_4, 5 HEPES, 2 Mg-ATP, 5 ethyleneglycolol-bis-(β-aminoethlyether)N,N,N',N-tetraacetic acid (EGTA), 70 K^+-glutamate and 70 TMA-Cl. The solution was titrated to pH of 7.2 at 22°C with KOH. This was the standard pipette solution unless otherwise stated. Alterations in the Na^+ concentration in pipette solutions was compensated for by alterations of the concentration of TMA-Cl to maintain constant the osmolality. Pipette solutions were filtered through a 0.2 µM syringe filter (Pall Corporation, Ann Arbor, MI, USA). When filled with solutions, patch pipettes had resistances of 0.8-1.1 MΩ.

Measurement of membrane capacitance and access resistance.

Membrane capacitance (C_m) of the cell was estimated after whole cell configuration was established, using the membrane test mode of pClamp 10 software. All currents measured were normalised using cell membrane capacitance and hence cell size as the C_m is indicative of the cell surface area. The membrane test mode also allowed estimation of the access resistance (Ra) which reflects the quality of access between the patch pipette and the intracellular compartment. The experiment was abandoned if Ra at 24^{o}C was greater than ~4.5 mΩ.

Measurement of I_p and Exponential Decay.

When the Ra was documented to be acceptable myocytes were voltage clamped at a test potential known to inactivate voltage sensitive Na^+ channels [73]. The test potential was -40 mV unless indicated otherwise. A trace of the holding current (I_h– the current required to hold the membrane potential at the test potential) was recorded using Axotape version 10 software. Once I_h was stable the superfusates were switched to Ca^{2+} free and K^+ free, Cd^{2+} and Ba^{2+} containing Tyrodes solution to inhibit Na^+-Ca^{2+} exchange and K^+ channel conductance [72] and the Na^+-K^+ pump. This causes a reduction in the outward current of the cell and a new steady state level is reached. This new level had to stabilise for a predetermined length of time (approximately 1 min unless otherwise stated) prior to the superfusates being switched to a Ca^{2+}-free, Cd^{2+} and Ba^{2+} containing solution with 7 mM KCl. This protocol generates a transient pump current (I_p) generated by the Na^+, K^+ ATPase that is identified by the outward shift in membrane current induced by K^+. I_p was identified at a holding potential of -40 mV as the difference between stable plateaus of holding current before and after Na^+, K^+ ATPase activation with 7 mol/L KCl at

least 5 min (unless otherwise stated) after establishing the whole-cell configuration. Sampling rate for all recordings was 20 Hz (1 sample every 50 ms).

Mathematical Model.

Computer simulations of the steady-state pump current observed experimentally via the whole-cell patch clamp technique were performed using the commercially available program Berkeley Madonna 8.0 and the variable step-size Rosenbrock integration method for stiff systems of differential equations. The simulations yielded the time course of the concentration of each enzyme intermediate involved and the outward current, i.e. the number of elementary charges transported per pump molecule per second. For the purposes of simulations of the steady-state current, each enzyme intermediate was normalized to a unitary concentration and the enzyme was assumed arbitrarily to initially be totally in the E1 state only. Each simulation was then carried out until the distribution between the different enzyme states no longer changed and the outward current reached a constant value.

A comprehensive explanation of the rate constants used can be found in the Appendix of chapter 3. This includes the equations used to calculate each of the enzyme intermediates and the where each rate constant was derived with the appropriate reference. In the chapters 4 and 5 only the altered equations are given in their appendix and calculations of the effect of the allosteric site and rate constants for glutathionylation are documented.

Data acquisition, analysis and storage.

Recording of membrane current, holding potential, passing of current and voltage steps were performed using continuous single electrode voltage- clamp mode of an Axoclamp 2B amplifier via DigiData 1200 series interface (Axon Instruments, Foster City, CA, USA). Voltage clamp pulses and stimulus protocols were applied using the pClamp 10 software run on an Dell PC computer. Continuous recording of V_m and I_h were made using a multichannel computerised data acquisition system (Axoscope Version 10, Axon Instruments, Foster City, CA, USA). Analyses of steady-state and transient currents were performed in Clampfit 10.2 and data was collated in Microsoft Office Excel 2007.

Chemicals and reagents.

Product	Source	Location
Adenosine 5- triphosphate magnesium salt	Sigma-Aldrich Chemical Co.	St Louis, Missouri, USA
Antibody to the α1 subunit of Na+ K+ ATPase	Millipore Bioscience	Billerica, Maryland, USA
Antibody to the β1 subunit of Na+ K+ ATPase	Millipore Bioscience	Billerica, Maryland, USA
Barium chloride	BDH	Australia
Bovine Cu,Zn superoxide dismutase	Sigma-Aldrich Chemical Co.	St Louis, Missouri, USA
Cadmium chloride	Sigma-Aldrich Chemical Co.	St Louis, Missouri, USA
Calcium chloride dehydrate	Sigma-Aldrich Chemical Co.	St Louis, Missouri, USA
Ethyleneglycolol-bis-(β-aminoethlyether)N,N,N',N-tetraacetic acid (EGTA)	Sigma-Aldrich Chemical Co.	St Louis, Missouri, USA
Gentamicin	Pfizer	Brooklyn, New York, USA
Glucose anhydrous	BDH	Australia
N-2-Hydroxyethylpiprazine-N-2-ethenesulphonic acid (HEPES)	Sigma-Aldrich Chemical Co.	St Louis, Missouri, USA
Hydrochloric acid (HCl)	Merck Biosciences	Darmstedt, Germany
Hydrogen Peroxide	Merck Biosciences	Darmstedt, Germany
Magnesium chloride hexahydrate (MgCl2.6H20)	Sigma-Aldrich Chemical Co.	St Louis, Missouri, USA
Magnesium sulphate (MgSO4)	Sigma-Aldrich Chemical Co.	St Louis, Missouri, USA
Monosodium glutamate	Sigma-Aldrich Chemical	St Louis, Missouri, USA

	Co.	
D(-)-methylglucamin (NMG)	Merck Biosciences	Darmstedt, Germany
Ouabain	Sigma-Aldrich Chemical Co.	St Louis, Missouri, USA
Potassium chloride	Sigma-Aldrich Chemical Co.	St Louis, Missouri, USA
Potassium dihydrogen orthophosphate (KH2PO4)	BDH	Australia
Potassium hydroxide (KOH)	Sigma-Aldrich Chemical Co.	St Louis, Missouri, USA
Potassium L-glutamate	Sigma-Aldrich Chemical Co.	St Louis, Missouri, USA
Sodium Chloride	Sigma-Aldrich Chemical Co.	St Louis, Missouri, USA
Sodium dihydrogen orthophosphate monohydrate (NaH2PO4.H2O)	BDH	Australia
Sodium dodecyl sulfate (SDS)	Sigma-Aldrich Chemical Co.	St Louis, Missouri, USA
Sodium hydrogen carbonate (NaHCO3)	Merck	Darmstedt, Germany
Sodium hydroxide (NaOH)	Sigma-Aldrich Chemical Co.	St Louis, Missouri, USA
Taurine	Sigma-Aldrich Chemical Co.	St Louis, Missouri, USA
Tetramethylammonium chloride (TMA.Cl)	Fluka Chemicals	Switzerland
Tris.HCl	Sigma-Aldrich Chemical Co.	St Louis, Missouri, USA

CHAPTER THREE

INTRODUCTION

The mechanism of the complete reaction cycle of the Na^+, K^+ ATPase is generally described by the Albers-Post formalism. A simplified version of this cycle is shown in figure 3.1. Much information has been gathered on the kinetics of the partial reactions of this cycle. However, this information has been gained from the study of a small number of purified enzyme systems. The reason for this is that, in comparison to ion channels, individual ion pumps such as the Na^+, K^+ ATPase produce a relatively low ion flux across the membrane. Therefore, the measurement of ion pump activity, in particular of partial reactions, has been limited to tissues in which the Na^+, K^+ ATPase naturally occurs at a very high level of expression. By far the most commonly studied source of Na^+, K^+ ATPase has been mammalian kidney, for which Peter Jørgensen developed a purification procedure in the 1970s [74,75]. A large amount of valuable information has been gained on the transport modes of the Na^+, K^+ ATPase from ion flux measurements carried out using red blood cells or resealed red cell ghosts [76,77]. However, as pointed out by Kaplan [78], the low expression level of the enzyme in human red blood cells (about 250 copies per cell) limits the scope for partial reaction kinetic studies in this system.

In a less complicated world kinetic and thermodynamic data obtained from the study of the Na^+, K^+ ATPase in one animal species or one tissue would be valid for all other species and tissues. Unfortunately, this seems not to be the case. Recently it has been shown that the Na^+, K^+ ATPase from pig kidney is significantly more thermally stable than that derived from shark rectal gland [79] and that the two

enzymes display significant differences in their kinetics, i.e., different rate-determining steps [80]. This is in spite of these two enzymes having very similar amino acid sequences and three dimensional structures [81-83]. The amino acid sequences of the α-subunits of both enzymes show 87% identity. In the case of the smaller β- and γ-subunits the sequence identities are 66% and 23%, respectively [79]. Via experiments in which both enzymes were independently reconstituted into synthetic lipid vesicles, Hansen *et al* [79] recently showed that that the bulk properties of the lipid membrane are not responsible for the difference in thermal stability of the pig and shark enzymes and they suggested that it may be due to relatively few differences in the enzyme's overall sequence.

In this paper we compare the Na^+, K^+ ATPase of mammalian heart and kidney. For the related enzyme, the sarcoplasmic reticulum Ca^{2+} ATPase, it has already been established that the kinetics of this enzyme are significantly different between skeletal muscle and heart muscle [84]. In skeletal muscle ion pumping is stimulated by ATP binding to an allosteric site on a phosphorylated form of the enzyme, whereas in cardiac muscle ATP accelerates ion pumping by binding to a non-phosphorylated form of the enzyme. If such major differences occur in the Ca^{2+} ATPase mechanism between different tissues, the Na^+, K^+ ATPase may also display significant differences. Therien and Blostein [85] reported in 1999 that the Na^+, K^+ ATPase of heart tissue possesses a somewhat higher degree of K^+/Na^+ antagonism at its cytoplasmic face in comparison to the Na^+, K^+ ATPase of kidney, i.e., K^+ more effectively competes with Na^+ for binding to the E1 state in the heart. However, this may not be the only difference. Gadsby and Nakao [86] also reported that the maximum turnover rate of the Na^+, K^+ ATPase in heart muscle cells is only about half that of Na^+, K^+ ATPase from kidney at a similar temperature. Significant kinetic

differences also exist between the Na^+, K^+ ATPase of kidney and that of red blood cells. For example, at 0 ºC the Na^+, K^+ ATPase phosphoenzyme of red blood cells is insensitive to the addition of K^+ ions and is rapidly dephosphorylated by ADP, whereas at higher temperatures it is dephosphorylated by both K^+ and ADP [87,88]. This difference in behaviour at different temperatures is not observed in the kidney enzyme [89-91].

Because of the large amount of data that has been gathered on the partial reactions of the kidney enzyme, it is now possible to reconstruct the kinetics of its entire reaction cycle and make predictions on its steady state behaviour under different experimental conditions. In this chapter we present a mathematical model which allows this and we compare the predictions of the kidney-based model to experimental results obtained on the Na^+, K^+ ATPase in heart muscle cells via the whole-cell patch clamp technique. For this comparison we have concentrated on two well-established observations made on heart muscle cells. These are the significant inhibition of pump current by inside-negative membrane potentials [86] and the significant inhibition of pump current by high concentrations of extracellular Na^+ (up to 150 mM) observed at negative holding potentials [27]. This comparison indicates that there could well be significant differences in the kinetic behaviour of heart and kidney Na^+, K^+ ATPase, in particular with respect to their voltage dependence. These differences are most likely due to the different levels of expression of isoforms of the Na^+, K^+ ATPase's major catalytic α-subunit. Whereas in the kidney enzyme the α_1 isoform constitutes >99% of the expression of the α-subunit [92], in cardiac myocytes results from Gao *et al* [93] indicate that the α_1 subunit is expressed to 82%, with 18% of the α-subunits being expressed as the α_2 isoform.

METHODS

Pump current simulations.

Computer simulations of the steady-state pump current observed experimentally via the whole-cell patch clamp technique yielded the time course of the concentration of each enzyme intermediate involved and the outward current, i.e. the number of elementary charges transported per pump molecule per second.

In simulations of transient kinetic data, prior to simulating the time course of the current transients caused by any sudden change in the experimental conditions (e.g. Na^+ concentration or membrane voltage), the initial steady-state distribution of the enzyme between the E1, E1P$(Na^+)_3$, E2P and E2$(K^+)_2$ states was calculated by performing a simulation, as described in the previous paragraph, in which the enzyme was assumed to be initially totally in the E1 state. The simulation was carried out until the distribution between the various enzyme states no longer changed. This distribution was then used as a starting condition for the simulation of concentration jump or voltage jump experiments.

RESULTS

Kinetic model.

Under experimental conditions in which inorganic phosphate and ADP are absent the complex Albers-Post cycle describing the Na^+, K^+ ATPase's partial reactions can be reduced to the simpler 4-state model shown in figure 3.1. E1P$(Na^+)_3$ and E2$(K^+)_2$ represent here occluded states of the protein, i.e. states in which the respective ions are enclosed within the protein and have no direct access to either the cytoplasm or

the extracellular fluid. In contrast, E1 and E2P represent states in which the ion binding sites have access to the cytoplasm and the extracellular fluid, respectively. In the case of the occluded states, $E1P(Na^+)_3$ and $E2(K^+)_2$, no exchange of the occluded ions with either the cytoplasm or the extracellular fluid is possible. However, in the case of the non-occluded states, we assume that rapid exchange of Na^+ and K^+ between the binding sites and either the cytoplasm or the extracellular fluid can occur. Thus, in the case of the E2P state we assume that there is a rapid exchange of Na^+ ions and K^+ ions between the extracellular fluid and two of the ion transport binding sites. It has been well established that the stoichiometry of the Na^+, K^+ ATPase is $3Na^+/2K^+$/ATP. Therefore, one of the ion binding sites is considered to be completely specific for Na^+, whereas Na^+ or K^+ can both bind with differing affinities to the other two. Therefore, ion binding to E2P can be treated as a series of coupled equilibria, as shown in figure 3.2. An analogous scheme can be drawn for the E1 state.

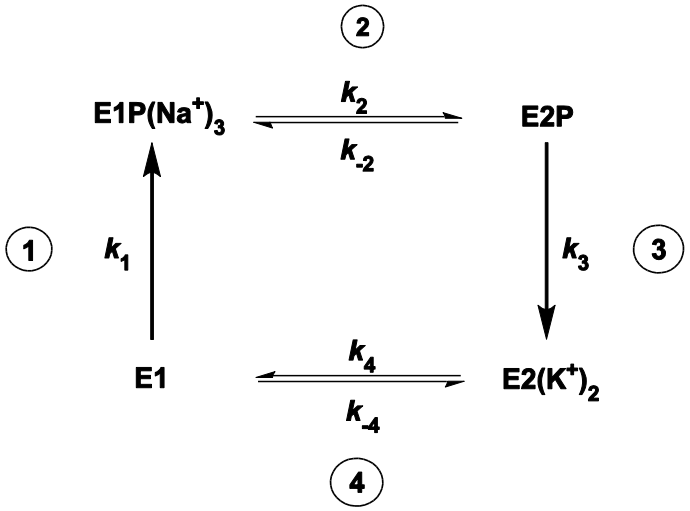

Figure 13.1. Simplified representation of the Albers-Post scheme describing the Na^+,K^+-ATPase catalytic cycle. Step 1: Binding of 3 Na^+ ions from the cytoplasm, phosphorylation by ATP and occlusion of Na^+ within the protein. Step 2: Conformational change of the phosphorylated protein releasing the Na^+ ions to the extracellular medium. Step 3: Binding of 2 K^+ ions from the extracellular medium, occlusion of K^+ within the protein and dephosphorylation. Step 4: Conformational change of the unphosphorylated protein releasing K^+ ions to the cytoplasm.

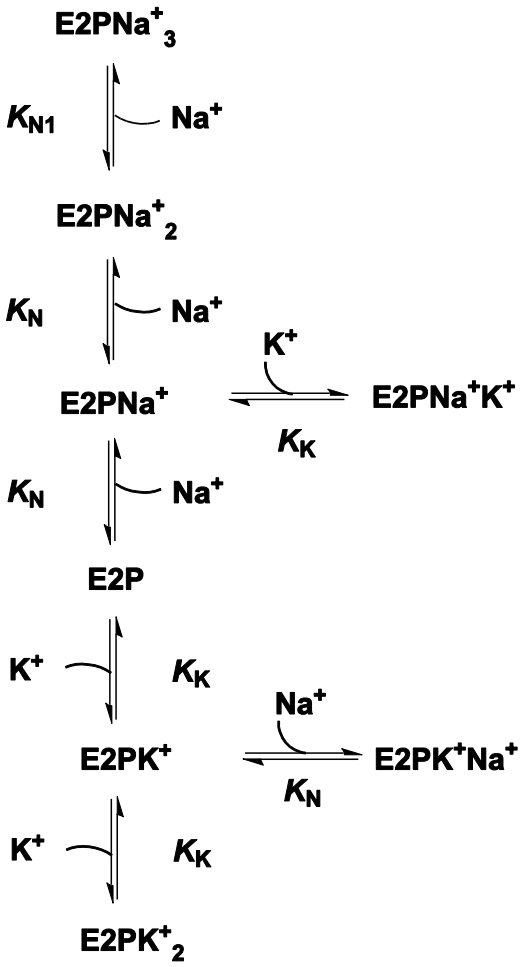

Figure 3.2. Scheme describing the coupled equilibria of Na^+ and K^+ binding to the E2P conformation of the enzyme. The model assumes competition between Na^+ and K^+ at two of the transport sites with dissociation constants K_N and K_K, respectively, and one specific Na^+ transport site with a dissociation constant K_{N1}.

In the 4-state model of figure 3.1, we, therefore, only show explicitly the major rate-determining steps of the enzyme cycle. In our computer model (see Appendix), furthermore, we only include differential rate equations for the E1, E1P(Na^+)$_3$, E_2 and E2(K^+)$_2$ states, because we consider ion binding to E1 and E2P to be very rapid, such that the binding reactions to these two states relax instantaneously on the time-scale of the four rate-determining steps, i.e. ion binding reactions are treated as equilibria. The four reactions whose kinetics are explicitly included in the model in sequence starting from E1 are then:

1) Phosphorylation of the enzyme by ATP and simultaneous occlusion of 3 Na^+ ions within the protein,
2) Conformational change of phosphorylated enzyme involving a de-occlusion of Na^+ and opening of the binding sites to the extracellular fluid (and its reverse reaction),
3) Occlusion of 2 K^+ ions within the phosphorylated enzyme, stimulating a dephosphorylation of the protein, and
4) Conformational change of unphosphorylated enzyme involving a de-occlusion of K^+ and opening of the binding sites to the cytoplasm (and its reverse reaction).

Oka *et al* [94] used a similar 4-state model, also assuming rapid equilibria for ion and ATP binding, to model the steady-state activity of cardiac Na^+, K^+ ATPase. However, the mathematical procedure used here to determine the steady-state activity is very different from that used by Oka *et al* [94], who calculated the pump current analytically by applying the King-Altman method [95], in which the steady-state turnover of the enzyme is directly calculated from the observed rate constants of all the reaction steps. Here we have used a numerical procedure (see Materials and Methods),

which also allows the kinetics of transient changes in steady-state pump current to be simulated.

In the model we consider that each of the four rate-determining reactions only reaches its maximum observable rate constant when the reactant state is fully saturated by the appropriate substrates. For example, the maximum rate constant for phosphorylation, k_1, is only achieved when the enzyme is fully saturated with 3 Na^+ ions and ATP. Although it doesn't explicitly appear in figure 3.1, the model assumes that high affinity binding of ATP to E1 is required to stimulate the reactions E1 → E1P$(Na^+)_3$ and E1 → E2$(K^+)_2$. Low affinity binding of ATP to the E2 state is also assumed to stimulate the reaction E2$(K^+)_2$ → E1. As in the case of Na^+ and K^+ binding, ATP binding is also treated in the model as a rapid equilibrium.

This simple kinetic model excludes a number of partial reactions which experimentally are known to occur. Thus, the model doesn't take into account ADP-stimulated dephosphorylation of E1P$(Na^+)_3$, P_i-stimulated phosphorylation of E2, dephosphorylation of E2P in the absence of occluded K^+ and conformational changes of unphosphorylated enzyme in the absence of bound ATP. However, under conditions of physiological levels of Na^+, K^+ and ATP in the cytoplasm and the absence of any added inorganic phosphate or ADP, these reactions are either effectively suppressed or their rate constants are negligible in comparison to those of the four major reactions shown in figure 3.1. Therefore, we consider that the extra complexity that the model would gain by including these reactions is not at this stage warranted.

In addition to differential rate equations for the each of the four major enzyme states, to complete the model we have included differential rate equations to describe the

transient current across the membrane. Because the enzyme pumps three Na^+ out of the cell in exchange for two K^+ ions in, there is a net transport of one positive charge out. In our model we assume that ion binding reactions are rapid equilibria. Therefore, when the enzyme is actively pumping both Na^+ and K^+, the release of two Na^+ ions to the extracellular fluid would immediately be neutralised by the uptake of two K^+ ions. Similarly, in the cytoplasm, when two K^+ ions are released, this is immediately neutralised by the uptake of two Na^+ ions. Therefore, the rate of change of the outward current at any point in time can be described by the rate of release of one Na^+ ion from the E2P state, which is given by the rate of conversion of $E1P(Na^+)_3$ to E2P minus the rate of the backward reaction (see Appendix, eq. 15). This is an important difference to the kinetic model which our group has published previously [29], which only allows steady-state currents to be estimated from the steady-state rate of phosphate production.

A final important point regarding the construction of the model is the incorporation of voltage dependence. In patch clamp measurements it's possible to accurately control the transmembrane voltage. This has a significant influence on the kinetics of charge-transporting (electrogenic) partial reactions of the enzyme. Therefore, this also needs to be included in the model. This can be done by multiplying the rate or equilibrium constants of all the electrogenic reactions by Boltzmann factors, i.e. $\exp(aFV_m/RT)$ (see Appendix, eqs. 9-14). Here F is the Faraday constant, V_m is the total transmembrane potential difference, R is the ideal gas constant and T is the absolute temperature. a is termed a dielectric coefficient and is the fraction of the total membrane potential difference influencing the electrogenic reaction concerned. It is sometimes approximated as the fractional distance across the membrane that an ion is transported during an electrogenic reaction [96,97]. Because there is a net

transport of one positive charge due to ion pumping, if one proceeds around the Na^+, K^+ ATPase cycle in the normal forward direction the dielectric coefficients of all the electrogenic reactions must add up to +1. The values of the dielectric coefficients we have used in our model are based on values estimated in the group of Rakowski from voltage jump studies [24,98,99]. Values of all the rate and equilibrium constants used in the simulations as well as the values of the dielectric coefficients are given in Table 1 of the Appendix to this chapter. All of the rate and equilibrium constants have been derived from measurements on mammalian kidney Na^+, K^+ ATPase.

Simulations of the expected kinetic behaviour of kidney Na^+, K^+ ATPase.

Simulations of the expected dependence of the pump current, I_p, per pump molecule on the extracellular Na^+ concentration and the total transmembrane potential difference, V_m, based on the Albers-Post model and the kinetic parameters given in Table 1 for mammalian kidney enzyme are shown in figure 3.3. For comparison, experimental results of Nakao and Gadsby [27] for the dependence of I_p for heart muscle Na^+, K^+ ATPase on both the extracellular Na^+ and V_m have also been reproduced. The experimental results indicate that for heart muscle Na^+, K^+ ATPase there is a significant positive slope in the I-V_m curve at negative membrane potentials, which becomes more pronounced as the extracellular Na^+ concentration increases, i.e., at large negative membrane potentials I_p increases with increasing V_m. The effect saturates as one moves to positive membrane potentials, at which I_p becomes virtually voltage-independent.

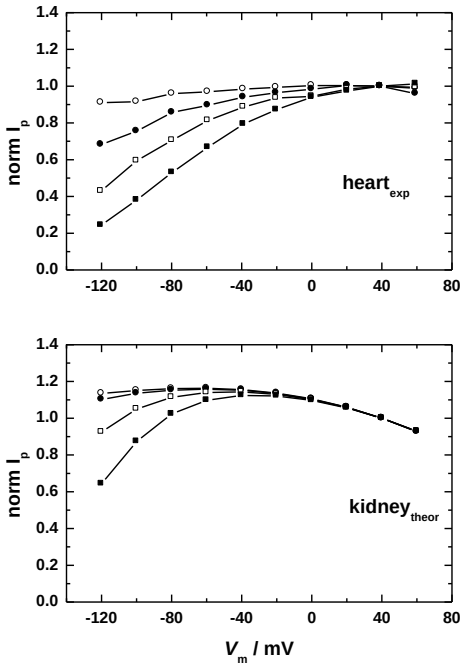

Figure 3.3. Dependence of the Na^+,K^+-ATPase current-voltage relationship (I-V_m curve) on the extracellular Na^+ concentration. Each symbol corresponds to the following Na^+ concentrations: 1.5 mM (○), 50 mM (●), 100 mM (□) and 150 mM (■). The solid lines between the points have simply been drawn to aid the eye of the reader. Upper curve: Experimental results for guinea pig heart ventricular myocytes, obtained via the whole-cell patch clamp technique, reproduced from Figure 3 of Nakao and Gadsby [27]. The pump current, I_p, of each curve has been normalized to the value obtained at a holding potential of + 40 mV. The experimental conditions were $[Na^+]_{cyt}$ = 50 mM, $[K^+]_{cyt}$ = 0 mM, $[K^+]_{ext}$ = 5.4 mM, $[ATP]_{cyt}$ = 10 mM, T = 36ºC. Lower curve: Computer simulations of the expected I-V_m curve for mammalian kidney Na^+,K^+-ATPase pump current based on the kinetic and equilibrium parameters given in Table 3.1 and the Albers-Post scheme described by Figs. 3.1 and 3.2. The ion concentrations, ATP concentration and temperature used for the simulations were the same as for the upper curve.

In comparison, the predicted behaviour of kidney Na^+,K^+-ATPase is different in some respects. At negative holding potentials there is still a positive slope of the I-V_m curve and the magnitude of the slope is still more pronounced at high extracellular Na^+ concentrations, but the magnitude of the drop in pump current on going from 1.5 to 150 mM extracellular Na^+ is significantly less. For example, at 150 mM extracellular Na^+ and -120 mV, the normalized I_p has dropped to approximately 0.6, whereas for the heart enzyme I_p drops experimentally to around 0.2. The other difference between the experimental heart results and the simulated kidney results is that the kidney results predict a slight negative slope in the I-V_m curve at positive potentials, which is independent of the extracellular Na^+ concentration, in contrast to an apparent saturation in the pump current at positive potentials in the case of the heart results. If all of the experimental parameters used in the simulations are correct, this result indicates that heart and kidney Na^+, K^+ ATPases must have some slightly different kinetic or equilibrium parameters, at least with respect to one of the partial reactions which determines the overall pump turnover, i.e. a rate-determining steps, the steps leading into rate-determining steps or the degree of charge displacement associated with these steps transport charge.

Voltage-jump transient simulation.

To demonstrate the applicability of the model in reproducing the results of transient kinetic experiments, we have carried out simulations in which the membrane voltage is rapidly changed from -120 mV to 0 mV. This corresponds to the experimental procedure used by Gadsby *et al* [100] on the Na^+, K^+ ATPase in squid giant axons. However, voltage-jump experiments of this type have been reported on the Na^+, K^+ ATPase within cardiac myocytes and *Xenopus* oocytes in addition to squid giant axons [24,98-100].

A voltage-jump simulation using the kinetic and equilibrium parameters given in Table 1 is shown in figure 3.4 (upper panel). In accord with the experimental conditions used by Gadsby *et al* (2012), the ion and ATP concentrations used were $[Na^+]_o$ = 25 mM. $[Na^+]_i$ = 80 mM, $[K^+]_o$ = $[K^+]_i$ = 0 mM and [ATP] = 5 mM. In the absence of any intracellular ADP or extracellular K^+, the enzyme can be assumed, both before and after the voltage-jump, to be distributed totally between the $E1P(Na^+)_3$ state and the E2P states (including occupation by zero, one or two Na^+ ions). Prior to the voltage jump from -120 to 0 mV, the simulation indicates that 56% of the enzyme should be in the $E1P(Na^+)_3$ state and 44% should be in E2P states. After the voltage-jump the final distribution at the end of the voltage transient becomes 0.2% in the $E1P(Na^+)_3$ state and 99.8% in E2P states. This significant redistribution of the enzyme from $E1P(Na^+)_3$ to E2P is accompanied by the release of Na^+ from the specific Na^+ ion binding site. Therefore, the voltage-jump is associated with a rapid rise in the outward current transient as the Na^+ ions are released to the extracellular fluid and a slower decay back to zero current because movement of the enzyme around its catalytic cycle past the E2P state in the absence

of extracellular K^+ is inhibited (Figure 3.4, upper panel). The decay back to zero current is exponential, with a relaxation time of 4 ms. This value is controlled predominantly by the reciprocal of the rate constant for the $E1P(Na^+)_3 \rightarrow E2P$ transition at 0 mV of 225 s^{-1} (see Table 3.1). This simulated result is in good agreement with the slowest current transient observed by Gadsby *et al* [100] with a time constant of 1-10 ms, which they also attributed to the release of occluded Na^+ from the enzyme as a consequence of the $E1P(Na^+)_3 \rightarrow E2P$ transition. Gadsby *et al* [100] also observed two faster, but smaller amplitude, transients, which they attributed to the release from E2P of the two Na^+ ions bound to the nonspecific sites, i.e. $E2PNa^+_2 \rightarrow E2PNa^+ + Na^+$ and $E2PNa^+ \rightarrow E2P + Na^+$. These two transients had time constants of 0.2-0.5 ms and ≤ 28 μs. These two faster transients are not reproduced by the simulations. The reason for this is that the model assumes that ion binding to and release from the E2P state are rapid equilibria on the timescale of the four reactions explicitly included in the model (Figures 3.1 and 3.2). To reproduce these smaller rapid transients the model would have to be extended to explicitly include the kinetics of ion binding. Thus, the model as it stands is applicable to the simulation of transients from the millisecond time range and beyond, but cannot be applied to simulations into the submillisecond range. The ability of the model to reproduce current transients arises because of its basis on the numerical integration of differential rate equations. This is a significant advantage of this approach over a fully analytical one, such as that used in the model of Oka *et al* [94], which can only be used to calculate steady-state currents.

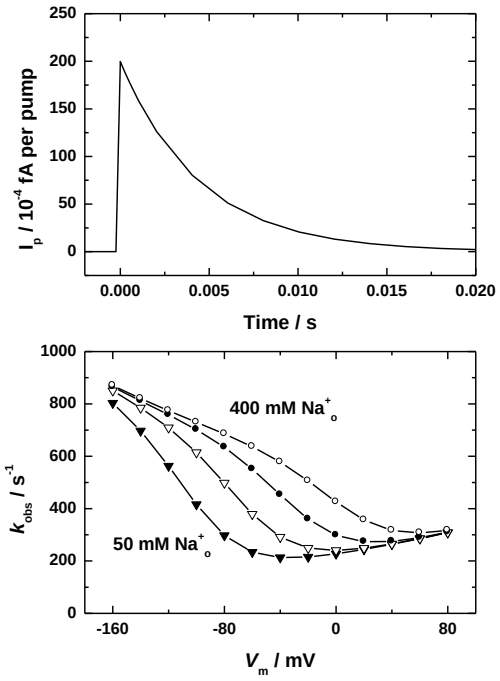

Figure 3.4. Simulation of a voltage-jump transient. The initial conditions were $[Na^+]_{cyt}$ = 80 mM, $[Na^+]_{ext}$ = 25 mM, $[K^+]_{cyt}$ = $[K^+]_{ext}$ = 0 mM, $[ATP]_{cyt}$ = 5 mM, V_m = -120 mV, T = 22ºC, as in experiments of Gadsby *et al* [100]. At time = 0, the membrane voltage was jumped to 0 mV. The current transient is attributed to the voltage-dependent release of Na^+ from the E2P state, which is rate-limited by the $E1P(Na^+)_3 \rightarrow E2PNa^+_3$ transition.

The lower panel of figure 3.4 presents the results of calculations of the expected observed rate constant, k_{obs}, (i.e. the reciprocal of the time constant) of the decaying phase of the voltage-jump transient and its dependence on both the final transmembrane voltage and the extracellular Na^+ concentration. Using the values given in for the kidney enzyme in Table 1 the value of k_{obs} can be calculated directly from the equation:

$$k_{obs} = k_2 + k_{-2} f(3Na_o) \qquad (1)$$

where $f(3Na_o)$ is the fraction of enzyme in the E2P state with 3 Na^+ ions bound. k_2 and k_{-2} are the voltage-dependent forward and backward rate constants of the $E1P(Na^+)_3 \rightarrow E2P$ transition (see eqs. A10 and A11 in the Appendix). The simulated results show a significant increase in k_{obs} as the extracellular Na^+ concentration increases and as the membrane potential becomes more negative. Both of these effects can be explained by an increase in occupation of sites on E2P by Na^+ ions, which increases the value of the term $f(3Na_o)$ in eq. 1 and hence causes k_{obs} to increase. At positive membrane potentials there is a smaller increase in k_{obs} with increasing membrane potential. This effect can be explained by the relatively small voltage dependence of k_2 (see eq. A10). Qualitatively similar behaviour to that shown in figure 3.4 has been experimentally observed by Holmgren *et al* [24] in measurements on the Na^+,K^+-ATPase of squid giant axons. The only noteworthy difference between our calculations and the experimental results of Holmgren *et al* [24] is the range of k_{obs} values. The measurements showed a saturating value of ~1,400 s^{-1} at negative potentials and a minimum value of ~100 s^{-1}, whereas the calculations indicate a saturating value of ~900 s^{-1} at negative potentials and a minimum value of

~200 s^{-1}. These differences must be due to different magnitudes of the rate constants $k_{2,V=0}$ and $k_{-2,V=0}$ for the kidney and squid enzymes.

Na^+, K^+ ATPase regulation.

Because the Na^+, K^+ ATPase plays such a crucial role in animal physiology, it must adapt to changing cellular conditions and physiological stimuli [41], and, therefore, its activity must be regulated. In principle, membrane proteins can be regulated by changes in the level of their expression, changes in delivery and incorporation into the membrane or by post-translational modifications to their structure that changes the activity of the protein itself. Such modifications are termed acute mechanisms of regulation because they are fast-acting in comparison to changes in expression level. Both phosphorylation and glutathionylation have been suggested as possible acute regulatory mechanisms. Recently, Massey *et al* [101] reported that in the kidney a differential regulatory phosphorylation of the Na^+, K^+ ATPase occurred depending on the enzyme's conformational state. Liu *et al* [102] found in the heart that the β-subunit of the Na^+, K^+ ATPase undergoes glutathionylation, also depending on the pump's conformational state. These results suggest that any shift in the enzyme's distribution between different conformational states could influence its propensity towards regulatory post-translational modification. A physiological mechanism whereby the enzyme's conformational distribution could be shifted is via an increase in the cytoplasmic Na^+ concentration. This would occur transiently in nerve and muscle cells at the onset of an action potential as a normal part of their physiological activity. Sustained increases in the cytoplasmic Na^+ concentration level are observed in red blood cells in certain hereditary blood conditions, i.e., spherocytosis and

elliptocytosis, in which the plasma membrane has a higher than normal ion permeability. The cytoplasmic Na^+ level influences the enzyme's conformational distribution because it is not saturating under normal physiological conditions for most cells and the phosphorylation of the enzyme by ATP, which is dependent on cytoplasmic Na^+ binding, is a major rate-determining step of the enzyme's pump cycle [29]. The kinetic model presented here allows the time course and magnitude of any shifts in the enzyme's conformational equilibrium to be calculated. To demonstrate this we have simulated the time courses of the population of enzyme in the states E1, E2, E1P and E2P following a sudden jump in the cytoplasmic Na^+ concentration from a normal physiological level of 15 mM to a concentration of 150 mM (Figure 3.5).

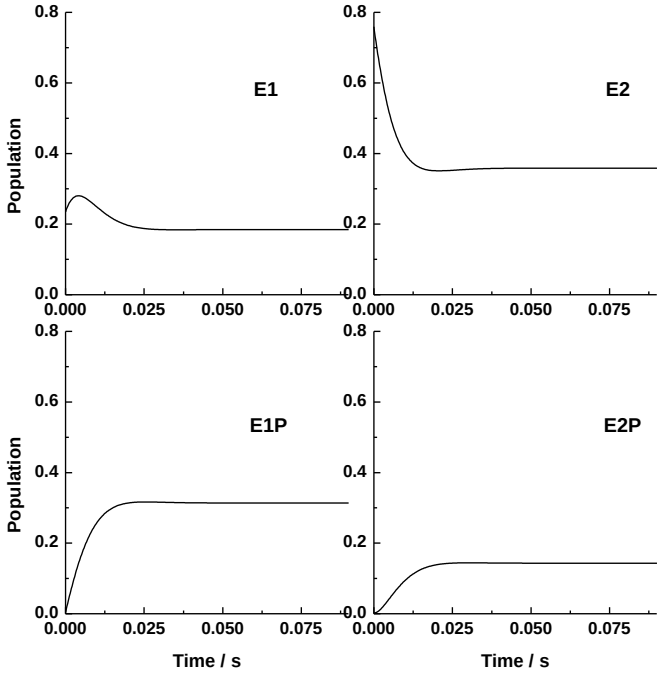

Figure 3.5. Simulations of the time courses of the relative populations of the Na^+, K^+ ATPase in the conformational states E1, E2, E1P and E2P following a jump in the cytoplasmic Na^+ concentration from 15 to 150 mM. All other conditions were held constant: $[Na^+]_{ext}$ = 140 mM, $[K^+]_{cyt}$ = 120 mM, $[K^+]_{ext}$ = 4 mM, $[ATP]_{cyt}$ = 3 mM, V_m = -80 mV, T = 24ºC. The simulations were based upon the kinetic and equilibrium parameters given in Table 3.1.

Overall the simulations predict that an increase in the cytoplasmic Na^+ concentration should be accompanied by increases in the populations of phosphorylated states (E1P and E2P) at the expense of the population of unphosphorylated states (particularly E2). The E1 state shows an initial transient increase in its population, due to the shift in the E1/E2 distribution in favour of the Na^+-selective E1 state, which is followed by a drop in its population. At the initial cytoplasmic Na^+ concentration of 15 mM, the enzyme is almost entirely in unphosphorylated states (76% in E2 and 19% in E1). The reason for this is that at this concentration the slowest steps of the pump cycle are the transition $E2(K^+)_2 \rightarrow E1 + 2K+$ and the phosphorylation step $E1(Na^+)_3 + ATP \rightarrow E1P(Na^+)_3 + ADP$. Hence the enzyme accumulates in the states leading into the major rate-determining steps, $E1(Na^+)_3$ and $E2(K^+)_2$. However, after jumping the cytoplasmic Na^+ concentration to 150 mM, the effective rate constant for the phosphorylation reaction dramatically increases because of the increase in level of saturation of the ion binding sites on E1 by cytoplasmic Na^+. With the phosphorylation reaction no longer contributing so strongly to rate-determination of the cycle, there is a significant increase in the level of enzyme in the phosphorylated states, i.e., 31% in E1P and 14% in E2P (from 0.4% and 0.2% initially).

Within a living cell any increase in the cytoplasmic Na^+ concentration would be overlaid also by a consequent change in the membrane voltage, which would also cause a shift in the enzyme's conformational distribution (as demonstrated by the simulations in figure 3.4). This hasn't been taken into account in the simulations shown in figure 3.5. The simulations of figure 3.4 and 3.5 nevertheless demonstrate that the model is capable of predicting conformational distribution changes due to both voltage and concentration jumps, which could potentially be used to rationalise changes in conformationally-dependent regulatory modifications to the pump.

DISCUSSION

The Na^+, K^+ ATPase is an electrogenic ion pump, i.e. it carries out a net transport of charge across the plasma membrane. This is due to its stoichiometry under normal physiological conditions of $3Na^+$ ions transported out of the cell and $2K^+$ transported into the cell during each turnover. Because the Na^+, K^+ ATPase transports net charge across the membrane its activity must in principle be dependent on the electrical membrane potential. However, whether or not a voltage dependence of its activity is apparent over physiologically relevant membrane potentials (i.e. approx. -80 to +60 mV in the case of the heart) depends on how strongly the charge transporting steps influence the overall turnover of the enzyme. A significant voltage dependence of the enzyme's steady-state activity will only be apparent when either the charge-transporting steps themselves are rate-determining steps of the cycle or the charge-transporting steps influence the population of an enzyme intermediate which is a reactant leading into a rate-determining step.

The simulations presented in figure 3.3, based on kinetic and equilibrium parameters derived from mammalian kidney enzyme, indicate that for the kidney Na^+, K^+ ATPase a lower degree of voltage dependence would be expected across the membrane potential range 0 to -120 mV than that observed experimentally for heart muscle Na^+, K^+ ATPase [27,86] (see figure 3.3). This suggests some differences in the kinetic or equilibrium parameters of the heart and kidney enzymes.

Simulations showing a very different result were, however, recently reported by Oka *et al* [94]. These authors also carried out simulations based on kidney data, but they found a strong voltage dependence and extracellular Na^+ concentration dependence identical to that measured in heart cells [27,86]. The decisive difference between the

simulations of Oka *et al* [94] and those presented here lies in the values of the rate constants used. The major charge-transporting step of the Na^+, K^+ ATPase is widely accepted to be the release of the first Na^+ to the extracellular medium, which is rate-limited by the E1P → E2P transition [24,98] [100,103]. Increasingly negative membrane potentials would cause Na^+ from the extracellular medium to rebind to the E2P state, driving the enzyme back towards the E1P$(Na^+)_3$ state. Whether this effect has a major influence on the overall turnover depends on the forward and backward rate constants of the E1P → E2P reaction. In their model Oka *et al* [94] chose values of 80 s^{-1} and 8 s^{-1} at 37ºC (or 31 s^{-1} and 3.1 s^{-1} at 20ºC) for the forward and backward rate constants, respectively. This makes the E1P → E2P reaction the slowest forward reaction of their entire kinetic model, i.e. the major rate-determining step of their cycle. If the charge-transporting step of the cycle is simultaneously the major rate-determining step of the cycle it is to be expected that under these conditions significant voltage dependence would be predicted.

There is, however, a large body of experimental evidence that the E1P → E2P transition is not a major rate-determining step of the kidney enzyme [104-108]. All of these studies indicate a rate constant for the E1P → E2P transition of 200 s^{-1} or greater at 24ºC. Also for heart muscle Na^+, K^+ ATPase, the E1P → E2P transition has been shown to be a fast reaction. Lu *et al* [109] estimated a rate constant for the heart enzyme in the range 300 to 900 s^{-1}. Based on their data, Gadsby and Nakao [86] also came to the conclusion that the major voltage-sensitive step of the heart Na^+, K^+ ATPase isn't rate-limiting, but rather that the voltage-sensitive step controls the concentration of the enzyme intermediate entering the rate-limiting step. Therefore, it would appear that the good agreement in voltage dependence and extracellular Na^+ dependence between the simulations of Oka *et al* [94] and the measurements of

Gadsby and Nakao [86] is simply fortuitous, because the simulations were based on an artificially low rate parameter. In the Discussion to their paper, Oka *et al* [94] in fact state that the rate constants they used may require revision.

For mammalian kidney Na^+, K^+ ATPase it is widely agreed that under saturating conditions of all substrates and no membrane potential the major rate-determining step is the E2 → E1 transition (see figure 3.1) and its associated release of K^+ to the cytoplasm [110-113]. Experiments on solid supported membranes have shown that this reaction doesn't involve any significant charge transport [114]. This being the case, one would not expect any major voltage dependence of the activity of mammalian kidney Na^+, K^+ ATPase when no electrical potential is applied across the membrane (i.e. at V_m = 0), which were the conditions under which the rate constant for the E2 → E1 transition were made [110-113]. This is what the simulations in figure 3.3 show. The experimental measurements on the heart enzyme (Figure 3.3) also show no significant voltage dependence (i.e. approximately a zero slope of the I-V_m curve) around 0 mV. This would be consistent with the E2 → E1 transition also being the major rate-determining step of the heart enzyme around 0 mV.

However, both the experimental heart enzyme results and, to a lesser degree, the simulations of kidney enzyme show a significant dependence of the pump current on the extracellular Na^+ concentration (Figure 3.3). If the observed extracellular Na^+ concentration dependence isn't due to a rate-limiting E1P → E2P transition or to any other rate-limiting charge-transporting step, then Gadsby and Nakao [86] must be correct that a reaction directly following the charge-transporting step must become rate-limiting at negative potentials. The reaction immediately following the release of Na^+ from the E2P state is the occlusion of K^+ from the extracellular medium. As far as we are aware, no direct measurements on the rate constant of this reaction for

the heart enzyme have been made. For the pig kidney enzyme the reaction is fast when the E2P state is completely saturated with K^+, with a rate constant of around 340 s^{-1} at 24ºC [80]. However, this reaction could contribute significantly to rate-limitation at negative potentials because a negative potential would promote electrogenic Na^+ binding to the E2P state and shift the E1P/E2P distribution back towards the E1P$(Na^+)_3$ state. The consequent depletion in population of the E2PK^+_2 state would decrease the effective rate constant of K^+ occlusion by E2P, leading to possible decrease in the pump turnover.

Whether this effect does in fact cause a decrease in turnover depends on the rate constants of the individual reaction steps. For the kidney enzyme, using the parameters given in Table 3.1, the simulations shown in figure 3.3 indicate that it does. The simulations carried out at 150 mM extracellular Na^+ and -120 mV yield a degree of occupation of the E2P state by 2 K^+ ions of 0.093. This is in comparison to a value of 0.634 at 1.5 mM Na^+ and -120 mV. Thus, the higher Na^+ causes a dramatic decrease in the occupation of the E2P state by 2 K^+ ions. Taking into account the voltage of -120 mV via eq. 14, one can then calculate an apparent rate constant for K^+ occlusion by the E2P state. Thus, multiplying the value of k_3 at zero membrane potential of 342 s^{-1} by 0.093 and the Boltzmann factor shows that the apparent rate constant reduces to a value of 169 s^{-1}. This is not far above the slowest rate constant in the cycle, i.e. that for the E2 → E1 transition of 90 s^{-1} (k_4). Thus, the voltage-induced drop in occupation of E2P by K^+ would be expected to make K^+ occlusion by E2P a significant contributor to rate determination at negative potentials. In contrast, at 1.5 mM extracellular Na^+ and -120 mV, if one does the same calculation one arrives at an apparent rate constant for K^+ occlusion by E2P of 1151 s^{-1}. This is so far above the rate constant for the E2 → E1 transition that one

wouldn't expect any significant contribution of K^+ occlusion by E2P to rate limitation of the overall pump turnover. This accounts for the very low dependence of the pump current on voltage at low extracellular Na^+ concentrations.

A possible explanation for the differences between the heart enzyme behaviour and that predicted by the simulations for the kidney enzyme is that they are composed of different isoforms of the enzyme. In the kidney the major catalytic subunit of the enzyme is present predominantly as the α_1 isoform [92], whereas in heart muscle both the α_1 and α_2 isoforms are present [93,115]. Horisberger and Kharoubi-Hess [116] did in fact find that when the α_1 subunit is expressed together with the β_1 subunit in *Xenopus* oocytes it displays a smaller voltage dependence at negative potentials than the α_2 subunit when expressed with β_1. They did not co-express any FXYD proteins together with the α- and β-subunits. In agreement with the results of Horisberger and Kharoubi-Hess [116], Apell and Bersch [117] found very little voltage dependence of the activity of the $\alpha_1\beta_1$ form of the enzyme over the membrane potential range -100 – 0 mV when they reconstituted it from rabbit kidney into synthetic lipid vesicles. Thus, it seems to be the case that the difference in the I-V_m behaviour of the heart and kidney most likely arises from intrinsic structural differences in the α-subunit and different degrees of expression of the α-isoforms between heart and kidney tissue. Horisberger and Kharoubi-Hess [116] also found that the α_2 isoform of the enzyme had a slightly lower apparent affinity for K^+ ions than the α_1 isoform. This is further supported by the results of Segall *et al* [118], who reported that the α_2 isoform favours more strongly the Na^+-stabilized E1 state over the K^+-stabilized E2 state. Via kinetic studies on α-subunit chimeras they attributed this difference primarily to sequence differences in the N-terminal third of the α-subunit. A difference in Na^+/K^+ ion selectivity could be the underlying physical reason

for the increased voltage dependence of the heart enzyme. A lower affinity of the E2P state for K^+ ions means that Na^+ can more effectively compete for occupation of the nonspecific ion sites on E2P, even at less negative potentials. This helps to drive the enzyme back towards the $E1P(Na^+)_3$ state and simultaneously reduces the degree of occupation of E2P by 2 K^+ ions. The consequence of this is a reduced effective rate constant for K^+ occlusion by E2P and hence a reduced overall turnover of the enzyme. Apart from a decrease in K^+ affinity, an increase in Na^+ affinity to E2P and an increase in the rate constant for the backward rate constant, $E2PNa^+_3 \rightarrow E1P(Na^+)_3$ are also possible mechanisms by which the voltage dependence of the enzyme could be increased. Quenched-flow results from Segall *et al* [118] indicate that there is unlikely to be any difference in the rate constant of the forward reaction $E1P(Na^+)_3 \rightarrow E2P(Na^+)_3$ for the heart and kidney enzymes.

The good agreement between the predictions of the model and the experimental behaviour of the $\alpha_1\beta_1$ enzyme gives one confidence that the model could be used to investigate the kinetics of regulation of the kidney enzyme, as described in the Results section, and, with minor modifications, also the kinetics of regulation of the heart enzyme. In the case of the heart enzyme, however, it would be important to bear in mind that the kinetic and equilibrium parameters used in the modelling would be apparent values, because, as described earlier, the expressed enzyme in that tissue consists of a mixed population of α-subunit isoforms [93,115].

Finally, it is interesting to consider the significance of the results shown in figure 3.3 within the physiological context of heart and kidney function. A typical extracellular Na^+ concentration of a heart muscle cell is 150 mM and a typical resting potential is approximately -80 mV. However, prior to each contraction the membrane potential increases to +60 mV (the action potential) due to the influx of Na^+ through

voltage-sensitive Na^+ channels. According to the results of Nakao and Gadsby [27], shown in the upper panel of figure 3.3, at the physiological extracellular Na^+ concentration of 150 mM this increase in membrane potential should alone cause a roughly 100% increase in the pump turnover. This would be advantageous for the cell, because it would make it easier for the Na^+, K^+ ATPase to pump out the excess Na^+ ions which had just entered via the Na^+ channels during the extended plateau-phase of the cardiac action potential and, thus, to re-establish resting conditions prior to the next action potential. This voltage-dependent increase in Na^+, K^+ ATPase activity would further enhance the stimulation of the enzyme already expected by the increase in intracellular Na^+ concentration, which under physiological conditions is not at a saturating level. A lower activity of the heart Na^+, K^+ ATPase under resting conditions of -80 mV also has the advantage of conserving ATP when high ion pumping rates are not essential. In the case of kidney cells, however, there are no changes in membrane potential associated with their activity. The membrane potential is always approximately -80 mV. Thus, there is no advantage for a kidney cell in possessing a voltage-dependent Na^+, K^+ ATPase. Thus, a kidney cell should not suffer at all by possessing a lower voltage dependence of its Na^+, K^+ ATPase. Thus, the experimental and predicted results of heart and kidney Na^+, K^+ ATPase shown in figure 3.3 seem to make sense in terms of the physiological function of these two types of cells.

APPENDIX

Simulation of the steady-state pump current.

Based on the four-state Albers-Post model of the Na^+, K^+ ATPase enzymatic cycle shown in figure 3.1, the differential rate equations describing the changes in concentrations of all the enzyme intermediates are:

$$\frac{d[E1]}{dt} = -k_1 f(3Na_i) f(ATP_{E1})[E1] + k_4 f(ATP_{E2})[E2] - k_{-4} f(2K_i) f(ATP_{E1})[E1] \quad \text{(A1)}$$

$$\frac{d[E1P]}{dt} = -k_2[E1P] + k_1 f(3Na_i) f(ATP_{E1})[E1] + k_{-2} f(3Na_o)[E2P] \quad \text{(A2)}$$

$$\frac{d[E2P]}{dt} = -k_3 f(2K_o)[E2P] - k_{-2} f(3Na_o)[E2P] + k_2[E1P] \quad \text{(A3)}$$

$$\frac{d[E2]}{dt} = -k_4 f(ATP_{E2})[E2] + k_3 f(2K_o)[E2P] + k_{-4} f(2K_i) f(ATP_{E1})[E1] \quad \text{(A4)}$$

In these equations the term $f(3Na_i)$ represents the fraction of enzyme in the E1 state occupied by 3 Na^+ ions. Similarly $f(ATP_{E1})$ represents the fraction of enzyme in the E1 state occupied by ATP. The significance of these *f*-terms can be easily understood if we take the phosphorylation reaction as an example. The maximum rate constant for phosphorylation, k_1, is only achieved when the E1 state of the enzyme is completely saturated by $3Na^+$ ions and one ATP molecule. Thus the observed rate constant, k_1^{obs}, for the reaction is given by k_1 multiplied by the probability that E1 has 3 bound Na^+ ions (= $f(3Na_i)$) and by the probability that E1

has a bound ATP molecule (=$f(ATP_{E1})$). This simple mathematical formulation of the rates will break down at very low cytoplasmic Na^+ and ATP concentrations, when second-order binding of the substrates to the enzyme becomes slower than the following first-order phosphorylation and occlusion of Na^+. However, under normal physiological conditions the assumption of rapid binding equilibria, on which equations (A1) - (A4) and the 4-state scheme shown in figure 3.1 are based, can be considered a good approximation.

Also appearing in equations (A1) – (A4) are the fraction of enzyme in the E2 state with ATP bound, *f*(ATPE2), the fraction of enzyme in the E2P state with 3 Na^+ ions bound, $f(3Na_o)$, the fraction of enzyme in the E2P state with 2 K^+ ions bound, $f(2K_o)$ and the fraction of enzyme in the E1 state with 2 K^+ ions bound, $f(2K_i)$. In a similar way to that described for the phosphorylation reaction, these fractions or probabilities modify the observed rate constant for each relevant reaction step, as shown in eqs. (A1) – (A4). Since in our model we consider all of the substrate binding reactions to be equilibria, the *f*-terms are determined solely by the substrate concentrations and the relevant equilibrium (or dissociation) constants of each substrate. Thus,

$$f(ATP_{E1}) = ([ATP]/K_{A1})/(1+[ATP]/K_{A1}) \qquad \text{(A5)}$$

$$f(ATP_{E2}) = ([ATP]/K_{A2})/(1+[ATP]/K_{A2}) \qquad \text{(A6)}$$

In contrast to ATP binding, the expressions for the *f*-terms describing Na^+ and K^+ binding are much more complex because here one must consider competition between 2 Na^+ ions and 2 K^+ ions for the same binding sites, as shown in figure 3.3. The relevant expression for Na^+ binding to E2P is:

$$f(3Na_o) = \frac{[Na^+]_o^3}{\left[K_{N1}^o K_N^{o2} + \frac{2K_{N1}^o K_N^{o2}[K^+]_o^2}{K_K^o} + \frac{K_{N1}^o K_N^{o2}[K^+]_o^2}{K_K^o} + 2K_{N1}^o K_N^o [Na^+]_o + K_{N1}^o [Na^+]_o^2 + [Na^+]_o^3 + \frac{4K_{N1}^o K_N^o [K^+]_o [Na^+]_o}{K_K^o} \right]} \quad \text{(A7)}$$

An analogous expression to eq. (A7) can be written for $f(3Na_i)$, in which all of the superscript and subscript o's are replaced by i's, to indicate binding to E1 from the intracellular fluid (cytoplasm) rather than the outer medium (extracellular fluid). The relevant expression for K^+ binding to E2P is:

$$f(2K_o) = \frac{[K^+]_o^2 / K_K^{o2}}{\left(1 + \frac{[K^+]_o}{K_K^o}\right)^2 + \frac{[Na^+]_o}{K_N^o}\left(\frac{[Na^+]_o^2}{K_{N1}^o K_N^o} + \frac{[Na^+]_o}{K_N^o} + \frac{4[K^+]_o}{K_K^o} + 2\right)} \quad \text{(A8)}$$

An analogous expression to eq. (A7) can also be written for $f(2K_i)$, in which all the superscript and subscript o's are replaced by i's, to indicate binding to E1 from the cytoplasm.

Our use of the fraction of enzyme in the E2P state with 3 Na^+ ions bound, $f(3Na_o)$, as a measure of the probability of the reverse reaction E2P → E1P$(Na^+)_3$ occurring is based on the assumption that this transition can only occur after three Na^+ ions have bound to the E2P state. Experimental data indicating that this is indeed the case has recently been achieved via voltage-jump measurements on the Na^+, K^+ ATPase of giant squid axons (25).

The effects of transmembrane electrical potential difference *V* (defined as electrical potential in minus electrical potential out) are taken into account in the model by the following Boltzmann expressions:

$$K_{N1}^{i} = K_{N1,V=0}^{i} \exp(-0.25FV / RT) \quad \text{(A9)}$$

$$k_{2} = k_{2,V=0} \exp(+0.1FV / RT) \quad \text{(A10)}$$

$$k_{-2} = k_{-2,V=0} \exp(-0.1FV / RT) \quad \text{(A11)}$$

$$K_{N1}^{o} = K_{N1,V=0}^{o} \exp(0.65FV / RT) \quad \text{(A12)}$$

$$K_{N}^{i} = K_{N,V=0}^{i} \exp(0.37FV / RT) \quad \text{(A13)}$$

$$k_{3} = k_{3,V=0} \exp(-0.37FV / RT) \quad \text{(A14)}$$

F, *R* and *T* represent here the Faraday constant, the universal gas constant and the absolute temperature, respectively. The numerical factors preceding *F* in each expression are the relevant dielectric coefficients for each reaction, as given in Table 3.1.

Based on the model, the differential rate equation for the transient outward current due to the Na^+, K^+ ATPase, I_p, is given by:

$$\frac{dI_p}{dt} = k_2[E1P] - k_{-2} f(3Na_o)[E2P] \qquad \text{(A15)}$$

The outward current at any point in time can be determined by numerically integrating the coupled series of differential rate equations (A1)-(A4) and (A15). For the purposes of this paper, the simulations were carried out until I_p no longer changed. This was then taken as its steady-state value.

Table 3.1. Values of the rate constants, equilibrium constants and dielectric coefficients of the four-state model used for the simulations shown in Figure 3.3.

Parameter	Reaction*	Value	Reference
k_1	$E1 \rightarrow E1P(Na^+)_3$	200 s^{-1}	100
$k_{2,V=0}$	$E1P(Na^+)_3 \rightarrow E2P$	225 s^{-1}	103
$k_{-2,V=0}$	$E2P \rightarrow E1P(Na^+)_3$	401 s^{-1}	103
$k_{3,V=0}$	$E2P \rightarrow E2(K^+)_2$	342 s^{-1}	74
k_4^{max}	$E2(K^+)_2 \rightarrow E1$	90 s^{-1}	107
k_4^{min}	$E2(K^+)_2 \rightarrow E1$	11 s^{-1}	108
k_{-4}	$E1 \rightarrow E2(K^+)_2$	550 s^{-1}	114
$K_{N1}^{i},_{V=0}$	$E1Na^+_3 \leftrightarrow E1Na^+_2 + Na^+$	1.8 mM	100
K_N^i	microscopic dissociation constant for the first 2 Na^+ ions from E1	8 mM	100
$K_{N1}^{o},_{V=0}$	$E2PNa^+_3 \leftrightarrow E2PNa^+_2 + Na^+$	100 mM	98
$K_N^{o},_{V=0}$	microscopic dissociation constant for the last 2 Na^+ ions from E2P	400 mM	103
K_K^i	microscopic dissociation constant for 2 K^+ ions from E1	10 mM	79
K_K^o	microscopic dissociation constant for $2K^+$ from E2P	1.33 mM	101
K_{A1}	$E1ATP \leftrightarrow E1 + ATP$	8 μM	100
K_{A2}	$E2(K^+)_2ATP \leftrightarrow E2(K^+)_2 + ATP$	71 μM	100
$a(K_{N1}^i)$	$E1Na^+_3 \leftrightarrow E1Na^+_2 + Na^+$	-0.25	115
$a(k_2)$	$E1P(Na^+)_3 \rightarrow E2P$	+0.1	98
$a(k_{-2})$	$E2P \rightarrow E1P(Na^+)_3$	-0.1	98

$a(K_{N1}^{o})$	$E2PNa^{+}_{3} \leftrightarrow E2PNa^{+}_{2} + Na^{+}$	+0.65	93, 97, 98
$a(K_{N}^{o})$	dissociation of the last 2 Na^{+} ions from E2P	+0.37*	
$a(k_3)$	$E2P \rightarrow E2(K^{+})_2$	-0.37	114

* This value was chosen to balance the dielectric coefficient of -0.37 determined by Rakowski *et al* [38] for extracellular K^{+} binding and yield on overall transfer of one positive charge into the extracellular medium.

CHAPTER FOUR

INTRODUCTION

Within the Albers-Post formalism, Na^+ ions bind from the cytoplasm to the E1 conformation of the enzyme and, following phosphorylation by ATP and conformational relaxation of the E1P$(Na^+)_3$ state, are released to the extracellular medium from the E2P conformation. K^+ ions then bind from the extracellular medium to the E2P conformation, stimulate dephosphorylation, and are transported to the cytoplasm (Figure 3.1). In the E1P$(Na^+)_3$ state the Na^+ ions are enclosed within the protein and have no direct access to either the cytoplasm or the extracellular fluid, whereas in the E2P state the transport sites are open to the extracellular fluid.

In the simple scheme outlined in figure 3.1 one would expect cytoplasmic Na^+ ions, by promoting phosphorylation, to stimulate pump activity. Extracellular Na^+, on the other hand, would be expected to inhibit the release of Na^+ to the extracellular medium, drive the enzyme from the E2P conformation back towards the E1P$(Na^+)_3$ conformation and compete with K^+ for binding to the E2P state. Because K^+ promotes dephosphorylation of the enzyme much more effectively than Na^+, any decrease in the occupation of the sites on E2P by K^+ would slow down the dephosphorylation step of the cycle. Thus, based on the simple version of the Albers-Post cycle shown in figure 3.1 one would predict that extracellular Na^+ ions should inhibit turnover. However, in earlier work on purified Na^+, K^+ ATPase in native membrane fragments we discovered [113] a stimulation of the enzyme's rate-determining E2 → E1 transition by Na^+ which could not be explained by this scheme.

The Na^+-induced stimulation of the E2 → E1 transition could only be explained by Na^+ binding to the E2 state prior to the enzyme undergoing the transition to the E1 state. On the basis of steady-state activity studies of the effect of the Na^+ concentration on vanadate inhibition, Sachs [121] concluded that cytoplasmic Na^+ doesn't bind to the transport sites of the protein prior to the release of K^+. In the $E2(K^+)_2$ state the K^+ ions are occluded within the protein, with no access of the transport sites to the cytoplasm. Therefore, the Na^+ ions which stimulate the E2 → E1 transition cannot be the same ones which bind in exchange for K^+ on the cytoplasmic face of the protein once the enzyme has already undergone its transition to the E1 state.

While it appeared likely that the acceleration of the E2 → E1 transition was due to Na^+ acting from the extracellular face of the protein no definite conclusion could be reached regarding the side of action because the experiments were conducted using open membrane fragments with simultaneous access of Na^+ to both faces of the protein. Nevertheless, based on kinetic measurements on Na^+, K^+ ATPase reconstituted into lipid vesicles, a number of authors have supported the presence of a Na^+ allosteric site with access from the extracellular medium [122-124]. The site appears, however, to be not very specific for Na^+, with many buffer cations also exhibiting a Na^+-like action in stabilising the E1 conformation relative to the E2 conformation [112,124-132].

The purpose of this study was to investigate the effect of the Na^+ allosteric site on Na^+, K^+ ATPase activity in cardiac myocytes. In particular we aimed to determine from which side of the protein the ions are acting in this cellular system. Furthermore, now that 3D-crystal structural information on the Na^+, K^+ ATPase is

available [81-83,133-135], it is possible to consider where the Na^+ allosteric site within the protein might be.

METHODS

Measurement of electrogenic Na^+, K^+ ATPase current (I_p).

We measured currents (arising from the 3: 2 Na^+:K^+ exchange ratio) in single myocytes using the whole-cell patch clamp technique. The composition of the patch pipette solutions perfusing the intracellular compartment were designed to take into account features of Na^+, K^+ ATPase kinetics. The solution included 20 mM Na^+, a concentration higher than physiological intracellular levels, to obtain a substantial K^+ activated current at 24 °C. Wide-tipped patch pipettes (4-5 μm) were filled with solutions containing (in mM): HEPES 5; MgATP 2; ethylene glycol-bis(β-aminoethyl ether)-N,N,N',N'-tetraacetic acid (EGTA) 5; potassium glutamate 70, sodium glutamate 20 and tetramethylammonium chloride (TMA-Cl) 70. They were titrated to a pH of 7.2 at 24 °C with KOH. In some experiments Na^+ and K^+ concentrations were varied in the pipette solution and the concentration of TMA-Cl was adjusted accordingly to maintain a constant osmolality.

While we were establishing the whole-cell configuration myocytes were superfused with solution containing (in mM): NaCl 140; KCl 5.6; $CaCl_2$ 2.16; $MgCl_2$ 1; glucose 10; NaH_2PO_4 0.44; HEPES 10. It was titrated to a pH of 7.4 at 24 °C with NaOH. Two to three minutes after the whole cell configuration was established we switched to a superfusate that was designed to minimize non-pump membrane currents by blocking current arising from transmembrane K^+ and Ca^{2+} gradients. It was nominally Ca^{2+}, K^+-free and contained 0.2 mM $CdCl_2$ and 2 mM $BaCl_2$. Unless otherwise

indicated, the solution contained 7 mM KCl. The K^+-dependent shift in holding current was used to identify I_p. Control experiments using Na^+ free patch pipette solutions to eliminate pump currents indicated that there were no residual K^+-induced membrane currents at the holding potential of -40 mV used. We measured I_p using Na^+ concentrations in the superfusate ranging from 0 to 140 mM. We included *N*-methyl-D-glucamine to compensate for changes in the Na^+ concentration and hence maintain the osmolality of the extracellular solution. In experiments performed to measure the I-V_m relationship I_p was identified as the shift in holding current induced by Na^+, K^+ ATPase blockade with 200 µM ouabain. Holding currents were recorded during voltage steps of 5 s duration in 20-mV increments to test potentials from −100 to +40 mV. Recordings were averaged from three applications of the voltage-clamp protocol and the holding current was taken as the mean value of currents sampled with an electronic cursor.

All experiments were performed at a temperature of 24 °C, maintained with Warner Instruments automatic temperature controllers and in-line heaters. TMA-Cl and *N*-methyl-D-glucamine were purum grade and were obtained from Fluka Chemicals (Switzerland). All other chemicals used in solutions were analytical grade and were obtained from BDH (Australia).

We used Axoclamp 2A and 2B voltage clamp amplifiers, supported by pClamp version 7 and Axotape version 2 (Axon Instruments, CA, USA) to record currents. Currents were identified as the difference between holding currents with and without 7 mM extracellular K^+, sampled at 20 Hz before and after Na^+, K^+ ATPase activation.

Statistical analysis.

The experimental results are expressed as the means ± S.E. Student's *t* tests for unpaired data were used for the comparison of the mean levels of I_p. Wilcoxon ranked sum test was used to compare the means of the I-V_m curves.

Pump current simulations.

Computer simulations yielded the time course of the concentration of each enzyme intermediate involved, the outward current and the amount of charge transported. For the purposes of the simulations, each enzyme intermediate was normalized to a unitary concentration and the enzyme was assumed arbitrarily to be initially in the E1 state. Each simulation was then carried out until the distribution between the different enzyme states no longer changed and the outward current reached a constant value.

RESULTS

Steady-state pump current measured via the whole-cell patch clamp technique.

Typical whole-cell current recordings are shown in figure 4.1. The steady-state I_p produced by the Na^+, K^+ ATPase in voltage-clamped myocytes as a function of the extracellular Na^+ concentration is shown in Figure 3. There is an increase in I_p with increasing extracellular Na^+ concentration over the range 0 – 50 mM. With an increase in the Na^+ concentration of the pipette solution above 80 mM there was no significant difference in I_p at 0 vs 50 mM extracellular Na^+ (I_p = 0.87 ±0.1 pA/pF, n = 6, vs I_p = 0.92 ±0.12 pA/pF, n = 6, P = 0.76). We also performed experiments in which we maintained the Na^+ concentration in pipette solutions at 20 mM but

eliminated K^+, replaced with TMA-Cl. With elimination of K^+ in the pipette solution there was no significant difference in I_p at 0 vs. 50 mM extracellular Na^+ (I_p = 1.12 ±0.12 pA/pF, n = 5, vs. I_p = 1.28 ±0.09 pA/pF, n = 5, P = 0.31).

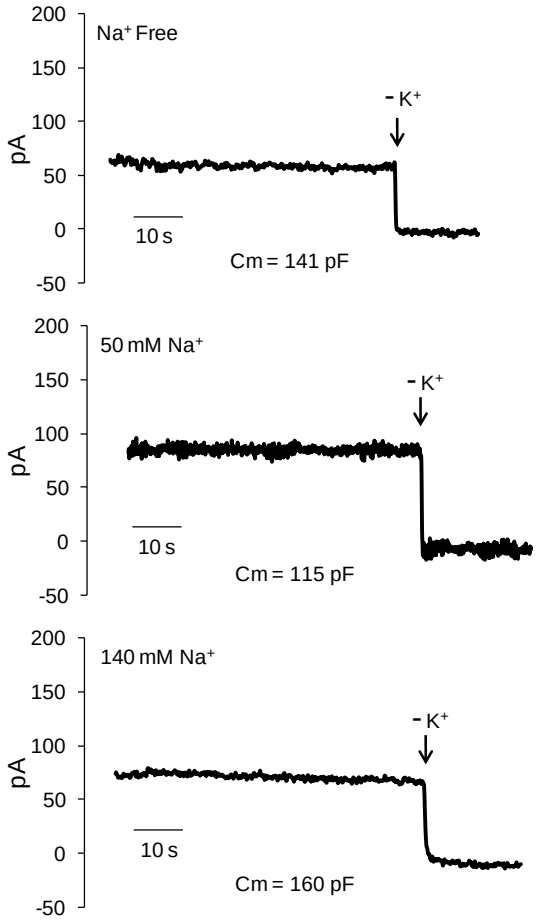

Figure 4.1. Whole-cell current recordings. K^+-sensitive membrane currents recorded in extracellular solutions that were Na^+ free or contained 50 or 140 mM Na^+. Pipette solutions included 20 mM Na^+ and 80 mM K^+. The membrane capacitance (C_m) is included for each recording for comparison. The arrow in each recording indicates the point at which the cardiomyocyte was exposed to K^+ free superfusate. Prior to this point the superfusate included 7 mM K^+.

Since the K^+-sensitive current that identifies I_p here can be affected by competition between K^+ and Na^+ to pump binding sites we performed additional experiments using a high extracellular K^+ concentration of 15 mM. Experiments using this K^+ concentration were performed using Na^+ concentrations of 50 or 140 mM. Since the extracellular transport sites are expected to be completely saturated by K^+ at an extracellular K^+ concentration of 7 mM in the absence of extracellular Na^+, additional experiments at 15 mM extracellular K^+ were not performed in the Na^+-free superfusates. Mean I_p for experiments using 15 mM K^+ have been included in figure 4.2. The K^+-dependent increase between currents recorded at 0 and 50 mM extracellular Na^+ was significant also when 15 mM K^+ was used at the higher Na^+ concentration and the decrease in I_p that occurred when the extracellular Na^+ concentration was increased further to 140 mM appeared qualitatively similar to the decrease that occurred when 7 mM K^+ was used in the superfusate.

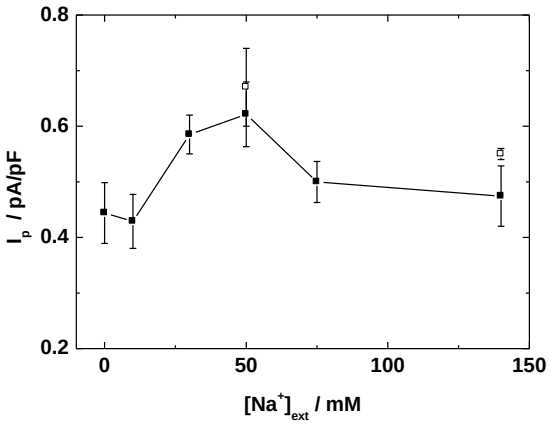

Figure 4.2. Dependence of the Na^+,K^+-pump current of cardiac myocytes (I_p) normalized to the membrane capacitance, on the extracellular Na^+ concentration. Pipette solutions included 20 mM Na^+ and 80 mM K^+. Extracellular solutions included 7 (closed symbols) or 15 mM K^+ (the latter at 50 and 140 mM extracellular Na^+ only). Other experimental conditions were: [ATP] = 2 mM, V = -40 mV, T = 24ºC, pH 7.2.

We examined if the difference in I_p recorded in Na^+-free extracellular solutions and solutions containing 50 mM Na^+ arise from a voltage dependent step in the pump cycle. Myocytes were voltage clamped using Na^+ and K^+ concentrations of 20 and 80 mM, respectively, in the patch pipette solutions. The extracellular K^+ concentration was 7 mM. To eliminate any contamination of the small Na^+, K^+ ATPase currents that might arise from voltage-dependent inwardly rectifying K^+-activated K^+ channels despite use of 2 mM Ba^{2+} in the superfusate we used 200 µM ouabain to inhibit the Na^+, K^+ ATPase. Ouabain in this concentration causes near complete pump blockade in rabbit cardiac myocytes [136]. Holding currents were recorded before and after exposure to ouabain [137]. An example of holding currents used to derive the voltage dependence of pump currents is shown in figure 4.3A. Results of all experiments in Na^+-free solutions and solutions containing 50 mM Na^+ are

summarized in figure 4.3B. The currents recorded in solutions containing 50 mM Na^+ were significantly larger than currents in Na^+-free solutions ($P < 0.01$). To examine if there was a difference in voltage dependence at 0 and 50 mM extracellular Na^+ we normalized currents at the different holding potentials to the current recorded at 0 mV (Figure 4.3C). The normalized data did not support the hypothesis that the difference in I_p between 0 and 50 mM extracellular Na^+ is voltage dependent ($P = 0.21$).

The increase in the enzyme's pump activity with 20 mM Na^+ in the patch pipette solution with an increase in the extracellular Na^+ concentration is not predicted by the simple Albers-Post scheme shown in Figure 3.1, in which only transport sites for Na^+ and K^+ are considered. Based on this scheme the only effect one would expect is an inhibition by extracellular Na^+. Extracellular Na^+ is expected to compete with extracellular K^+ ions at the transport sites on the E2P conformation.

The coupled equilibria describing the competition between extracellular Na^+ and K^+ ions for the transport sites on the E2P state of the enzyme can be found in Figure 3.2 of Chapter 3. This scheme incorporates the generally accepted hypothesis of two transport sites, which can be occupied with different affinities by Na^+ and K^+, plus a single site which is specific for Na^+. To demonstrate the expected dependence of I_p on the extracellular Na^+ concentration based on this scheme, we have performed calculations described in the following section, with the mathematical details given in the Appendix of this Chapter.

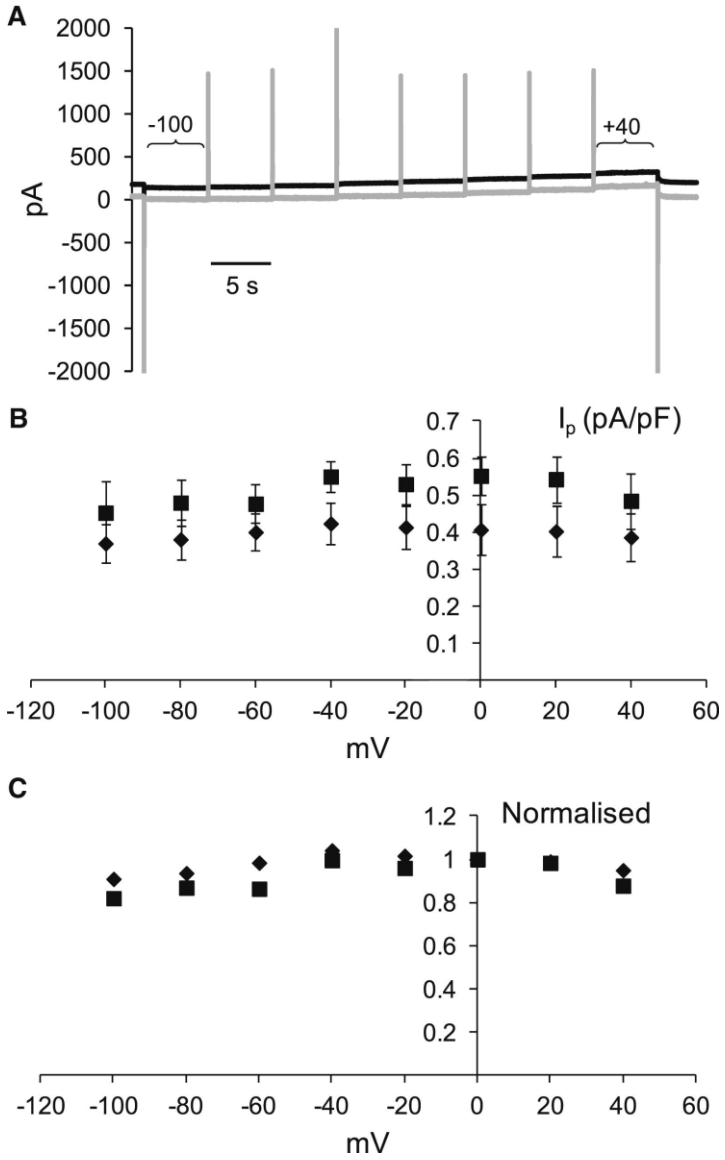

Figure 4.3. Voltage dependence of the Na^+,K^+-pump current at 0 and 50 mM extracellular Na^+. A. Examples of holding currents before (black trace) or after (grey trace) exposure of a myocyte to 200 µM ouabain. Pipette solutions included 20 mM Na^+ and 80 mM K^+. The holding potential was stepped from -40 to -100 mV at the beginning of the traces and then in 20 mV increments to +40 mV at the end of the traces before returning to -40 mV. I_p at each potential was identified as the difference in current recorded before and after exposure to ouabain. B. Voltage dependence of mean I_p at either 50 mM (■) or 0 mM extracellular Na^+ (♦). Currents recorded at 0 mM extracellular Na^+ were significantly larger than currents at 0 mM Na^+ (Wilcoxon's

replicate rank test). C. Mean I_p normalized to I_p recorded at 0 mV. Voltage dependence of the normalized currents was not statistically significant (P = 0.21, Wilcoxon's replicate rank test).

Modelling of heart Na^+, K^+ ATPase transported charge-voltage behaviour.

Under experimental conditions which are not too far removed from physiological conditions the complex Albers-Post cycle describing the Na^+, K^+ ATPase's partial reactions can be reduced to the simpler 4-state model shown in figure 3.1. We have used this simple model to describe current-voltage behaviour of the Na^+, K^+ ATPase previously [137]. The mathematical detail of the model and the assumptions on which it is based are described in detail there. Here we describe only the essential points of the model. $E1P(Na^+)_3$ and $E2(K^+)_2$ represent here occluded states of the protein. In contrast, E1 and E2P represent states in which the ion binding sites have access to the cytoplasm and the extracellular fluid, respectively. In the case of the non-occluded states, we assume that rapid exchange of Na^+ and K^+ between the binding sites and either the cytoplasm or the extracellular fluid can occur. Thus, in the case of the E2P state we assume that there is a rapid exchange of Na^+ ions and K^+ ions between the extracellular fluid and two of the ion transport binding sites. The stoichiometry of the Na^+, K^+ ATPase is $3Na^+/2K^+/ATP$. One of the ion binding sites is considered to be specific for Na^+, whereas Na^+ or K^+ can both bind with differing affinities to the other two. Thus, we treat ion binding to E2P as a series of coupled equilibria, as shown in Figure 3.2 of Chapter 3. An analogous scheme can be drawn for the E1 state. Only the kinetics of the four major rate-determining reactions shown in Figure 3.1 is explicitly considered. We consider that each of the four rate-determining reactions only reaches its maximum observable rate when the reactant state is fully saturated by the appropriate substrates.

Because the enzyme pumps three Na^+ ions in exchange for two K^+ ions in, there is a net transport of one positive charge out of cells. Thus, the overall steady-state

turnover of the enzyme equals the outward flux of ions, and can be easily converted to an outward current. The voltage dependence of the charge-translocating reaction steps is taken into account by Boltzmann terms, as previously described in Chapter 3. The numerical simulation procedure outlined in Chapter 3 allows the time dependence of any changes in pump current to be calculated following rapid perturbations, e.g. due to a voltage jump, as well as the steady-state.

If one only wishes to calculate the steady-state pump currents, the differential rate equations describing the rate of change of each enzyme intermediate (shown in the Appendix of this Chapter) are all equal to zero. Therefore, in principle, if one makes use of the mass conservation law that the total concentration of the enzyme intermediates is constant, the coupled series of differential equations reduces to a series of simultaneous equations which can be solved analytically to obtain a single equation that allows the pump current to be calculated under varying experimental conditions. However, because of the complex reaction mechanism, the resultant equation for the pump current is unwieldy, and we only present the mathematics for the numerical solution here. Whether one uses a numerical procedure or the analytical solution to the simultaneous equations, the results of the calculations are identical. An advantage of the numerical procedure is that by integration of the time-dependent pump current, the amount of charge transported by the Na^+, K^+ ATPase can be calculated. We will use this feature of the numerical model to compare with experimental voltage-jump data.

The kinetic and equilibrium parameters used for modelling of the outward sodium pump current, I_p, in Chapter 3 were derived from measurements on purified mammalian kidney enzyme. Significant differences existed between the experimentally observed current-voltage behaviour of heart muscle Na^+, K^+ ATPase

in intact cardiac myocytes and the predicted behaviour of kidney Na^+, K^+ ATPase. In particular, the kidney enzyme displayed significantly lower voltage dependence of the pump current at a physiologically relevant extracellular Na^+ concentration of 150 mM.

The comparison between the heart and kidney enzymes demonstrates that, if one wishes to simulate the behaviour of heart Na^+, K^+ ATPase, modifications to the rate or equilibrium parameters used in the model must be made. The steep positive slope in the I_p-V_m curve of the heart enzyme over the membrane voltage range -120 to 0 mV has its origin in Na^+ competition for transport sites on the E2P state. To determine more reliable values for the equilibrium dissociation constants of describing the interaction of Na^+ with the E2P state, we have compared the results of simulations of the total charge transported by the Na^+, K^+ ATPase following a voltage jump with experimental results obtained by Peluffo [138] using rat cardiac myocytes. Because the experiments were performed in the absence of extracellular K^+, the comparison allows us to estimate the Na^+ dissociation constants without any competition from K^+. Peluffo's experimental data is reproduced in figure 4.4 together with the simulations based on our kinetic model. Good agreement between the experimental data and the simulations was achieved. To obtain this agreement it was necessary to significantly reduce the Na^+ dissociation constants of the E2P state relative to the values previously determined for the kidney enzyme. The microscopic dissociation constant for interaction of Na^+ with the two nonspecific sites at a membrane potential of 0 mV, K_{No}, was reduced from 400 mM (kidney) to 180 mM (heart). Similarly, the dissociation constant for interaction of Na^+ with the specific Na^+ site, K_{N1o}, was reduced from 100 mM (kidney) to 40 mM (heart).

A direct quantitative comparison of the actual amounts of charge transported experimentally and that calculated from the model is not possible, because the total charge transported depends on the number of Na^+, K^+ ATPase molecules expressed per cell, which depends on the size of the cell. To account for varying cell sizes Peluffo [138] divided the measured current by the capacitance of each cell, which should be proportional to the cell surface area. Thus, his measured current in units of femto-Coulombs per pico-Farad should be proportional to the current per pump molecule, which is the quantity we calculate in our simulations.

To judge the agreement between the experimental data and the simulated results it is important to look at the plateaus in charge transported after voltage jumps to very high positive or very low negative potentials. If the magnitudes of these plateaus are equal, at the extracellular Na^+ concentration corresponding to this situation the enzyme is half-saturated by Na^+, i.e., the number of bound Na^+ ions capable of being released on shifting to inside-positive potentials equals the number of available binding sites and hence the number of free Na^+ ions capable of binding on shifting to inside-negative potentials. Although only three different extracellular Na^+ concentrations were measured by Peluffo [138], the results indicate that the half-saturating Na^+ concentration is in the range 72.5 – 145 mM, probably closer to the 72.5 mM than 145 mM.

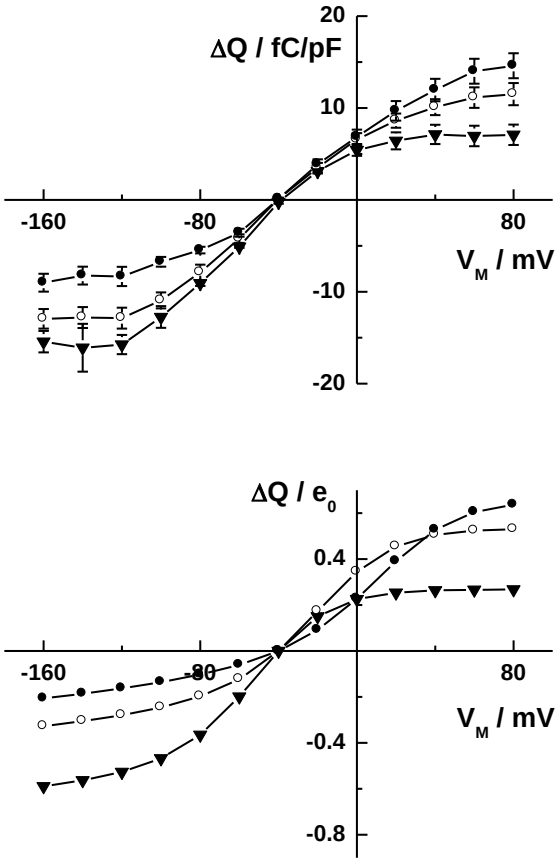

Figure 4.4. Dependence of the Na^+,K^+-ATPase transported charge-voltage relationship (ΔQ-V curve) on the extracellular Na^+ concentration after voltage jumps from the membrane voltage V_m to -40 mV. Each symbol corresponds to the following Na^+ concentrations: 36.3 mM (▼), 72.5 mM (○) and 145 mM (●). The solid lines between the points have been drawn to aid the eye.

Upper curve: Experimental results for rat heart myocytes, obtained via the voltage clamp technique, reproduced from Figure 3C of Peluffo [138]. The transported charge, ΔQ, has been divided by the capacitance of each cell to correct for variations in cell size. The experimental conditions were cytoplasmic [Na^+] = 120 mM, cytoplasmic [K^+] = extracellular [K^+] = 0 mM, cytoplasmic [ATP] = 15 mM, T = 23ºC.

Lower curve: Computer simulations of the ΔQ-V curve for mammalian heart Na^+, K^+ ATPase current based on the Albers-Post scheme described by Figs. 3.1 and 3.3 and the kinetic and equilibrium parameters given in Table 3.1 of Chapter 3, except that a microscopic dissociation constant of Na^+ for the nonspecific transport sites on E2P state of 180 mM and a dissociation constant of Na^+ to the specific site on E2P of 40 mM have been used. The ion concentrations, ATP concentration and temperature used for the simulations were the same as for the upper curve.

Modelling of heart Na^+,K^+ ATPase current-voltage behaviour.

We extended the modelling to competition between Na^+ and K^+ for the transport sites and thus estimate the E2P microscopic dissociation constant for K^+ of the heart enzyme. For this purpose we compare with the experimental steady-state pump current data for heart Na^+, K^+ ATPase reported by Nakao and Gadsby [27]. We showed previously in Chapter 3 that it was not possible to adequately reproduce the current-voltage ($I\text{-}V_m$) behaviour reported by Nakao and Gadsby [27] if we used equilibrium dissociation constants for the E2P state derived from measurements on kidney enzyme. We changed the values of K_{No} and K_{N1o} from 400 mM and 100 mM derived from the kidney enzyme to 180 mM and 40 mM, the values derived from the comparison with Peluffo's data in the previous section, and have then varied the value of K_{Ko} (the microscopic dissociation constant of K^+ with the E2P state at a membrane potential of 0 mV) until we obtained the best reproduction of experimental behaviour.

Nakao and Gadsby's experimental data together with the results of the simulations showing the closest agreement with their data are shown in figure 4.5. To achieve this agreement we increased the value of K_{Ko} slightly from 1.33 mM (kidney value) to 1.8 mM. The higher value of K_{Ko} together with the lower values of K_{No} and K_{N1o} relative to the values obtained using enzyme derived from mammalian kidney, indicates that Na^+ competes with K^+ much more strongly for binding to the E2P state in the heart enzyme than the kidney enzyme. Because binding/release of Na^+ to the specific site on E2P is the major charge-transporting step of the Na^+, K^+ ATPase pump cycle, the stronger competition from Na^+ ions explains the much greater

voltage dependence of the heart enzyme's steady-state turnover than that predicted for the kidney enzyme.

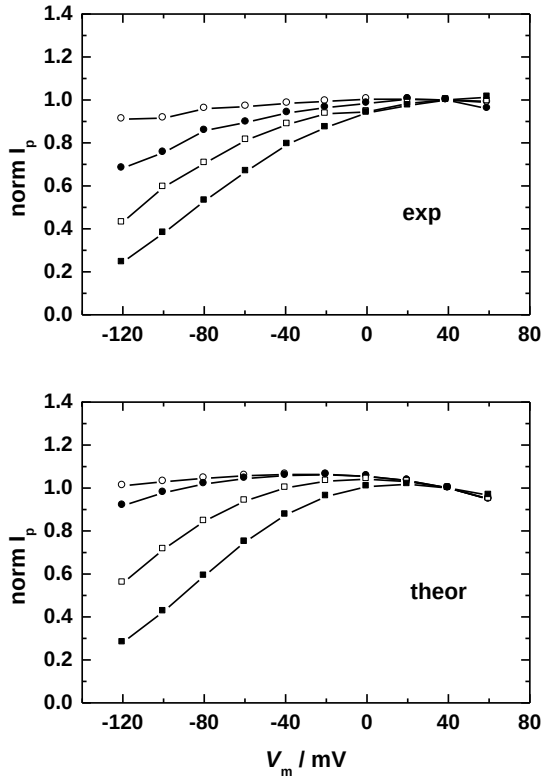

Figure 4.5. Dependence of the Na^+, K^+ ATPase current-voltage relationship (I-V_m curve) on the extracellular Na^+ concentration. Symbols correspond to the Na^+ concentrations of 1.5 mM (○), 50 mM (●), 100 mM (□) and 150 mM (■). The solid lines between the points have been drawn to aid the eye.

Upper curve: Experimental results for guinea pig heart ventricular myocytes, obtained via the whole-cell patch clamp technique, reproduced from Figure 3 of Nakao and Gadsby [27]. The pump current, I_p, of each curve has been normalized to the value at a holding potential of + 40 mV. The experimental conditions were cytoplasmic [Na^+] = 50 mM, cytoplasmic [K^+] = 0 mM, extracellular [K^+] = 5.4 mM, cytoplasmic [ATP] = 10 mM, T = 36ºC.

Lower curve: Simulations of the I-V curve for mammalian heart Na^+,K^+-ATPase pump current based on the Albers-Post scheme described by Figs. 1 and 3 and the kinetic and equilibrium parameters given in Table 1 of Chapter 3, except that a microscopic dissociation constant of K^+ for the E2P state of 6.2 mM has been used and the dielectric coefficients of binding of both Na^+ and K^+ to this state have been reduced to 0.1. The ion concentrations, ATP concentration and temperature used for the simulations were the same as for the upper curve.

Modelling of the extracellular Na^+ concentration dependence of I_p.

Now that we have a kinetic model based on the Albers-Post scheme capable of reproducing data from the literature on the transported charge- and current-voltage behaviour of heart Na^+, K^+ ATPase, we can test whether this model explains the experimentally observed dependence of I_p on the extracellular Na^+ concentration shown in figure 4.2. Calculations of the expected dependence of the pump current, I_p, per pump molecule on the extracellular Na^+ concentration based on the Albers-Post model are shown in figure 4.6 (dotted line). Based on the values of the dissociation constants for extracellular K^+ and Na^+ interaction with the transport sites derived from the data of Peluffo [138] and Nakao and Gadsby [27] in the previous two sections, it is apparent that the Albers-Post model only predicts a monotonic decrease in steady-state activity of around 2 – 3 % between 0 and 150 mM Na^+ if one only considers interaction of extracellular Na^+ with the enzyme's transport sites. This is not in agreement with the experimental results (Figure 4.1), which show an increase in activity between 0 and 50 mM. For these calculations we have used a value of the rate constant, k_4, of the $E2(K^+)_2 \rightarrow E1$ transition of 18 s^{-1}. This value is based on the finding of Humphrey *et al* [113] on purified enzyme that Na^+ ions cause a roughly 5-fold increase in the rate constant of this reaction and the finding of Lüpfert

et al [112] that at physiological levels of Na^+, Mg^{2+} and ATP the reaction occurs with a rate constant of around 90 s^{-1}.

To account for the increase in pump current experimentally observed we have expanded the Albers-Post model to incorporate extracellular Na^+ binding to an allosteric site and an associated acceleration of the E2 → E1 conformational transition, as indicated by kinetic experiments on purified enzyme [113]. The extensions and changes to the mathematics necessary for these calculations are described in the Appendix of this chapter. Based on the kinetic results on purified enzyme [113] we have used a dissociation constant for the interaction of Na^+ with the allosteric site, K_{allo}, of 31 mM. The results of the simulations, utilizing the values of K_{Ko} = 1.8 mM, K_{No} = 180 mM, and K_{N1o} = 40 mM derived from the simulations of Peluffo's [138] and Nakao and Gadsby's [27] data, are shown in figure 4.6 (dashed line). The model predicts a roughly hyperbolic increase in the pump current over the 0 – 50 mM extracellular Na^+ concentration range. At Na^+ concentrations above 100 mM there is a very gradual drop in pump current, i.e., qualitatively in agreement with the experimental observations (Figure 4.2). Therefore, the experimental results are consistent with the existence of an allosteric activating Na^+ site with access from the extracellular medium. The drop in I_p at high extracellular Na^+ concentrations is, however, much more pronounced than that predicted by the model (Figure 4.6). However, if the values of K_{No} and K_{N1o} are decreased to 68 mM and 15 mM, respectively, a significant drop in I_p is observed over the Na^+ concentration range 50 – 150 mM, i.e., in much closer agreement with the experimentally observed behaviour (Figure 4.2). Therefore, it appears likely that competition from Na^+ for binding to the extracellular transport sites on the E2P state of the enzyme is much

stronger in the rabbit cardiac myocytes used in our study in comparison to the guinea pig myocytes used by Nakao and Gadsby [27].

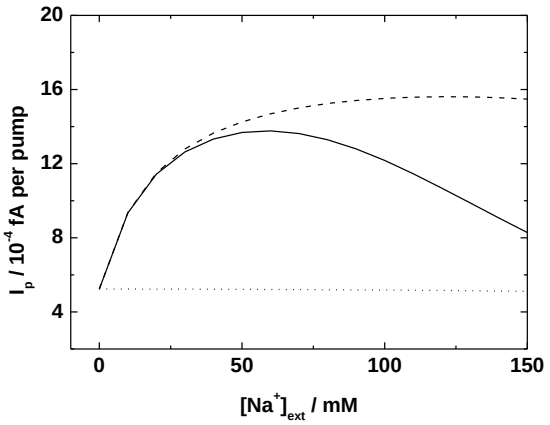

Figure 4.6. Simulations of expected dependence of Na^+, K^+ ATPase current, I_p, per pump molecule on the extracellular Na^+ concentration based on the Albers-Post model (dotted line, K_{Ko} = 1.8 mM, K_{No} = 180 mM, and K_{N1o} = 40 mM) and an expanded Albers-Post model incorporating extracellular allosteric Na^+ binding (dashed line, K_{Ko} = 1.8, K_{No} = 180 mM, and K_{N1o} = 40 mM). The solid line also represents a simulation based on the same model incorporating allosteric Na^+ binding, but with reduced dissociation constants for extracellular Na^+ interaction with the transport sites (K_{Ko} = 1.8 mM, K_{No} = 68 mM, and K_{N1o} = 15 mM). The experimental conditions used for the simulations were identical to those of the actual experiments (see legend for Figure 4.2).

DISCUSSION

Much information regarding the molecular mechanism of Na^+, K^+ ATPase has been gained by studies of the purified protein, either in the form of enzyme-containing membrane fragments or reconstituted into synthetic lipid vesicles. However, the goal of any mechanistic work on the Na^+, K^+ ATPase must be to understand how the enzyme works in a living cell, and it is crucial that any discoveries made on purified Na^+, K^+ ATPase be reconciled with studies on the enzyme in situ in intact cells. Apart from this fundamental point, experiments on cells have the additional advantage over studies of Na^+, K^+ ATPase-containing membrane fragments that the cytoplasm and the extracellular medium are separated by the plasma membrane, allowing the side of action of the enzyme's substrates to be identified. Synthetic vesicles are sided preparations, but, in the case of small unilamellar vesicles generally used for reconstitution, their internal volume is much less than that of cells and it is impossible with vesicles to reproduce the natural membrane composition of a living cell. Therefore, the relevance of results obtained on the Na^+, K^+ ATPase using lipid vesicles for the enzyme in a cell always needs to be examined.

Because the Na^+, K^+ ATPase pumps Na^+ ions from the cytoplasm into the extracellular fluid, increased concentrations of extracellular Na^+ must inhibit its pumping activity, a simple example of product inhibition. However, studies on purified enzyme has suggested that extracellular Na^+ can also stimulate ion pumping by acting at an allosteric site [112,113,122-127,129-132,139]. Our results on whole cells confirm that prediction. This increase cannot be explained by Na^+ acting on transport sites alone and implicates the existence of a separate allosteric Na^+ site.

A logical question to ask, however, would be why no evidence for an extracellular allosteric Na^+ site was apparent in the results reported by Nakao and Gadsby [27], reproduced in figure 4.5. A likely explanation is that they used a higher Na^+ concentration of 50 mM in their patch pipette in comparison to 20 mM in the experiments shown in figure 4.2. In our study on increasing the cytoplasmic Na^+ concentration or eliminating the cytoplasmic K^+ concentration there was no longer a statistically significant increase in I_p with increasing extracellular Na^+ concentrations from 0 to 50 mM, which we attribute to extracellular allosteric Na^+ binding.

If the increase in I_p due to extracellular Na^+ is caused by an increase in the flux through the $E2(K^+)_2 \rightarrow E1$ transition, as measurements on purified enzyme suggest [113], then the disappearance of the effect of extracellular allosteric Na^+ site at high cytoplasmic Na^+ concentrations or low cytoplasmic K^+ concentrations implies a decrease in the contribution of the $E2(K^+)_2 \rightarrow E1$ transition to rate-determination of the entire pump cycle. Thus, the $E2(K^+)_2 \rightarrow E1$ transition must already be so fast that any increase in its rate has negligible effect on the enzyme's turnover. To understand how this might come about one should consider what effects an increase in the cytoplasmic Na^+ concentration or a decrease in the cytoplasmic K^+ concentration could have on the individual partial reactions of the enzyme.

An increase in the cytoplasmic Na^+ concentration would accelerate the phosphorylation reaction, $E1 \rightarrow E1P$, but this would tend to increase the contribution of the $E2(K^+)_2 \rightarrow E1$ transition towards overall rate determination of the pump cycle and hence one would expect an enhanced effect of extracellular Na^+ on I_p rather than the decreased effect experimentally observed. However, an increase in the cytoplasmic Na^+ concentration would also increase the degree of competition of Na^+ over K^+ for binding to the transport sites on E1. This would decrease the rate of the

backward reaction $E1K^+_2 \rightarrow E2(K^+)_2$ and, thus, increase the net flux in the forward direction $E2(K^+)_2 \rightarrow E1$.

A decrease in the cytoplasmic K^+ concentration would be expected to have the same effect as an increase in the cytoplasmic Na^+ concentration. The result of this would be a decrease in the contribution of the E2 → E1 transition to overall rate determination and a reduction in the allosteric effect of extracellular Na^+. The experimental results that the allosteric effect of extracellular Na^+ diminishes either on increasing the cytoplasmic Na^+ level or decreasing the cytoplasmic K^+ level indicates that for the heart enzyme the decrease in the rate of the backward reaction $E1K^+_2 \rightarrow E2(K^+)_2$ must dominate over the increase in rate of the E1 → E1P reaction by cytoplasmic Na^+. It is in fact likely that in the experiments performed by Nakao and Gadsby [27] there would have been very little competition to Na^+ binding to the E1 state, because they replaced K^+ with Cs^+ ions which compete with Na^+ with an approx. ten-fold higher $K_{1/2}$ than K^+ [140] Although not quantitatively the same, it is also worth mentioning that the theoretical model predicts the decrease in the allosteric effect of extracellular Na^+ at increasing intracellular Na^+ concentrations or decreasing intracellular K^+ concentrations. At an intracellular Na^+ concentration of 20 mM, the model predicts an increase in the relative value of I_p between 0 and 50 mM extracellular Na^+ of 172%. If the intracellular Na^+ concentration is increased to 80 mM, the model predicts that the increase in I_p over the same extracellular Na^+ concentration range should drop to 126%. If the intracellular K^+ concentration is decreased to zero, the model predicts that the increase in I_p over the same extracellular Na^+ concentration should drop to 93%.

From a consideration of recently published crystal structures of the Na^+, K^+ ATPase [81-83,133-135], we have identified a possible site of allosteric Na^+ binding. Based on the

sequence numbering of the shark enzyme (pdb 2ZXE), it seems that the Na^+ ion could possibly bind to the sequence of acidic amino acid residues Glu122, Asp123, Glu124 and Asp128. These residues are located in a cleft between the α- and β-subunits of the protein which has access from the extracellular medium. That this cleft has functional importance for the protein is evidenced by the fact that it is also occupied by the specific Na^+, K^+ ATPase inhibitor ouabain [83,133]. It is worthwhile pointing out that, based on X-ray crystallographic data, Ekberg *et al* [141] recently identified Asp92 and Asp95 as being involved in cation binding on the extracellular face of the plasma membrane H^+ ATPase, another P-type ATPase closely related to the Na^+, K^+ ATPase. These amino acid residues are in homologous positions to those which we suggest may be involved in extracellular allosteric Na^+ binding in the Na^+, K^+ ATPase. Based on the effects of mutations on the kinetics of partial reactions, amino acid residues in homologous positions have also been implicated [142] in extracellular ion binding in the sarcoplasmic reticulum Ca^{2+} ATPase.

I_p over the 0 – 50 mM extracellular Na^+ concentration range was only weakly voltage dependent and not significantly different between 0 and 50 mM Na^+ (Figure 4.3). This is consistent with the expectation that the major voltage-dependent step of extracellular Na^+ rebinding to E2P is not rate-limiting under the conditions of these experiments nor is K^+ occlusion by E2P, whose observed rate is dependent on the degree of occupation of the transport sites on E2P by K^+. At intracellular Na^+ and K^+ concentrations of 20 and 80 mM, the forward $E2(K^+)_2 \rightarrow E1K^+_2$ and backward $E1K^+_2 \rightarrow E2(K^+)_2$ are major reactions determining the overall forward reaction rate and hence I_p. The absence of significant voltage dependence also indicates that binding of Na^+ to the extracellular allosteric site we invoke is not voltage dependent, i.e. the allosteric site is not buried within the transmembrane domains of the protein.

Finally, it is interesting to speculate if allosteric Na^+ binding has a role in regulation of cell Na^+. At a normal physiological extracellular Na^+ concentration of ~140 mM the Na^+ allosteric site should be nearly fully occupied and hence unlikely to have a regulatory role. It might simply be an evolutionary adaptation of the enzyme to optimize its activity under normal physiological conditions in the presence of a relatively high concentration of extracellular Na^+ and to compensate for any inhibition which would arise from extracellular binding to the ion transport sites. However, the allosteric site might also have a role under pathophysiological conditions of low extracellular Na^+. Extracellular concentrations as low as ~100 mM can be encountered in severe hyponatremia in humans. Due to an associated decrease in inward passive Na^+ leak this decreases the intracellular Na^+ concentration [143]. The decrease in intracellular concentration arising from decreased leak would be amplified if the low extracellular Na^+ increases the occupation of the transport sites on E2P by K^+ and hence increases forward Na^+, K^+ ATPase rate. At an extracellular Na^+ concentration of 100 mM and above the contribution of K^+ occlusion by E2P to overall rate determination is expected to be enhanced in cardiac myocytes [136]. The allosteric site is expected to reduce such an acceleration of pump rate in hyponatremic states (Figure 4.6) and may therefore serve in a the tight control of intracellular Na^+ to optimize cell function.

APPENDIX

Calculation of the steady-state pump current.

Simple Albers-Post model.

Extracellular Na^+ can have two possible effects on the ion pumping activity of the Na^+, K^+ ATPase:

1) By (re-)binding to the transport sites on the E2P state, Na^+ can inhibit pump activity,

2) By binding to an allosteric site, Na^+ can stimulate the E2 → E1 transition and increase pump activity.

Because these two effects involve widely separated reactions of the Albers-Post cycle, the only quantitative way to consider the influences they would both have on the overall steady-state pump current is to carry out calculations of the entire pump cycle.

Based on the four-state Albers-Post model of the Na^+, K^+ ATPase enzymatic cycle shown in figure 3.1, the differential rate equations describing the changes in concentrations of all the enzyme intermediates are:

$$\frac{d[E1]}{dt} = -k_1 f(3Na_i) f(ATP_{E1})[E1] + k_4 f(ATP_{E2})[E2] - k_{-4} f(2K_i) f(ATP_{E1})[E1] \quad (1)$$

$$\frac{d[E1P]}{dt} = -k_2[E1P] + k_1 f(3Na_i) f(ATP_{E1})[E1] + k_{-2} f(3Na_o)[E2P] \quad (2)$$

$$\frac{d[E2P]}{dt} = -k_3 f(2K_o)[E2P] - k_{-2} f(3Na_o)[E2P] + k_2[E1P] \quad (3)$$

$$\frac{d[E2]}{dt} = -k_4 f(ATP_{E2})[E2] + k_3 f(2K_o)[E2P] + k_{-4} f(2K_i) f(ATP_{E1})[E1] \quad (4)$$

In these equations the term $f(3Na_i)$ represents the fraction of enzyme in the E1 state occupied by 3 Na^+ ions, which is determined by the current cytoplasmic Na^+ and K^+ concentrations and the binding affinities of the ion sites. Similarly $f(ATP_{E1})$ represents the fraction of enzyme in the E1 state occupied by ATP. The significance of these *f*-terms can be easily understood if we take the phosphorylation reaction as an example. The maximum rate constant for phosphorylation, k_1, is only achieved when the E1 state of the enzyme is completely saturated by $3Na^+$ ions and one ATP molecule. Thus the observed rate constant, k_1^{obs}, for the reaction is given by k_1 multiplied by the probability that E1 has 3 bound Na^+ ions (= $f(3Na_i)$) and by the probability that E1 has a bound ATP molecule (=$f(ATP_{E1})$). This simple mathematical formulation of the rates will break down at very low cytoplasmic Na^+ and ATP concentrations, when second-order binding of the substrates to the enzyme becomes slower than the following first-order phosphorylation and occlusion of Na^+. However, under normal physiological conditions the assumption of rapid binding equilibria, on which equations (1) - (4) and the 4-state scheme shown in figure 3.1 are based, can be considered a good approximation.

Also appearing in equations (1) – (4) are the fraction of enzyme in the E2 state with ATP bound, $f(ATP_{E2})$, the fraction of enzyme in the E2P state with 3 Na^+ ions bound, $f(3Na_o)$, the fraction of enzyme in the E2P state with 2 K^+ ions bound, $f(2K_o)$ and the fraction of enzyme in the E1 state with 2 K^+ ions bound, $f(2K_i)$. In a similar way to that described for the phosphorylation reaction, these fractions or probabilities modify the observed rate constant for each relevant reaction step, as shown in eqs. (1) – (4). Since in our model we consider all of the substrate binding reactions to be equilibria, the *f*-terms are determined solely by the substrate concentrations and the relevant equilibrium (or dissociation) constants of each substrate. Equations for all of the *f*-terms are given in the Appendix of Chapter 3.

Based on the model, the transient outward current due to the Na^+, K^+ ATPase at any moment in time, $I_p(t)$, is given by:

$$I_p(t) = k_2[E1P] - k_{-2} f(3Na_o)[E2P] \qquad (5)$$

Thus, eqs. (1) – (4) and (5) represent a coupled series of equations which can be solved numerically to derive the value of $I_p(t)$ at any combination of ion and ATP concentrations.

Once a steady-state has been reached, $I_p(t)$ represents the flux through the reaction E1P → E2P, in which Na^+ ions are released to the external medium, and is hence equal to the turnover of the enzyme. The amount of charge transported by the Na^+, K^+ ATPase across the membrane can also be calculated by integrating $I_p(t)$ with respect to time.

Expanded Albers-Post model including extracellular allosteric Na^+ binding.

To take into account the effect of extracellular allosteric Na^+ binding on the steady-state pump current requires some relatively small modifications to the basic model. Because experimental evidence on purified enzyme indicates [113] that extracellular Na^+ accelerates the $E2(K^+)_2 \rightarrow E1$ conformational transition, the differential rate equations describing the change in concentrations of the E1 and E2 states, i.e. eqs. (1) and (4), need to be changed. The modified equations are:

$$\frac{d[E1]}{dt} = -k_1 f(3Na_i) f(ATP_{E1})[E1] + (k_4^{\min} f(ATP_{E2}) + (k_4^{\max} - k_4^{\min}) f(ATP_{E2}) f(Na_o^{allo}))[E2] \\ -k_{-4} f(2K_i) f(ATP_{E1})[E1] \qquad (6)$$

$$\frac{d[E2]}{dt} = -(k_4^{\min} f(ATP_{E2}) + (k_4^{\max} - k_4^{\min}) f(ATP_{E2}) f(Na_o^{allo}))[E2] + k_3 f(2K_o)[E2P] \\ +k_{-4} f(2K_i) f(ATP_{E1})[E1] \qquad (7)$$

In these two equations $k_4^{\max}$ represents the maximum value of the rate constant for the $E2(K^+)_2 \rightarrow E1$ transition when the extracellular Na^+ allosteric site is fully occupied by Na^+ and simultaneously the low affinity ATP site on E2 is fully occupied by ATP. Similarly, $k_4^{\min}$ represents the minimum value of the rate constant for the same transition when the extracellular Na^+ allosteric site is completely free of Na^+ but the

low affinity ATP site on E2 is still fully occupied by ATP. The term $f(Na_o^{allo})$ in eqs. (6) and (7) represents the fraction of Na^+ allosteric sites occupied by Na^+. It is given by:

$$f(Na_o^{allo}) = ([Na^+]_o / K_{allo}) / (1 + [Na^+]_o / K_{allo}) \quad (8)$$

K_{allo} is here the dissociation constant of the extracellular allosteric Na^+ site.

CHAPTER FIVE

INTRODUCTION

With the whole-cell patch clamp technique [35], extensively used to study functional properties of the pump in cardiac myocytes I_p is identified as the difference in membrane current recorded with and without blockade of the pump by exposure of myocytes to a cardiac glycoside or to K^+-free extracellular solutions. Many studies have reported that when voltage clamped cardiac myocytes are re-exposed to K^+ after a period of pump inhibition in K^+-free solutions, a rapid increase in I_p is recorded followed by a decrease to a new steady state level. The transient peak current is attributed to the outward pumping of Na^+ that accumulated in a diffusion-restricted space near the inner membrane leaflet while the pump was inhibited [59]. A sub-sarcolemmal space with restricted diffusion for Na^+ has important cardiac physiological, pathophysiological and therapeutic implications [67,144,145] and restricted Na^+ diffusion has become included in mathematical models of the cardiac action potentials [146,147], for example used to predict effects of drugs in the setting of disease process and for screening for efficacy and potential adverse effects [148,149].

While restricted diffusion of Na^+ in a sub-sarcolemmal space in principle might provide an explanation for the K^+-activated transient peak current in cardiac myocytes after exposure to K^+-free solutions, the diffusion rate for Na^+ near the membrane relative to the bulk phase of the cytosol would have to be dramatically reduced relative to diffusion in the bulk phase of the cytosol to account for accumulation of Na^+ [150]. Physical barriers to account for such restricted diffusion have not been identified. We have examined if K^+-induced Na^+, K^+ ATPase activity initially might be enhanced because glutathionylation of the pump's β_1 subunit

decreases during the period in K^+-free extracellular solutions. Glutathionylation of the β_1 subunit is causally related to inhibition of activity [151] and susceptibility to glutathionylation depends on the pumps conformational poise during the catalytic cycle [102]. The poise must depend on the transmembrane gradients of Na^+, K^+ ATPase ligands and we hypothesized that there is a decrease in glutathionylation during exposure to K^+-free extracellular solutions. This would cause Na^+, K^+ ATPase activity to be enhanced with initial K^+-induced reactivation. According to this scheme a subsequent decline in activity would then be due to re-glutathionylation to a new steady state level during turnover.

METHODS

Measurement of electrogenic Na^+, K^+ ATPase current (I_p) in myocytes.

We measured I_p in single myocytes using the whole-cell patch clamp technique. In most experiments wide-tipped patch pipettes (4-5 μm) were filled with solutions containing (in mmol/L): HEPES 5; MgATP 2; ethylene glycol-bis(β-aminoethyl ether)-N,N,N',N'-tetraacetic acid (EGTA) 5; potassium glutamate 70, sodium glutamate 20 and tetramethylammonium chloride (TMA-Cl) 70. They were titrated to a pH of 7.2 at 25 °C with KOH. In experiments that varied the pipette concentrations of Na^+ or K^+ we adjusted the concentration of TMA-Cl to maintain constant osmolality. Human recombinant glutaredoxin 1 (Grx1, 10 μg/mL), and superoxide dismutase (SOD, 200 IU/ml) or apocynin (100 μmol/L) were included in pipette solutions when indicated.

While we established the whole-cell configuration myocytes were superfused with solution containing (in mmol/L): NaCl 140; KCl 5.6; $CaCl_2$ 2.16; $MgCl_2$ 1; glucose 10; NaH_2PO_4 0.44; HEPES 10. It was titrated to a pH of 7.4 at 25 °C with NaOH. Two to three minutes after the whole cell configuration was established we switched to a

superfusate designed to minimize non-pump membrane currents. It was nominally Ca^{2+}-free and contained 0.2 mmol/L $CdCl_2$ and 2 mmol/L $BaCl_2$. Na^+-K^+ pump currents were blocked by exposing voltage clamped myocytes to K^+-free extracellular solutions and re-activated by exposure to solutions containing 7 mmol/L K^+.

In some experiments we varied the extracellular concentration of Na^+ with osmolality maintained by the addition of *N*-methyl-D-glutamine chloride (NMG.Cl). TMA.Cl and NMG were purum grade and were obtained from Fluke Chemicals (Switzerland). All other chemicals used in solutions were analytical grade and were obtained from BDH (Australia). Ouabain, Grx1, SOD and Apocynin were obtained from Sigma Chemical Co., (St Louis, MO).

We used Axoclamp 2A and 2B voltage clamp amplifiers, supported by pClamp version 10 and Axotape version 2 (Axon Instruments, CA, USA) to record membrane currents. Currents were sampled at 20 Hz before and after Na^+, K^+ ATPase inhibition and activation in K^+-free and K^+-containing extracellular solutions. Clampfit was used to analyse current traces. Unless indicated, we used a holding potential of -40 mV to inactivate voltage-sensitive Na^+ channels. A rapid solution switcher (Warner Instruments) assured changes in the extracellular K^+ concentration were complete within 1 ms. However, due to diffusion delay in the t-tubular system [152] uniform activation of all Na^+, K^+ ATPase in rabbit cardiac myocytes cannot be expected in less than ~100 ms [153]. Experiments were performed near room temperature at 24 ^oC to minimize artefacts from changes in temperature with solution switches [153].

Trypsin cleavage of Na^+, K^+ ATPase and glutathionylation of its β_1 Subunit.

Na^+, K^+ ATPase-enriched membrane fragments from the outer medulla of pig kidney were prepared according to the method of Jørgensen using SDS extraction followed by differential centrifugation [154]. The specific activity was ~1800 μmol· mg^{-1} ·h^{-1} at 37 ^oC. Na^+, K^+ ATPase was stabilized in two different conformational states as described by the nomenclature of the Albers-Post scheme. The E2-P ground state and a state analogous to the E1~P·ADP·3Na^+ like state were stabilized in solutions that included beryllium fluoride and aluminium fluoride with ADP, respectively, as described [71]. We induced oxidative stress by exposing the membrane fragments to hydrogen peroxide (H_2O_2) in a concentration of 0.5 % Vol/Vol. This concentration is only nominal because of the short half-life of the compound. Controlled trypsin proteolysis of Na^+, K^+ ATPase stabilized in the two conformations and detection of glutathionylation of the β_1 Na^+, K^+ ATPase subunit with the GSH antibody technique were performed as described previously [102]. The Na^+, K^+ ATPase preparation contains GSH at a level that gives clear signals for detection of glutathionylation and GSH was not added when we measured glutathionylation. However, we did add 0.5 mmol/L GSH to enhance detection of glutathionylation-dependent differences in trypsin digest patterns.

Data Analysis.

Data are expressed as mean ± S.E. Statistical comparisons were made with a Student's *t* test or 1 way ANOVA as appropriate. $P < 0.05$ was considered to be statistically significant. Curve fittings of the transient current traces were performed with Clampfit 10.2.

Pump current simulations.

Computer simulations of the experimental steady-state pump current were performed using the commercially available program Berkeley Madonna 8.0 and the variable step-size Rosenbrock integration method for stiff systems of differential equations. The simulations yielded the time course of the concentration of each enzyme intermediate involved, the outward current and the amount of charge transported. For the purposes of the simulations, each enzyme intermediate was normalized to a unitary concentration. To simulate the K+ activated transient currents the model was run for 1 minute in the absence of extracellular K+ and the distribution of enzyme intermediates obtained from this was subsequently used for the K+ activation experiments. The K+ activation simulation was then carried out for 1 minute to replicate the experimental protocol. The protocol for the membrane voltage stimulations followed the protocol used in the experimental procedures to obtain the distribution of the enzyme intermediates.

RESULTS

K^+-induced Na^+, K^+ ATPase membrane currents.

The decline of the peak I_p on re-exposure of voltage clamped cardiac myocyte to K^+ after exposure to K^+-free extracellular solutions is reported to be a composite of fast and slow phases, with no detectable decline in the intracellular Na^+ concentration ($[Na^+_i]$) during the fast phase but with a parallel decline of I_p and $[Na^+_i]$ in the slow phase. This is compatible with an early Na^+ concentration gradient between Na^+-K^+ pump sites and the bulk phase where $[Na^+_i]$ is measured, as reviewed [67]. We voltage

clamped myocytes using patch pipette solutions that included 20 mmol/L Na^+ and 70 mmol/L K^+. When we re-exposed a myocyte to K^+ after exposure to K^+-free extracellular solutions we could reproduce fast and slow components that could be fitted by a biexponential function (Figure 5.1A). However, when we increased the size of the patch pipette to facilitate diffusion of Na^+ between its filling solution and the cytosol the time course of I_p on re-exposure to K^+ was well fitted by a single exponential function (Figure 5.1B). Such pipettes were used in all subsequent experiments we report.

The amplitude of the transient increase in I_p increased with duration of the pre-conditioning exposure to K^+-free solution but saturated beyond 30 s (data not shown). The duration of exposure to K^+-free solutions in experiments we report is ≥ 30 s unless indicated otherwise.

Persistence of large K^+-induced Na^+, K^+ ATPase current transients when myocytes are voltage clamped using Na^+-free patch pipette filling solutions has been utilised to support the existence of a diffusion-restricted sub-sarcolemmal space [59]. When using Na^+ free patch pipette filling solutions, we did not detect any K^+-induced shift in holding current (Figure 5.1C) indicating that there was no Na^+ in the cytosolic compartment, including in a sub-sarcolemmal space, that could support detectable Na^+, K^+ ATPase activity. To independently ascertain that the K^+-induced currents are due to activation of an electrogenic Na^+, K^+ ATPase current we exposed myocytes to ouabain. Ouabain eliminated K^+-induced membrane currents. Holding currents recorded during periods in K^+-free solutions were similar to currents recorded after the full effect of ouabain was achieved (Figure 5.1D) indicating that K^+-sensitive and ouabain-sensitive currents are similar.

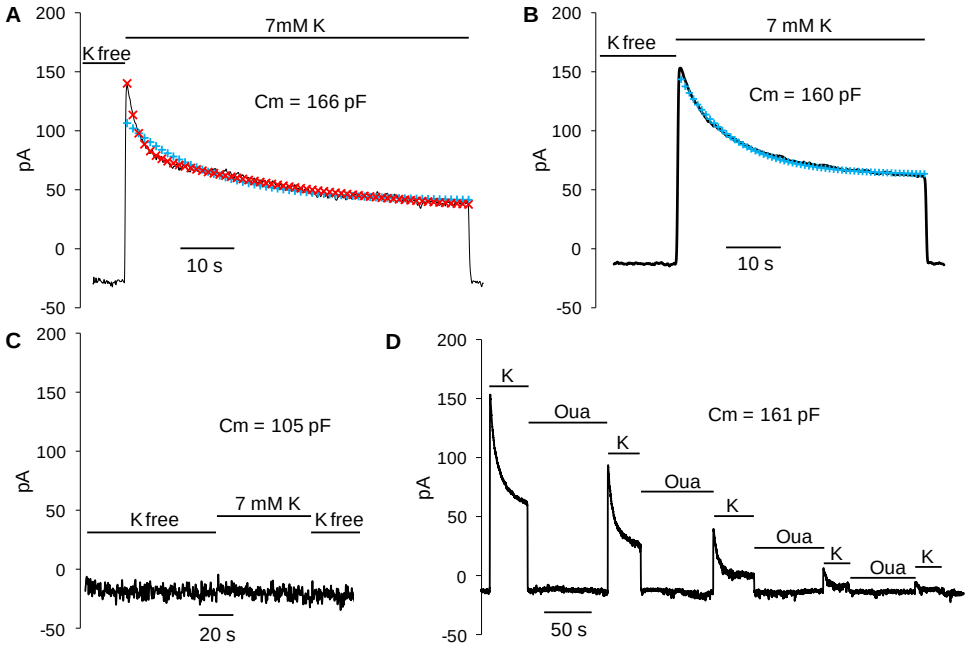

Figure 5.1. K^+-induced activation of the Na^+, K^+ ATPase current. A. Membrane currents of a voltage clamped myocyte exposed to K^+-free superfusate for 60 s before re-exposure to K^+. The superfusate included 140 mmol/L Na^+ while patch pipette solutions included 20 mmol/l Na^+ and 70 mmol/L K^+. Cm indicates membrane capacitance, reflecting cell size. The series resistance after establishing the whole-cell configuration was 7.1 MΩ. A single exponential function (+) gave a poor fit to the decay of a transient peak pump current while the decay was well fitted by a double exponential function (x) with time constants of 4.5 s and 61 s for fast and slow phases. B. K^+-induced activation of the Na^+-K^+ pump current using wide-tipped patch pipettes. The series resistance was 4.7 MΩ. A single exponential function gave a good fit to the decay of a transient peak pump current. C. Effect of K^+ in the superfusate when the patch pipette solution was Na^+-free. No K^+-dependent current was detected in tracing shown or in two other experiments. D. Sensitivity of K^+-induced membrane currents to ouabain. Patch pipette solution included 20 mmol/l Na^+ and 70 mmol/L K^+. The myocyte was exposed to 50 nmol/L ouabain as indicated.

Dependence of Na^+, K^+ ATPase transients on $[Na^+_i]$ and $[K^+_i]$.

Elimination of the K^+-induced transient peak I_p by an increase of the Na^+ concentration of patch pipette solutions has been taken to indicate that a concentration gradient between the bulk phase of the cytosol and the binding sites for Na^+ to the pump accounts for the transient currents recorded at lower concentrations [150]. However, the transient currents persisted when we increased the Na^+ concentration to 80 mmol/L while maintaining the K^+ concentration at 70 mmol/L (Figure 5.2A). Experiments performed using Na^+ concentrations of 20 or 80 mmol/L in patch pipette solutions while maintaining the K^+ concentration constant at 70 mmol/L are summarised in Figure 5.2B.

Since K^+ in patch pipette solutions reduces I_p [137], consistent with competition of K^+ for binding of Na^+ at intracellular sites [134], elimination of K^+ in the solution should increase I_p and hence amplify depletion of Na^+ on reactivation of the Na^+, K^+ ATPase. We reduced the Na^+ concentration in pipette solutions to 10 mmol/L to facilitate detection of a transient peak I_p arising from a difference between the Na^+ concentration in the bulk phase of the cytosol and in a diffusion-restricted sub-sarcolemmal space. The solutions contained 70 mmol/L K^+ or they were K^+-free. There was no transient peak I_p when pipette solutions were K^+-free (Figure 5.2C). A transient peak I_p was recorded when pipettes contained K^+ as for experiments performed using 20 or 80 mmol/L Na^+ in pipette solutions. The time course of I_p in experiments with K^+-containing or K^+-free patch pipette solutions are summarized in Figure 5.2D.

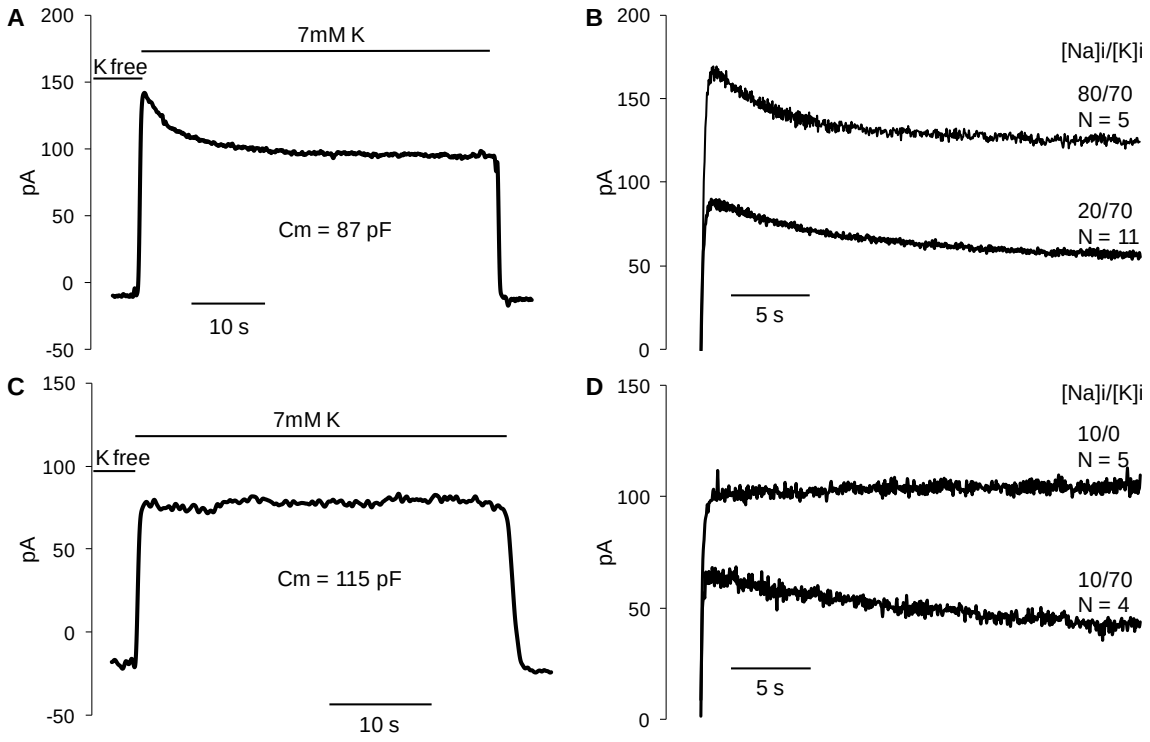

Figure 5.2. Dependence of Na^+, K^+ ATPase current transients on concentration of Na^+ and K^+ in patch pipette solutions. A. K^+-induced Na^+-K^+ pump currents using patch pipette solution including 80 mmol/L Na^+ and 70 mmol/L K^+. B. Comparison of average K^+-induced Na^+-K^+ pump currents. The concentration of Na^+ and K^+ (mmol/L) in patch pipette solutions and the number of experiments are indicated. C. K^+-induced Na^+-K^+ pump current using a K^+-free patch pipette solution. The solution included 10 mmol/L Na^+. D. Comparison of average K^+-induced Na^+-K^+ pump currents recorded using patch pipette solutions that were K^+-free or included 70 mmol/L K^+.

Dependence of Na^+, K^+ ATPase current transients on extracellular Na^+.

The transient peak I_p on K^+-induced reactivation is reported to persist in Na^+-free extracellular solutions [61,155]. In principle, this might be explained by an increase in the Na^+ concentration in a diffusion-restricted sub-sarcolemmal space during pump inhibition relative to what the concentration is during turnover. This would enhance activity when relative excess Na^+ is cleared on activation. We attempted to reproduce these results. Pipette solutions included 20 mmol/L Na^+ and 70 mmol/L K^+. In contrast to the initial transient peak of I_p recorded in Na^+-containing solutions, I_p recovered gradually from an initially low value with re-exposure to K^+ (Figure 5.3A). We also performed experiments in which the extracellular Na^+ concentration was 10 or 75 mmol/L. The time course of I_p on K^+-induced reactivation of the pump in these experiments and experiments performed using Na^+-free extracellular solutions are summarized in Figure 5.3B. A summary of experiments performed using solutions containing 140 mmol/L Na^+ is also included. I_p integrated over the first 5 s after K^+ induced reactivation of the Na^+, K^+ ATPase increased significantly with an increase in the extracellular Na^+ concentration (Figure 5.3C). In contrast to elimination of the transient peak I_p by use of K^+-free patch pipette solutions when external solution contained 140 mmol/L Na^+, using K^+-free pipette solutions did not alter the initially low value of I_p followed by a gradual recovery of K^+-induced activation of the Na^+-K^+ pump in Na^+-free external solutions (Figure 5.3D and 5.3E).

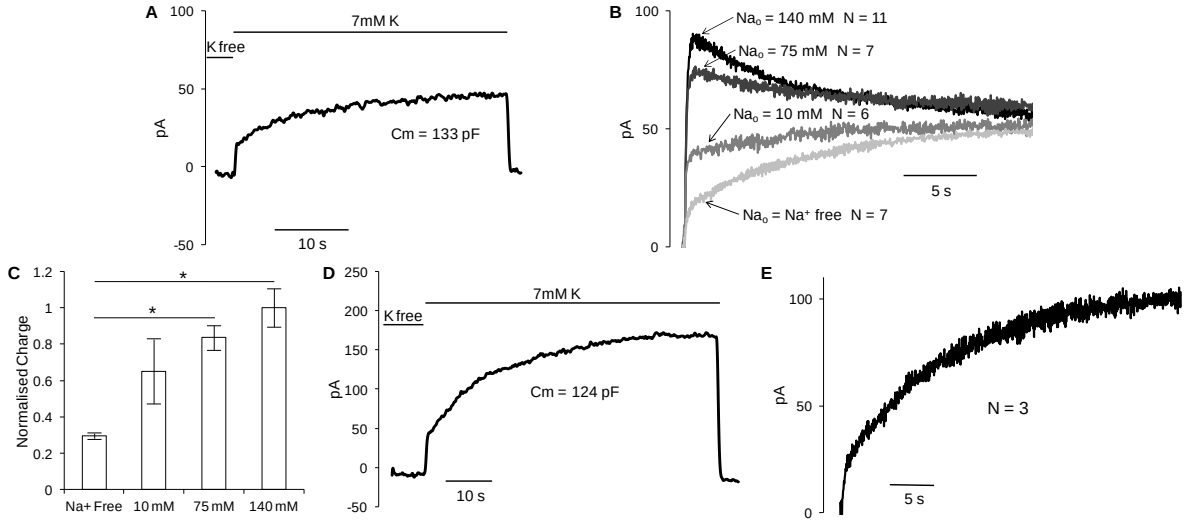

Figure 5.3. Dependence of K^+-induced Na^+, K^+ ATPase current transients on extracellular Na^+. A. Na^+, K^+ ATPase current in Na^+-free superfusate. The patch pipette solution included 20 mmol/L Na^+ and 70 mmol/L K^+. B. Average K^+-induced Na^+, K^+ ATPase currents with Na^+ concentrations in superfusate (Na_o) of 0 – 140 mmol/L. Number of experiments (N) for each Na_o is indicated. C. Na^+, K^+ ATPase current integrated over the first 5 s after re-exposure to K^+ normalised to the mean charge at a Na_o of 140 mmol/L. The charge transported increased with an increase in Na_o * indicates a significant difference ($P < 0.05$). D. Na^+, K^+ ATPase current using K^+-free patch pipette solution and a Na^+-free superfusate. The patterns of K^+-induced activation of pump current were similar in two additional experiments. E. Average Na^+, K^+ ATPase current using K^+-free patch pipette solution and a Na^+-free superfusate.

Dependence of Na^+, K^+ ATPase current transients on membrane voltage.

The different transmembrane concentration gradients for Na^+ and K^+ used in the voltage clamp experiments must impose different conformational states of the Na^+-K^+ pump. In the terminology of the Albers-Post scheme, all pump molecules assume the E2-P conformation in Na^+-free, K^+-free extracellular solutions but due to the backward E2-P + $3Na^+ \rightarrow$ E1~P$[Na^+]_3$ reaction (reaction (3) in Figure 5.4) a balance between E2-P and E1~P$[Na^+]_3$ species will exist in K^+-free, Na^+-containing solutions. Voltage dependence of the reaction [36] will shift the balance towards E2-P at positive potentials and towards the occluded E1~P$[Na^+]_3$ state at negative potentials. We examined if transient K^+-induced pump currents depend on membrane voltage during the preceding exposure to a K^+-free, Na^+-containing solution.

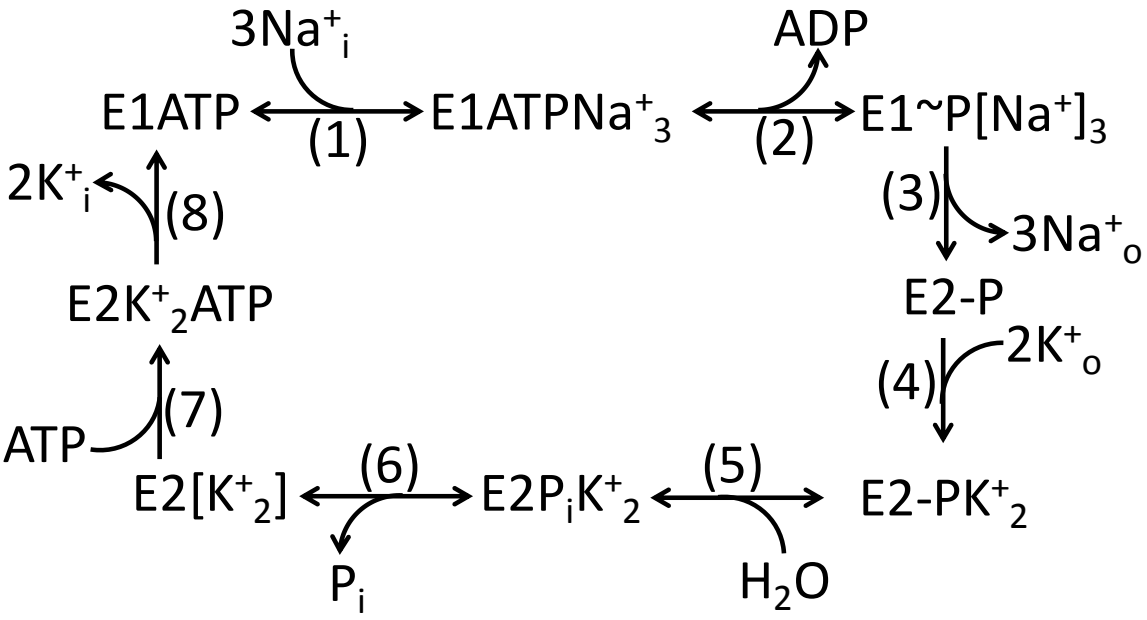

Figure 5.4. Albers-Post scheme for catalytic cycle of Na^+, K^+ ATPase. When 3 cytoplasmic Na^+ ions (Na^+_i) have bound to the E1 conformation (1) the cytoplasmic access gate is closed and locked when the α subunit is phosphorylated (2), causing occlusion of Na^+ ($[Na^+]_3$) within the molecule. A gate opens to the outside, and Na^+ is released (3) when its binding affinity decreases with the E1P→E2-P change. Extracellular K^+ is bound (K^+_o) (4) and the gate is closed and locked with dephosphorylation causing occlusion of K^+ within the molecule (6). De-occlusion (7) is facilitated by allosteric binding of ATP and K^+ is released to the cytoplasm (8) when its binding affinity decreases with the E2ATP → E1ATP change. In a voltage clamped internally perfused myocyte, the E2-P state accumulates in K^+-free, Na^+-free superfusate. In K^+-free, Na^+ containing superfusates a balance between E2-P and E1~P[Na^+_3] states depends on the extracellular Na^+ concentration and membrane voltage.

We voltage clamped myocytes at +10, -40 or -90 mV during exposure to K^+-free solutions. The Na^+ concentration in extracellular solutions was 75 mmol/L. Since I_p is voltage dependent and since there is a path in the pump molecule in K^+-free extracellular solutions for a leak current that depends on membrane voltage and extracellular Na^+ [135] we switched the holding potential to -40 mV for 1 sec before re-exposing myocytes to K^+ for the other two pre-conditioning membrane voltages. Modelling of the Na^+, K^+ ATPase cycle in Chapter 3 indicated that the conformational poise of pumps after 1 s at -40 mV is identical regardless of pre-conditioning membrane voltages. The whole-cell configuration could only be consistently maintained throughout the protocol when the duration of repeated exposure to K^+-free solution at the different voltages was reduced to 10 s. The experimental protocol and corresponding membrane currents are shown in Figure 5.5A. We used two indices to compare K^+-induced currents: a derived estimate of the initial current and an integral of the current recorded the first 5 s after re-exposure to K^+. The relatively short duration of exposure to K^+-free solutions at different pre-conditioning membrane voltages and a shared holding potential of -40 mV for 1 s before re-exposure to K^+ is expected to reduce the measured effect of membrane voltage. Despite this, both indices for pump activity were significantly larger for pre-conditioning membrane voltages of -90 mV than for +10 mV (Figure 5.5B).

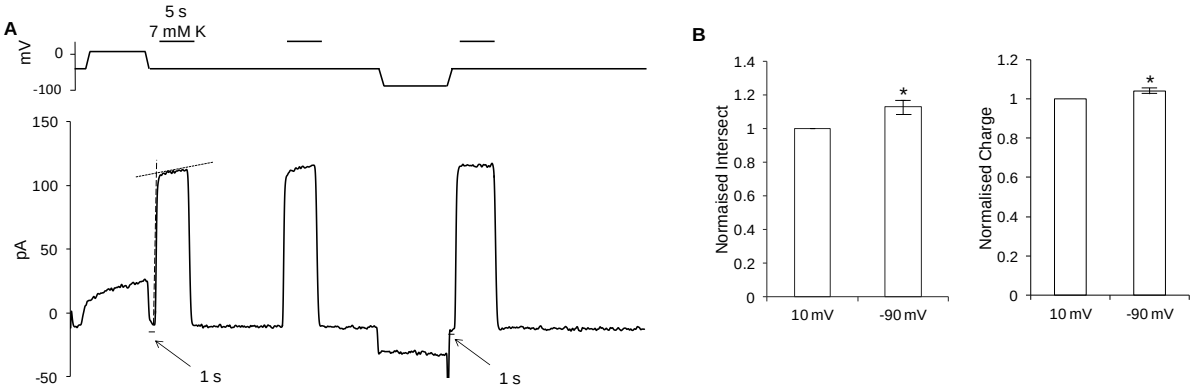

Figure 5.5. Dependence of K^+-induced Na^+, K^+ ATPase current on membrane voltage. A. Experimental protocol and K^+-induced Na^+, K^+ ATPase currents in myocyte exposed to K^+-free superfusate for 10 s at preconditioning holding potentials of -90 mV, -40 mV and +10 mV. A shared holding potential of -40 mV was used for 1 s (arrows) before re-exposure to K^+. The intersection of regression lines fitted to the fast upstroke and subsequent slower change in pump current with re-exposure to K^+ (shown for the pre-conditioning holding potential of +10 mV only) was used as an index of Na^+, K^+ ATPases that were not glutathionylated and available for early K^+-induced activation. B. Summary of derived estimate of the initial pump current and the integral of the current recorded the first 5 s after re-exposure to K^+ in 5 experiments. Data is normalized to the indices with a pre-conditioning holding potential of +10 mV. * indicates significant difference.

Effect of conformational poise and glutathionylation of the β_1 subunit on ATPase current transients.

The dependence of K^+-induced Na^+, K^+ ATPase current transients on transmembrane electrochemical gradients for Na^+ and K^+ we report here cannot be accounted for by accumulation and depletion of Na^+ in a diffusion-restricted sub-sarcolemmal space. However, the β_1 Na^+, K^+ ATPase subunit is susceptible to glutathionylation in some conformational states and resistant in others [102]. Since glutathionylation is reversible and causally related to pump inhibition [151] we hypothesized that conformation-dependent glutathionylation and de-glutathionylation accounts for the patterns of I_p recorded on K^+-induced Na^+, K^+ ATPase activation.

Susceptibility of the E2-P- and resistance of the E1~P$[Na^+]_3$ conformation to glutathionylation might account for the dependence of pump current transients on extracellular Na^+ and membrane voltage (Figure 5.3 and 5.5). Susceptibility of the β_1 subunit to glutathionylation in these conformations has not been determined. We exposed Na^+, K^+ ATPase in pig kidney membrane fragments stabilised with BeF_x and AlF_x/ADP [71] to the chemical oxidant H_2O_2 to induce glutathionylation [102]. BeF_x produces an E2-P like state while AlF_x/ADP induces a stable analogue of the transition state (E1~P·ADP·3Na^+) preceding E1~P$[Na^+]_3$ in which the cytoplasmic gate is at least partly closed [134]. As for Na^+, K^+ ATPase in other conformational states [102], a signal for glutathionylation was detected at baseline. Exposure to H_2O_2 increased glutathionylation of the β_1 subunit of Na^+, K^+ ATPase stabilized in the E2-P but not in the E1~P·ADP·3Na^+ like state (Figure 5.6A).

We examined if the difference susceptibility of the β_1 subunit of Na^+-K^+ ATPase stabilized in the E2-P and E1~P·ADP·3Na^+ like states to glutathionylation is consistent with any difference in structure as it can be identified by the trypsin

digestion pattern (Figure 5.6B). The band for the α subunit was weaker for Na^+, K^+ ATPase stabilized in the E2-P- than the E1~P·ADP·3Na^+ like states *i.e.* more susceptible to trypsin digestion in E2-P. A single weak band of a cleavage product migrating at 50 kDa for the E1~P·ADP·3Na^+ like state remained detectable when Na^+, K^+ ATPase had been pre-exposed to $ONOO^-$. Sequencing indicated it was from β subunits. In the E2-P like state two stronger bands of cleavage products from α and β subunits also migrated at 50 kDa. Their sensitivities to trypsin digestion were markedly increased when Na^+, K^+ ATPase had been pre-exposed to $ONOO^-$ suggesting glutathionylation can change structure even when Na^+, K^+ ATPase is stabilized with BeF_x.

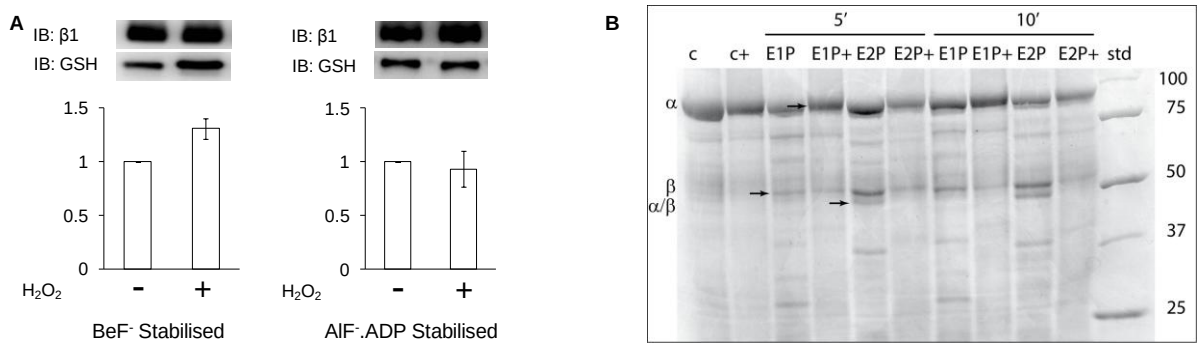

Figure 5.6. Conformational poise, glutathionylation of the β_1 subunit and trypsin digest pattern of Na^+, K^+ ATPase. A. glutathionylation of the β_1 subunit of Na^+, K^+ ATPase stabilized in E2-P (BeF) and E1~P·ADP·3Na^+ like (AlF) conformations. B. Trypsin digest of Na^+, K^+ ATPase stabilized in E2-P ground state (labelled E2P) and E1~P·ADP·3Na^+ (labelled E1P) conformations. Lanes 1 and 2 are controls without trypsin addition in the absence (c) and presence (c+) of $ONOO^-$. Subsequent 8 lanes are 5 and 10 min trypsin digests of BeF stabilized E2-P ground state and AlF/ADP stabilized E1~P·ADP·3Na^+ like state in the absence and presence of $ONOO^-$. The last lane shows molecular weight standards. The two bands around 50 kDa indicated by arrows were identified by sequencing to contain β (upper band) and α plus β (lower band).

When extracellular solutions contain Na^+ a switch to K^+-free solution should shift the E2-P + $3Na^+$ ↔ E1~P$[Na^+]_3$ reaction to the right [156] while Na^+ and Mg.ATP in patch pipette solutions promotes the forward E1ATP + $3Na^+$ → E1~P$[Na^+]_3$ reaction, causing E1~P$[Na^+]_3$ to accumulate. This alone will produce a large initial current due to the rapid release of bound Na^+ ions to the extracellular medium on exposure to extracellular K^+. However, based on the kinetics of the enzyme's partial reactions this transient current would be expected to decay in less than one second [23], in contrast to the transients shown in Figures 5.1 and 5.2 which decay into a steady state over tens of seconds. For this reason we consider changes in the glutathionylation state of the protein as the origin of these long-lived transients.

Resistance of E1~P·ADP·$3Na^+$ to glutathionylation suggests a relatively large proportion of pumps are free of glutathionylation-induced inhibition allowing for an initially high level of I_p on re-exposure to K^+. The subsequent decline of I_p might then be due to re-glutathionylation of susceptible conformational states during pump turnover. We included Grx1 (10 µg/mL), in patch pipette solutions to selectively eliminate glutathionylation-induced Na^+, K^+ ATPase inhibition [151]. The pipette solutions included 20 mmol/L Na^+ and 70 mmol/L K^+. Grx1 markedly reduced the decline of I_p following K^+-induced reactivation of the Na^+, K^+ ATPase (Figure 5.7A). The time course of I_p in experiments with Grx1 containing- or control patch pipette solutions are summarized in Figure 5.7B. The pump current integrated over the first 10 s after re-exposure to K^+ was significantly increased by addition of Grx1 to the pipette solution (Control 9.376 ± 0.69 pC/pF vs Grx1 14.023 ± 1.59 pC/pF; $P < 0.05$). Since Grx1 reverses glutathionylation of sulfhydryl residues in proteins with exclusive selectivity [157] this strongly supports the hypothesis that an increase in glutathionylation causes the decline of the transient peak I_p.

With the E2-P state susceptible to glutathionylation, a shift of the E2-P + $3Na^+$ ↔ E1~P$[Na^+]_3$ reaction to the left (Figure 5.4) in Na^+-free, K^+-free extracellular solutions will leave pumps susceptible to glutathionylation-induced inhibition, possibly accounting for the initially low value of I_p on re-exposure to K^+ in Na^+-free extracellular solutions. However, an initially low value of I_p on re-exposure to K^+ was also recorded when we included Grx1 in the patch pipette solution (Figure 5.7C). We examined if reducing oxidative stress and hence also the forward rate of glutathionylation affects the pattern of the initial I_p on reactivation of the Na^+, K^+ ATPase. Since NADPH oxidases are initiators and integrators of synthesis of reactive oxygen species via cross-talk with other cellular sources we included the NADPH oxidase inhibitor apocynin in patch pipette solutions [158]. We also included SOD in the solution to scavenge $O_2^{\cdot-}$. The combination of apocynin and SOD markedly increased the initial I_p on re-exposure to K^+ (Figure 5.7D) consistent with a role for an oxidative modification, including glutathionylation causing the early inhibition of I_p. Experiments performed in Na^+-free extracellular solutions with and without Grx1 or apocynin and SOD are summarized in Figure 5.7E. The charge integrated over the first 10 s after re-exposure to K^+ was significantly increased by the combination of apocynin and SOD (Control 4.436 ± 0.51 pC/pF vs SOD + APO 7.381 ± 0.34 pC/pF; $P < 0.05$).

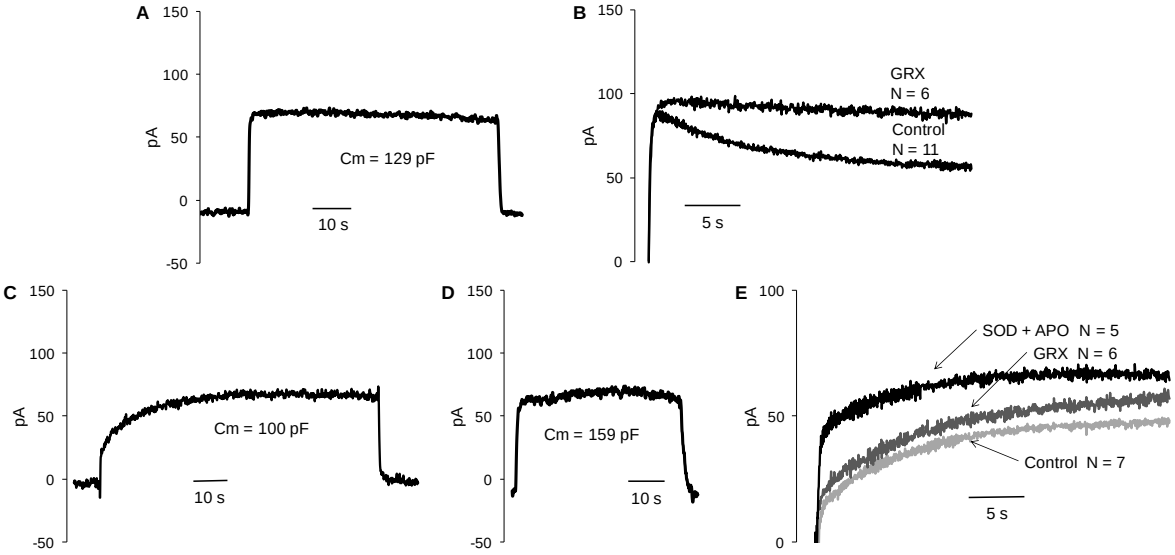

Figure 5.7. Oxidative stress and K^+-induced Na^+, K^+ ATPase current transients. Patch pipette solutions included 20 mmol/L Na^+, 70 mmol/L K^+. A. Effect of Grx1 on decay of transient peak Na^+, K^+ ATPase current. The superfusate included 140 mmol/L Na^+ and the pipette solution included Grx1 as indicated. B. Average K^+-induced Na^+, K^+ ATPase currents in Na^+ containing superfusate, with and without Grx1 in pipette solutions. The pump current integrated over the first 10 s after re-exposure to K^+ was significantly increased by Grx1. C. K^+-induced Na^+, K^+ ATPase current recorded in Na^+-free superfusate with Grx1 in the pipette solution. D. K^+-induced Na^+, K^+ ATPase current recorded in Na^+-free superfusate with SOD and apocynin in the pipette solution. E. Average K^+-induced Na^+, K^+ ATPase currents with Grx1 or apocynin and superoxide dismutase (SOD) in patch pipette solutions. There was no significant effect of Grx1 on pump currents integrated over the first 10 s after re-exposure to K^+ while the combination of SOD and apocynin significantly increased the integrated currents.

Modelling of K+ activated Transient Currents by Incorporating Glutathionylation.

The kinetic model from chapter 4, based on the Albers-Post scheme, is capable of reproducing data from the literature and thus we can test whether this model explains the experimentally observed K+ activated transient curves reported in this chapter. As observed in figure 5.8A the current model does not reproduce the transient curve observed with 140 mM Na+ in the extracellular solution. We propose the addition of glutathionylation at the E1 poise as predicted by Liu *et al* and glutathionylation at the E2P poise as predicted by the susceptibility of the β_1 subunit when the Na^+, K^+ ATPase enriched membrane fragments are incubated in BeF- and exposed to hydrogen peroxide. The extensions and alterations to the equations necessary for the calculation of enzyme intermediates are described in the Appendix of this chapter. The choice of glutathionylation rate constants was determined by how well they replicated the K^+ activated transient observed with 140 mM Na^+ in the extracellular solutions. The rate constants settled upon are within the range observed in the literature [159]. Once glutathionylation was included in the model simulations of the K^+ activated transient curves were possible with the dependence of extracellular Na^+ on the shape of the curve also replicated (Figure 5.8B). When we abolish K^+ from the patch pipette the transient current is not qualitatively altered and does fit the experimental data. This suggests that the reglutathionylation may be associated with K^+-dependent inhibition at the intracellular part of the pump cycle. Since the E1 poise in the mathematical model is a lumped parameter the model does not take into account which E1 species is likely to be glutathionylated. i.e. glutathionylation occurs at all E1 species and the model predicts that the transient

peak current and its subsequent decay curve should persist when the intracellular compartment is K^+-free (figure 5.8C), at odds with the experimental data.

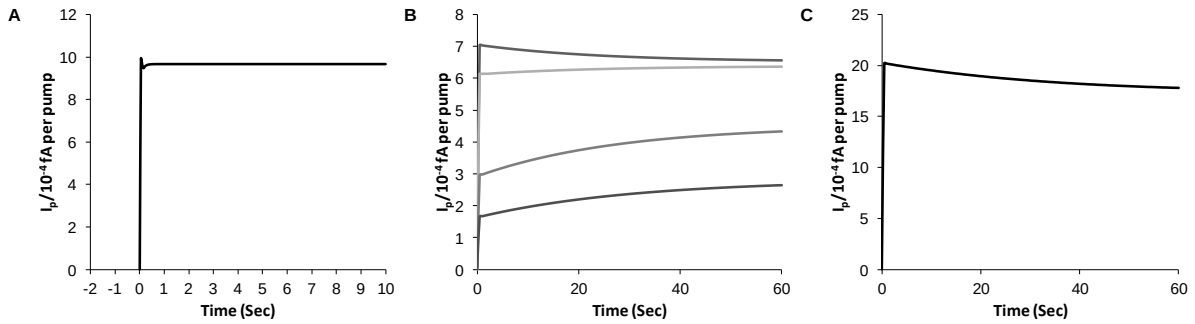

Figure 5.8. Modeling of the K^+-induced Na^+, K^+ ATPase current transients. A. Simulation of the K+ activated transient current without the incorporation of glutathionylation at E1 and E2P. B. Simulation of the K+ activated transient current with glutathionylation incorporated at all E1 species and E2P. The incorporation of glutathionylation at the non occluded sites replicates the Na+ dependence observed in the experimental results. C. Simulation of the K+ activated transient current with extracellular Na+ (140 mM) and K+ free intracellular solution. A transient current is still apparent, at odds with the experimental results shown in Figure 5.2.

The difference in the charged produced when the membrane voltage was manipulated (Figure 5.5) cannot be reconciled with the Na^+ subsarcolemmal space theory. As such, if we accept that susceptibility to glutathionylation of the E2P poise is partly responsible for the pattern in K^+ activated transients, that depends on Na^+, the balance in enzyme intermediates through alterations to the membrane voltage would change the proportion of pumps that are found in the E2P poise and thus susceptible to glutathionylation. Since the model has membrane voltage incorporated in its parameters we can predict this effect that arises from membrane voltage as seen in Table 5.1. When there is no glutathionylation at E2P the pump re-equilibrates to the balance at -40 mV within the one second before K^+-induced activation. Since the enzyme intermediates are equal then no difference in charge moved is observed. However, when E2P is susceptible to glutathionylation the model predicts that a small but significant change in the E2PG enzyme intermediate occurs after alteration of the membrane voltage. Since glutathionylation is the slowest step in the cycle it then cannot re-equilibrate after the change to -40 mV and produces a significant difference in the charged moved (10 mV protocol 28.7093 fC vs -90 mV protocol 32.1206 fC) replicating the experimental data qualitatively.

Table 5.1.

Without Glutathionylation			
	Initially	**7 sec**	**1 sec**
mV	-40	10	-40
E1	0	0	0
E1P	0.21902	0.05423	0.21902
E2P	0.78099	0.94577	0.78099
E2K2	0	0	0
	Initially	**7 sec**	**1 sec**
mV	-40	-90	-40
E1	0	0	0
E1P	0.21902	0.66496	0.21902
E2P	0.78099	0.33504	0.78099
E2K2	0	0	0

With Glutathionylation			
	Initially	**7 sec**	**1 sec**
mV	-40	10	-40
E1	0	0	0
E1P	0.28098	0.0778	0.26207
E2P	0.35951	0.51654	0.33532
E2PG	0.35951	0.40566	0.40262
E2K2	0	0	0
	Initially	**7 sec**	**1 sec**
mV	-40	-90	-40
E1	0	0	0
E1P	0.28098	0.48752	0.2992
E2P	0.35951	0.19742	0.38282
E2PG	0.35951	0.31508	0.318
E2K2	0	0	0

DISCUSSION

The cytosolic Na^+ concentration is determined by the balance between Na^+ influx and Na^+, K^+ ATPase-mediated efflux [160], and when Na^+, K^+ ATPase activity is blocked in K^+-free extracellular solutions Na^+ accumulates intracellularly unless blocking of pump-mediated efflux is compensated for by diffusion into the patch pipette solution. If accumulation does occur I_p is enhanced beyond steady state on re-exposure to K^+ until excess Na^+ is pumped out. Two components of the time course of decline of I_p after K^+-induced re-activation of the Na^+, K^+ ATPase have been reported [150,161] as we also found (Figure 5.1A). The slow phase is readily explained by clearing of excess Na^+ in the bulk phase of the cytosolic compartment [67,150] and was eliminated when we used wide-tipped patch pipettes to facilitate diffusion between pipette and the intracellular compartment.

Persistence of a transient peak of I_p when we used wide-tipped patch pipettes could be due to accumulation of Na^+ in a diffusion-restricted space near the cytosol-membrane interface [67,150]. However, with such accumulation the increase in the concentration of Na^+ in patch pipettes to a level nearly saturating Na^+ binding to the Na^+, K^+ ATPase should have reduced or eliminated the transient peak of I_p [59] and conversely, when patch pipette solutions were Na^+- or K^+-free a transient peak should still have been detectable. Since a Na^+, K^+ ATPase current, identified as a ouabain-sensitive current, can be detected with Na^+ in a concentration as low as 0.1 mmol/L in patch pipette solutions [137] Na^+ at most would have accumulated to a very low level in intracellular compartments including in any diffusion-restricted sub-sarcolemmal space.

Physical intracellular barriers to diffusion of Na^+ have not been reported and Despa and Bers [150] examined if an apparent restriction of diffusion might be mimicked by binding of Na^+ near the cytosol/membrane interface. They found only a modest degree of such binding. It has also been suggested that crowding of macromolecules near the inner membrane leaflet might restrict diffusion of Na^+ [67]. Our study indicates that macromolecular crowding or binding of Na^+ in a sub-sarcolemmal space does not occur to the extent that local restriction to the movement of Na^+ causes a transient K^+-induced peak of I_p. We cannot rule out brief local accumulation of Na^+ near the opening of Na^+ channels with the high rate of influx through the channel during the upstroke of the cardiac action potential but such accumulation should dissipate rapidly [162] and be unlikely to persist throughout the cardiac cycle. This implies some concepts important for cardiac physiology, pathophysiology and therapeutics must be revised.

Studies on voltage clamped cardiac myocytes indicate that Na^+, K^+ ATPase activation alters Na^+, Ca^{2+} exchange currents, [3,60,61,163,164] and on the basis of K^+-induced transient Na^+, K^+ ATPase current local depletion of Na^+ has been implicated in a Na^+, K^+ ATPase/Na^+, Ca^{2+} exchange interaction with implications for excitation-contraction coupling as reviewed [67]. Restricted movement of Na^+ is also expected to be a determinant of the cardiac action potential configuration because membrane currents generated by the Na^+, K^+ ATPase and the Na^+, Ca^{2+} exchanger contribute to the repolarisation phase and the net current depends on whether the Na^+, K^+ ATPase and the Na^+, Ca^{2+} exchanger sense the same Na^+ concentration [149].

A diffusion-restricted sub-sarcolemmal space would enhance the effect of increased Na^+ influx via non-inactivating Na^+ channels and Na^+, H^+ exchange to cause Na^+, Ca^{2+} exchange-dependent Ca^{2+} overload and injury during myocardial ischemia and

reperfusion. This suggests restricted Na^+ diffusion would make pharmacological inhibition of Na^+ influx particularly effective in reducing cardiac myocyte Ca^{2+} overload and its adverse consequences [144]. Restricted sub-sarcolemmal diffusion of Na^+ is also critical for the concept that the α_2 isoform of the Na^+, K^+ ATPase predominantly controls the Na^+ concentration in a sub-sarcolemmal space with particular importance for control of Na^+, Ca^{2+} exchange and excitation-contraction coupling while the α_1 isoform controls the Na^+ concentration in the bulk phase [165]. This concept has important pathophysiological implications for the change in expression of the isoforms with heart failure [163] and it suggests that α isoform-specific cardiac glycosides might be useful [166].

Since a diffusion-restricted sub-sarcolemmal space could not account for patterns of K^+-induced membrane currents in voltage clamp experiments we examined if they could be attributed to glutathionylation and de-glutathionylation. According to the Albers-Post scheme (Figure 5.4) the abundance of E1~P$[Na^+]_3$ species should increase when turnover is arrested in K^+-free, Na^+-containing extracellular solutions and the analogue E1~P·ADP·$3Na^+$ was resistant to glutathionylation. During turnover the E1ATP + $3Na^+$ → E1ATPNa^+_3 reaction is rate limiting when pipette solutions contain K^+ because K^+ competes for binding of Na^+ to E1ATP [134], causing E1ATP to accumulate. Since E1ATP is susceptible to glutathionylation [102] while E1~P$[Na^+]_3$ is resistant a decrease in glutathionylation in K^+-free solutions followed by an increase with reactivation might account for the initial peak I_p and its subsequent decline that depends on inclusion of K^+ in pipette solutions. The inhibition of the decline of I_p by Grx1 supported this scheme.

The time course of K^+-induced Na^+, K^+ ATPase activation in Na^+-free extracellular solutions is also compatible with glutathionylation that depends on conformational

state. In K^+-free, Na^+-free solutions E2-P will be the only prevalent species because the $E1{\sim}P[Na^+]_3 \rightarrow E2\text{-}P + 3Na^+$ reaction is driven to the right. Glutathionylation that develops in such solutions will initially inhibit I_p on re-exposure to K^+. Since turnover is stopped, the prevalence of E2-P will be independent of intracellular K^+ and, as expected from this, the time course of I_p on Na^+, K^+ ATPase activation was independent of K^+ in pipette solutions when extracellular solutions were Na^+-free.

Modelling of the data allows us to test the hypothesis that glutathionylation is involved in the K^+ activated transients. The peak transient is replicated once glutathionylation is incorporated in the E2P and E1 enzyme intermediates with the extracellular Na^+ dependence of the curves also being replicated (Figure 5.8B). Membrane voltage experiments confirm that there is a dependence of the transient curve upon the balance of the enzyme intermediates under Na^+/Na^+ exchange conditions. The necessity of glutathionylation at the E2P poise within the model to replicate the reported changes in the transient current strongly supports the existence of glutathionylation at E2P (Table 5.1). As such we can conclude that glutathionylation proffers an alternative to the hypothesis of the Na^+ diffusion restricted space being the origin of the transient currents observed in whole patch clamped cardiac myocytes.

We consider that prevalence of conformational states susceptible or not susceptible to glutathionylation in K^+-free and K^+-containing extracellular solutions relative to the prevalence of susceptible species during pump turnover determine whether an initial I_p on K^+-induced Na^+, K^+ ATPase activation is higher or lower than I_p in the subsequent steady state. This principle is illustrated by the effect the extracellular Na^+ concentration is expected to have on the $E2\text{-}P + 3Na^+ \leftrightarrow E1{\sim}P[Na^+]_3$ balance

which in turn is reflected by the dependence of the pattern of K^+-induced activation of I_p on extracellular Na^+ (Figure 5.3).

Resistance to glutathionylation in the E1~P$[Na^+]_3$ state is expected from the three-dimensional structure of the Na^+, K^+ ATPase molecule in a E1~P·ADP·3Na^+ state since the reactive cysteine residue of the β_1 Na^+, K^+ ATPase subunit is in the lipid phase of the transmembrane segment [134,135]. This is also the case for the E2·Pi·2K^+ structure [82]. However it seems that the β-subunit is significantly closer to transmembrane segment 10 of the α subunit in the E1~P·ADP·3Na^+ structure than in the E2·Pi·2K^+ structure [82,134]. This may add protection against β_1 subunit glutathionylation. The crystal structure for the E2-P ground state is not known but the difference in trypsin digest patterns of the β_1 subunit of Na^+, K^+ ATPase in E2-P and E1~P·ADP·3Na^+ like states stabilized by BeF_x and AlF_x/ADP indicate that a structural difference exists that might account for access of GSH to the reactive cysteine residue in E2-P.

A difference in the trypsin digest pattern between the E2-P like state we report here and E1~P·ADP·3Na^+ like species [102] may reflect a structural difference between *in situ* sarcolemmal Na^+, K^+ ATPases that accounts for access of the ~11 kDa Grx1 to reverse glutathionylation and counteract a decline in I_p after a transient peak on pump activation when extracellular solutions contained Na^+ (Figure 5.7B) but not access to prevent glutathionylation and pump inhibition to develop in K^+-free, Na^+-free solutions (Figure 5.7D). Consistent with this, access of Grx1 to target proteins may be conformation-dependent [157] as is co-immunoprecipitation of exogenous Grx1 with the β_1 subunit in Na^+, K^+ ATPase [102]. The molecular differences that accounts for this may not be major since molecular dynamics simulations suggest that

deformation of the inner membrane leaflet can change access to the reactive residue in the β_1 Na^+, K^+ ATPase subunit [167].

A K^+-induced transient peak Na^+, K^+ ATPase current in cardiac myocytes does not reflect cellular architecture at the membrane-cytosol interface as believed previously but can be accounted for by conformational states of the Na^+, K^+ ATPase molecule itself. With modifications of long-established experimental protocols used to study K^+-induced reactivation of the Na^+, K^+ ATPase the effect of oxidative modifications on selected partial reactions of the pump's catalytic cycle can be studied in intact cardiac myocytes and effects on function resolved with high resolution of its time-dependence. This is likely to be useful for studying the role of the Na^+, K^+ ATPase in cardiac myocyte physiology, pathophysiology and pharmacology.

APPENDIX

Expanded Albers-Post model including glutathionylation at E1 and E2P.

To take into account the effect of glutathionylation at E1 and E2P on the transient and steady-state pump currents requires some relatively small modifications to the model incorporating the Na^+ allosteric site. Because experimental evidence on purified enzyme indicates that the non occluded states are susceptible to glutathionylation, the differential rate equations describing the change in concentrations of the E1 and E2P states need to be changed. The modified equations are:

$$\frac{d[E1]}{dt} = -k_1 f(3Na_i) f(ATP_{E1})[E1] + (k_4^{\min} f(ATP_{E2}) + (k_4^{\max} - k_4^{\min}) f(ATP_{E2}) f(Na_o^{allo}))[E2] - k_{-4} f(2k_i) f(ATP_{E1})[E1] + kDG_1[E1G] - kG_1[E1]$$

$$\frac{d[E2P]}{dt} = -k_3 f(2K_o)[E2P] - k_{-2} f(3Na_o)[E2P] + k_2[E1P] + kDG_2[E2PG] - kG_2[E2P]$$

In these two equations the rate constants for glutathionylation are given as:

Parameter	Reaction	Value*
kG_1	E1 $\rightarrow$ E1G	0.06 s^{-1}
kDG_1	E1G $\rightarrow$ E1	0.028 s^{-1}
kG_2	E2P $\rightarrow$ E2PG	0.044 s^{-1}
kDG_2	E2PG $\rightarrow$ E2P	0.044 s^{-1}

* These values were chosen because they attained the simulations closest to the K^+ activated transient experimental data reported in this chapter.

CHAPTER SIX

CONCLUSIONS

Data presented in this thesis has produced the first published mathematical model of the Na^+, K^+ ATPase with the ability to simulate the kinetics of transient currents activated by extracellular K^+. The model describes significant differences between the kidney and heart enzyme populations that can be attributed to the variation in tissue specific expression of the Na^+, K^+ ATPase subunits. The addition of the Na^+ allosteric site effect from data obtained from whole cell patch clamped rabbit cardiac myocytes and Na^+, K^+ ATPase membrane enriched fragments shows the importance of understanding the effect of cation concentrations on the rate constants of the partial reactions. Experimental conditions such as the lowering of intracellular K^+ concentrations or the replacement of intracellular K^+ with a congener such as Cs^+ may give a larger pump current signal but will also mask the effect of the Na^+ allosteric sites ability to accelerate E2 to E1 conversion by reducing the effect of the reverse E1 to E2 conversion as reported in Chapter 4.

Incorporation of glutathionylation to the model to reproduce the K^+ activated transients, previously associated with a Na^+ restricted diffusion space, is a fundamental step towards predicting the effects on the Na^+, K^+ ATPase of changes in the redox balance of the cell. Hill and Bhatnagar review compilation of a list of cardiovascular proteins that are significantly altered with posttranslational modification of glutathionylation [50] offers an interesting perspective yet to be explored in cardiovascular pathologies. Chronic diseases have long been associated with significant changes in cellular redox balance [168-172] and now we are

beginning to understand how these changes in redox balance are affecting the molecular biology of the cell and its constituents.

The Na^+ subsarcolemmal space and its association with the Na^+, K^+ ATPase began with Bielen *et al* and their inability to abolish the K^+ activated transient current with control of the intracellular ionic concentrations via whole cell patch clamping [58]. Considering no hypothesis existed to explain such a counterintuitive observation the Na^+ subsarcolemmal space became lead hypothesis for this phenomenon [59]. Subsequently this has spawned almost 25 years of study, trying to understand and define the space itself [64,66,162] along with how this space may impact on the relationship between the Na^+, K^+ ATPase and the Na^+, Ca^{2+} exchanger [3,60,61,164,173]. The reporting of poise dependent glutathionylation of the β_1 subunit [102] offered the opportunity of re-evaluating the K^+ activated transient. Clearly the K^+ activated transient would occur if placing the ATPase in a Na^+/Na^+ exchange mode conferred some protection to the β_1 subunit as long as the proportion of glutathionylation dropped below that observed under the conditions of steady state turnover. Interestingly we observed an extracellular Na^+ dependence to the K^+ activated transient that has never been reported in the literature. As described in the Introduction the reported uses of both Tris.HCl and Choline Chloride as substitutes for extracellular Na^+ had significant methodological problems associated with their use. As such we hypothesised the potential for a poise dependent susceptibility to glutathionylation of the β_1 subunit in the phosphoenzyme intermediates of the Na^+, K^+ ATPase. This was supported by the metal fluoride stabilised enzyme exposure to oxidant stress and the observation recorded from the experimental membrane voltage protocol. The final significant piece of evidence that these transients cannot be associated with a Na^+ diffusion restricted space is the fact that when K^+-free

patch pipettes are used the transient is abolished considering that the relatively low concentration of Na^+ should have accentuated the Na^+ restricted diffusion space effect. This alternate explanation of the K^+ activated transients presents two significant new ideas that may alter the direction of research in the Na^+, K^+ ATPase. Firstly, the lack of evidence to support a significantly large Na^+ restricted diffusion space beneath the sarcolemma means that 25 years of research requires re-interpretation from a very different perspective. Secondly, the status of β_1 glutathionylation is firmly positioned as a significant form of posttranslational pump regulation as there is currently a lack of any competing explanation for the transient currents.

Novel Findings.

The following finds have not previously been described:

1. The first publication of a mathematical model of the Na^+, K^+ ATPase based on the partial reaction rate constants of the kidney enzyme with the ability to simulate transient changes in the steady-state pump current.

2. The first reported observation of the Na^+ allosteric site in whole cell voltage clamped cardiac myocytes as predicted by experiments in Na^+, K^+ ATPase-enriched isolated membrane fragments from pig kidney.

3. The existence of the Na^+ subsarcolemmal space as supported by K^+ activated transient currents from the Na^+, K^+ ATPase is impossible to reconcile with our data and as such places doubt upon the existence of this space.

4. Poise dependent glutathionylation is now an alternative explanation for the K^+-activated transient currents and the poise dependent glutathionylation of the phosphoenzyme intermediate.

5. Considering that glutathionylation is slower than any other kinetic rate constant within the pump cycle and is predicted to be heavily prevalent by the model during steady-state strongly supports its role as a regulator of pump activity.

6. For the first time a mathematical model of the Na^+, K^+ ATPase has been incorporated with a posttranslational modification associated with receptor coupled signalling.

Future Directions.

1. The four state model shows significant differences between the kidney enzyme and the heart enzyme. A preparation of the heart enzyme of enough purity can be obtained to measure the specific rate constants and ion dissociation constants to determine if this difference really exists.

2. The mathematical model, with the Na^+ allosteric site and glutathionylation incorporated, simulates the results reported in Chapter 5 qualitatively well. The simulation of a transient current when intracellular K^+ is abolished in the model signifies that improvements need to be made which may require using an extended model to target specific enzyme intermediates.

3. In every crystal structure model recently published of the Na^+, K^+ ATPase the susceptible cysteine of the β_1 subunit is found within the predicted membrane. As such the ability of a charged compound to reach the cysteine is

theoretically impossible. We need to come to an understanding of how a charged glutathione molecule can reach the cysteine 46 residue of the β_1 subunit and whether access is associated with membrane deformations or significant structural changes of the protein.

4. Under our conditions no effect of adding Glutaredoxin is observed on the peak transient current which is dependent on the level of E2P glutathionylation, but it seems to reduce re-glutathionylation at the E1 enzyme intermediate. This offers the possibility for an access issue for Glutaredoxin to the cysteine 46 residue of the β_1 subunit that hasn't been observed previously in the literature and may only surface under conditions were the ATPase is in situ.

REFERENCES

1. Skou, J.C. The influence of some cations on an adenosine triphosphatase from peripheral nerves. *Biochim Biophys Acta* **23**, 394-401 (1957).
2. ten Eick, R.E., Whalley, D.W. & Rasmussen, H.H. Connections: heart disease, cellular electrophysiology, and ion channels. *FASEB J* **6**, 2568-2580 (1992).
3. Swift, F.*, et al.* Functional coupling of alpha(2)-isoform Na(+)/K(+)-ATPase and Ca(2+) extrusion through the Na(+)/Ca(2+)-exchanger in cardiomyocytes. *Cell calcium* **48**, 54-60 (2010).
4. Vaughan-Jones, R.D.*, et al.* pH-Regulated Na(+) influx into the mammalian ventricular myocyte: the relative role of Na(+)-H(+) exchange and Na(+)-HCO Co-transport. *J Cardiovasc Electrophysiol* **17 Suppl 1**, S134-S140 (2006).
5. Banerjee, S.K., McGaffin, K.R., Pastor-Soler, N.M. & Ahmad, F. SGLT1 is a novel cardiac glucose transporter that is perturbed in disease states. *Cardiovasc Res* **84**, 111-118 (2009).
6. Mercer, R.W., Biemesderfer, D., Bliss, D.P., Jr., Collins, J.H. & Forbush, B., 3rd. Molecular cloning and immunological characterization of the gamma polypeptide, a small protein associated with the Na,K-ATPase. *J Cell Biol* **121**, 579-586 (1993).
7. Peters, W.H., de Pont, J.J., Koppers, A. & Bonting, S.L. Studies on (Na+ + K+)-activated ATPase. XLVII. Chemical composition, molecular weight and molar ratio of the subunits of the enzyme from rabbit kidney outer medulla. *Biochim Biophys Acta* **641**, 55-70 (1981).

8. Toyoshima, C., Kanai, R. & Cornelius, F. First crystal structures of Na+,K+-ATPase: new light on the oldest ion pump. *Structure* **19**, 1732-1738 (2011).

9. Geering, K. The functional role of beta subunits in oligomeric P-type ATPases. *Journal of bioenergetics and biomembranes* **33**, 425-438 (2001).

10. Geering, K. Functional roles of Na,K-ATPase subunits. *Current opinion in nephrology and hypertension* **17**, 526-532 (2008).

11. Lutsenko, S. & Kaplan, J.H. An essential role for the extracellular domain of the Na,K-ATPase beta-subunit in cation occlusion. *Biochemistry* **32**, 6737-6743 (1993).

12. Lemas, M.V., Hamrick, M., Takeyasu, K. & Fambrough, D.M. 26 amino acids of an extracellular domain of the Na,K-ATPase alpha-subunit are sufficient for assembly with the Na,K-ATPase beta-subunit. *The Journal of biological chemistry* **269**, 8255-8259 (1994).

13. Hokin, L.E.*, et al.* Studies on the characterization of the sodium-potassium transport adenosine triphosphatase. X. Purification of the enzyme from the rectal gland of Squalus acanthias. *The Journal of biological chemistry* **248**, 2593-2605 (1973).

14. Racker, E. Structure and function of ATP-driven ion pumps. *Trends in Biochemical Sciences* **1**, 244-247 (1976).

15. Dowd, F.J., Jr., Pitts, B.J. & Schwartz, A. Phosphorylation of a low molecular weight polypeptide in beef heart Na plus, K plus-ATPase preparations. *Archives of biochemistry and biophysics* **175**, 321-331 (1976).

16. Forbush, B., 3rd, Kaplan, J.H. & Hoffman, J.F. Characterization of a new photoaffinity derivative of ouabain: labeling of the large polypeptide and of a

proteolipid component of the Na, K-ATPase. *Biochemistry* **17**, 3667-3676 (1978).

17. Geering, K. Function of FXYD proteins, regulators of Na, K-ATPase. *Journal of bioenergetics and biomembranes* **37**, 387-392 (2005).
18. Geering, K. FXYD proteins: new regulators of Na-K-ATPase. *American journal of physiology. Renal physiology* **290**, F241-250 (2006).
19. Cornelius, F. & Mahmmoud, Y.A. Functional modulation of the sodium pump: the regulatory proteins "Fixit". *News in physiological sciences : an international journal of physiology produced jointly by the International Union of Physiological Sciences and the American Physiological Society* **18**, 119-124 (2003).
20. Schneeberger, A. & Apell, H.J. Ion selectivity of the cytoplasmic binding sites of the Na,K-ATPase: I. Sodium binding is associated with a conformational rearrangement. *The Journal of membrane biology* **168**, 221-228 (1999).
21. Ogawa, H. & Toyoshima, C. Homology modeling of the cation binding sites of Na+K+-ATPase. *Proceedings of the National Academy of Sciences of the United States of America* **99**, 15977-15982 (2002).
22. Hilgemann, D.W. From a pump to a pore: how palytoxin opens the gates. *Proceedings of the National Academy of Sciences of the United States of America* **100**, 386-388 (2003).
23. Blanco, G., DeTomaso, A.W., Koster, J., Xie, Z.J. & Mercer, R.W. The alpha-subunit of the Na,K-ATPase has catalytic activity independent of the beta-subunit. *The Journal of biological chemistry* **269**, 23420-23425 (1994).
24. Holmgren, M.*, et al.* Three distinct and sequential steps in the release of sodium ions by the Na+/K+-ATPase. *Nature* **403**, 898-901 (2000).

25. Buhler, R. & Apell, H.J. Sequential potassium binding at the extracellular side of the Na,K-pump. *The Journal of membrane biology* **145**, 165-173 (1995).

26. Eisner, D.A., Lederer, W.J. & Vaughan-Jones, R.D. The dependence of sodium pumping and tension on intracellular sodium activity in voltage-clamped sheep Purkinje fibres. *J Physiol* **317**, 163-187 (1981).

27. Nakao, M. & Gadsby, D.C. [Na] and [K] dependence of the Na/K pump current-voltage relationship in guinea pig ventricular myocytes. *The Journal of general physiology* **94**, 539-565 (1989).

28. Shattock, M.J., Matsuura, H. & Ward, J.P. Sodium pump current measured in cardiac ventricular myocytes isolated from control and potassium depleted rabbits. *Cardiovascular research* **28**, 1854-1862 (1994).

29. Kong, B.Y. & Clarke, R.J. Identification of potential regulatory sites of the Na+,K+-ATPase by kinetic analysis. *Biochemistry* **43**, 2241-2250 (2004).

30. Schulz, S. & Apell, H.J. Investigation of ion binding to the cytoplasmic binding sites of the Na,K-pump. *Eur Biophys J* **23**, 413-421 (1995).

31. Whittam, R. & Ager, M.E. Vectorial aspects of adenosine-triphosphatase activity in erythrocyte membranes. *Biochem J* **93**, 337-348 (1964).

32. Skou, J.C. Preparation from mammallian brain and kidney of the enzyme system involved in active transport of Na ions and K ions. *Biochimica et biophysica acta* **58**, 314-325 (1962).

33. Rega, A.F., Garrahan, P.J. & Pouchan, M.I. Potassium-activated phosphatase from human red blood cells : The asymmetrical effects of K(+), Na (+), Mg (++) and adenosine triphosphate. *J Membr Biol* **3**, 14-25 (1970).

34. Garrahan, P.J., Pouchan, M.I. & Rega, A.F. Potassium activated phosphatase from human red blood cells. The mechanism of potassium activation. *The Journal of physiology* **202**, 305-327 (1969).

35. Gadsby, D.C., Kimura, J. & Noma, A. Voltage dependence of Na/K pump current in isolated heart cells. *Nature* **315**, 63-65 (1985).

36. Nakao, M. & Gadsby, D.C. Voltage dependence of Na translocation by the Na/K pump. *Nature* **323**, 628-630 (1986).

37. Lafaire, A.V. & Schwarz, W. Voltage dependence of the rheogenic Na+/K+ ATPase in the membrane of oocytes of Xenopus laevis. *The Journal of membrane biology* **91**, 43-51 (1986).

38. Rakowski, R.F., Vasilets, L.A., LaTona, J. & Schwarz, W. A negative slope in the current-voltage relationship of the Na+/K+ pump in Xenopus oocytes produced by reduction of external [K+]. *The Journal of membrane biology* **121**, 177-187 (1991).

39. Peluffo, R.D. & Berlin, J.R. Electrogenic K+ transport by the Na(+)-K+ pump in rat cardiac ventricular myocytes. *The Journal of physiology* **501 (Pt 1)**, 33-40 (1997).

40. Berlin, J.R. & Peluffo, R.D. Mechanism of electrogenic reaction steps during K+ transport by the NA,K-ATPase. *Annals of the New York Academy of Sciences* **834**, 251-259 (1997).

41. Therien, A.G. & Blostein, R. Mechanisms of sodium pump regulation. *American journal of physiology. Cell physiology* **279**, C541-566 (2000).

42. Aperia, A.*, et al.* Cellular mechanisms for bi-directional regulation of tubular sodium reabsorption. *Kidney international* **49**, 1743-1747 (1996).

43. Bonvalet, J.P. Regulation of sodium transport by steroid hormones. *Kidney international. Supplement* **65**, S49-56 (1998).

44. Ramirez-Gil, J.F.*, et al.* Modifications of myocardial Na+,K(+)-ATPase isoforms and Na+/Ca2+ exchanger in aldosterone/salt-induced hypertension in guinea pigs. *Cardiovascular research* **38**, 451-462 (1998).

45. Buhagiar, K.A., Hansen, P.S., Gray, D.F., Mihailidou, A.S. & Rasmussen, H.H. Angiotensin regulates the selectivity of the Na+-K+ pump for intracellular Na+. *The American journal of physiology* **277**, C461-468 (1999).

46. Mihailidou, A.S.*, et al.* Hyperaldosteronemia in rabbits inhibits the cardiac sarcolemmal Na(+)-K(+) pump. *Circulation research* **86**, 37-42 (2000).

47. Hansen, P.S.*, et al.* Alloxan-induced diabetes reduces sarcolemmal Na+-K+ pump function in rabbit ventricular myocytes. *American journal of physiology. Cell physiology* **292**, C1070-1077 (2007).

48. William, M.*, et al.* Natriuretic peptides stimulate the cardiac sodium pump via NPR-C-coupled NOS activation. *American journal of physiology. Cell physiology* **294**, C1067-1073 (2008).

49. Figtree, G.A., Keyvan Karimi, G., Liu, C.C. & Rasmussen, H.H. Oxidative regulation of the Na(+)-K(+) pump in the cardiovascular system. *Free radical biology & medicine* **53**, 2263-2268 (2012).

50. Hill, B.G. & Bhatnagar, A. Protein S-glutathiolation: redox-sensitive regulation of protein function. *Journal of molecular and cellular cardiology* **52**, 559-567 (2012).

51. Figtree, G.A.*, et al.* Reversible oxidative modification: a key mechanism of Na+-K+ pump regulation. *Circulation research* **105**, 185-193 (2009).

52. Rasmussen, H.H., Hamilton, E.J., Liu, C.C. & Figtree, G.A. Reversible oxidative modification: implications for cardiovascular physiology and pathophysiology. *Trends in cardiovascular medicine* **20**, 85-90 (2010).

53. Liu, C.C.*, et al.* Susceptibility of beta1 Na+-K+ pump subunit to glutathionylation and oxidative inhibition depends on conformational state of pump. *The Journal of biological chemistry* **287**, 12353-12364 (2012).

54. Leblanc, N. & Hume, J.R. Sodium current-induced release of calcium from cardiac sarcoplasmic reticulum. *Science* **248**, 372-376 (1990).

55. Lederer, W.J., Niggli, E. & Hadley, R.W. Sodium-calcium exchange in excitable cells: fuzzy space. *Science* **248**, 283 (1990).

56. Miura, Y. & Kimura, J. Sodium-calcium exchange current. Dependence on internal Ca and Na and competitive binding of external Na and Ca. *The Journal of general physiology* **93**, 1129-1145 (1989).

57. Eisner, D.A., Lederer, W.J. & Vaughan-Jones, R.D. The dependence of sodium pumping and tension on intracellular sodium activity in voltage-clamped sheep Purkinje fibres. *The Journal of physiology* **317**, 163-187 (1981).

58. Bielen, F.V., Glitsch, H.G. & Verdonck, F. Changes of the subsarcolemmal Na+ concentration in internally perfused cardiac cells. *Biochimica et biophysica acta* **1065**, 269-271 (1991).

59. Carmeliet, E. A fuzzy subsarcolemmal space for intracellular Na+ in cardiac cells? *Cardiovascular research* **26**, 433-442 (1992).

60. Fujioka, Y., Matsuoka, S., Ban, T. & Noma, A. Interaction of the Na+-K+ pump and Na+-Ca2+ exchange via [Na+]i in a restricted space of guinea-pig ventricular cells. *The Journal of physiology* **509 (Pt 2)**, 457-470 (1998).

61. Su, Z.*, et al.* Influence of prior Na+ pump activity on pump and Na+/Ca2+ exchange currents in mouse ventricular myocytes. *The American journal of physiology* **275**, H1808-1817 (1998).

62. Davis, D.G., Murphy, E. & London, R.E. Uptake of cesium ions by human erythrocytes and perfused rat heart: a cesium-133 NMR study. *Biochemistry* **27**, 3547-3551 (1988).

63. Gruwel, M.L., Culic, O. & Schrader, J. A 133Cs nuclear magnetic resonance study of endothelial Na(+)-K(+)-ATPase activity: can actin regulate its activity? *Biophysical journal* **72**, 2775-2782 (1997).

64. Despa, S., Kockskamper, J., Blatter, L.A. & Bers, D.M. Na/K pump-induced [Na](i) gradients in rat ventricular myocytes measured with two-photon microscopy. *Biophysical journal* **87**, 1360-1368 (2004).

65. Silverman, B., Warley, A., Miller, J.I., James, A.F. & Shattock, M.J. Is there a transient rise in sub-sarcolemmal Na and activation of Na/K pump current following activation of I(Na) in ventricular myocardium? *Cardiovascular research* **57**, 1025-1034 (2003).

66. Wendt-Gallitelli, M.F., Voigt, T. & Isenberg, G. Microheterogeneity of subsarcolemmal sodium gradients. Electron probe microanalysis in guinea-pig ventricular myocytes. *The Journal of physiology* **472**, 33-44 (1993).

67. Aronsen, J.M., Swift, F. & Sejersted, O.M. Cardiac sodium transport and excitation-contraction coupling. *Journal of molecular and cellular cardiology* **61**, 11-19 (2013).

68. Swietach, P., Spitzer, K.W. & Vaughan-Jones, R.D. Intracellular Na+ Spatially Controls Ca2+ Signaling during Acidosis in the Ventricular Myocyte. *Biophysical Journal* **104**, 362a-362a (2013).

69. Haddad, J.*, et al.* Attachment and maintenance of adult rabbit cardiac myocytes in primary cell culture. *The American journal of physiology* **255**, C19-27 (1988).

70. Helin, P. & Lorenzen, I. Seasonal variations in the susceptibility of the aortic wall to atherosclerosis. Biochemical studies of glycosaminoglycans and collagen of rabbit atherosclerosis. *Atherosclerosis* **24**, 259-266 (1976).

71. Cornelius, F., Mahmmoud, Y.A. & Toyoshima, C. Metal fluoride complexes of Na,K-ATPase: characterization of fluoride-stabilized phosphoenzyme analogues and their interaction with cardiotonic steroids. *The Journal of biological chemistry* **286**, 29882-29892 (2011).

72. Tourneur, Y., Mitra, R., Morad, M. & Rougier, O. Activation properties of the inward-rectifying potassium channel on mammalian heart cells. *J Membr Biol* **97**, 127-135 (1987).

73. Follmer, C.H., ten Eick, R.E. & Yeh, J.Z. Sodium current kinetics in cat atrial myocytes. *J Physiol* **384**, 169-197 (1987).

74. Jorgensen, P.L. Purification and characterization of (Na+ plus K+)-ATPase. 3. Purification from the outer medulla of mammalian kidney after selective removal of membrane components by sodium dodecylsulphate. *Biochimica et biophysica acta* **356**, 36-52 (1974).

75. Jorgensen, P.L. Isolation of (Na+ plus K+)-ATPase. *Methods in enzymology* **32**, 277-290 (1974).

76. Glynn, I.M. The Na+, K+-Transporting Adenosine Triphosphatase. in *The Enzymes of Biological Membranes* (ed. Martonosi, A.) 35-114 (Springer US, 1985).

77. Sachs, J.R. Cation fluxes in the red blood cell: Na+,K+ pump. *Methods in enzymology* **173**, 80-93 (1989).

78. Kaplan, J.H. Ion movements through the sodium pump. *Annual review of physiology* **47**, 535-544 (1985).

79. Hansen, A.S., Kraglund, K.L., Fedosova, N.U. & Esmann, M. Bulk properties of the lipid bilayer are not essential for the thermal stability of Na,K-ATPase from shark rectal gland or pig kidney. *Biochemical and biophysical research communications* **406**, 580-583 (2011).

80. Myers, S.L., Cornelius, F., Apell, H.J. & Clarke, R.J. Kinetics of K(+) occlusion by the phosphoenzyme of the Na(+),K(+)-ATPase. *Biophysical journal* **100**, 70-79 (2011).

81. Morth, J.P.*, et al.* Crystal structure of the sodium-potassium pump. *Nature* **450**, 1043-1049 (2007).

82. Shinoda, T., Ogawa, H., Cornelius, F. & Toyoshima, C. Crystal structure of the sodium-potassium pump at 2.4 A resolution. *Nature* **459**, 446-450 (2009).

83. Ogawa, H., Shinoda, T., Cornelius, F. & Toyoshima, C. Crystal structure of the sodium-potassium pump (Na+,K+-ATPase) with bound potassium and ouabain. *Proceedings of the National Academy of Sciences of the United States of America* **106**, 13742-13747 (2009).

84. Cable, M.B. & Briggs, F.N. Allosteric regulation of cardiac sarcoplasmic reticulum Ca-ATPase: a comparative study. *Molecular and cellular biochemistry* **82**, 29-36 (1988).

85. Therien, A.G. & Blostein, R. K(+)/Na(+) antagonism at cytoplasmic sites of Na(+)-K(+)-ATPase: a tissue-specific mechanism of sodium pump regulation. *The American journal of physiology* **277**, C891-898 (1999).

86. Gadsby, D.C. & Nakao, M. Steady-state current-voltage relationship of the Na/K pump in guinea pig ventricular myocytes. *The Journal of general physiology* **94**, 511-537 (1989).

87. Blostein, R. Relationships between erythrocyte membrane phosphorylation and adenosine triphosphate hydrolysis. *The Journal of biological chemistry* **243**, 1957-1965 (1968).

88. Kaplan, J.H. & Kenney, L.J. Temperature effects on sodium pump phosphoenzyme distribution in human red blood cells. *The Journal of general physiology* **85**, 123-136 (1985).

89. Post, R.L., Kume, S., Tobin, T., Orcutt, B. & Sen, A.K. Flexibility of an active center in sodium-plus-potassium adenosine triphosphatase. *The Journal of general physiology* **54**, 306-326 (1969).

90. White, B. & Blostein, R. Comparison of red cell and kidney (Na+ +K+)-ATPase at 0 degrees C. *Biochimica et biophysica acta* **688**, 685-690 (1982).

91. Hara, Y. & Nakao, M. Sodium ion discharge from pig kidney Na+, K+-ATPase Na+-dependency of the E1P-E2P equilibrium in the absence of KCl. *Journal of biochemistry* **90**, 923-931 (1981).

92. Lucking, K., Nielsen, J.M., Pedersen, P.A. & Jorgensen, P.L. Na-K-ATPase isoform (alpha 3, alpha 2, alpha 1) abundance in rat kidney estimated by competitive RT-PCR and ouabain binding. *The American journal of physiology* **271**, F253-260 (1996).

93. Gao, J.*, et al.* Isoform-specific regulation of the sodium pump by alpha- and beta-adrenergic agonists in the guinea-pig ventricle. *The Journal of physiology* **516 (Pt 2)**, 377-383 (1999).

94. Oka, C., Cha, C.Y. & Noma, A. Characterization of the cardiac Na+/K+ pump by development of a comprehensive and mechanistic model. *Journal of theoretical biology* **265**, 68-77 (2010).

95. King, E.L. & Altman, C. A Schematic Method of Deriving the Rate Laws for Enzyme-Catalyzed Reactions. *The Journal of Physical Chemistry* **60**, 1375-1378 (1956).

96. Lauger, P. Thermodynamic and kinetic properties of electrogenic ion pumps. *Biochimica et biophysica acta* **779**, 307-341 (1984).

97. Läuger, P. & Apell, H.J. A microscopic model for the current-voltage behaviour of the Na,K-pump. *Eur Biophys J* **13**, 309-321 (1986).

98. Rakowski, R.F. Charge movement by the Na/K pump in Xenopus oocytes. *The Journal of general physiology* **101**, 117-144 (1993).

99. Holmgren, M. & Rakowski, R.F. Pre-steady-state transient currents mediated by the Na/K pump in internally perfused Xenopus oocytes. *Biophysical journal* **66**, 912-922 (1994).

100. Gadsby, D.C., Bezanilla, F., Rakowski, R.F., De Weer, P. & Holmgren, M. The dynamic relationships between the three events that release individual Na(+) ions from the Na(+)/K(+)-ATPase. *Nature communications* **3**, 669 (2012).

101. Massey, K.J., Li, Q., Rossi, N.F., Mattingly, R.R. & Yingst, D.R. Angiotensin II-dependent phosphorylation at Ser11/Ser18 and Ser938 shifts the E2 conformations of rat kidney Na+/K+-ATPase. *The Biochemical journal* **443**, 249-258 (2012).

102. Liu, C.C.*, et al.* Susceptibility of beta1 Na+-K+ pump subunit to glutathionylation and oxidative inhibition depends on conformational state of pump. *The Journal of biological chemistry* **287**, 12353-12364 (2012).

103. Wuddel, I. & Apell, H.J. Electrogenicity of the sodium transport pathway in the Na,K-ATPase probed by charge-pulse experiments. *Biophysical journal* **69**, 909-921 (1995).

104. Kane, D.J.*, et al.* Stopped-flow kinetic investigations of conformational changes of pig kidney Na+,K+-ATPase. *Biochemistry* **36**, 13406-13420 (1997).

105. Clarke, R.J., Kane, D.J., Apell, H.J., Roudna, M. & Bamberg, E. Kinetics of Na(+)-dependent conformational changes of rabbit kidney Na+,K(+)-ATPase. *Biophysical journal* **75**, 1340-1353 (1998).

106. Kane, D.J., Grell, E., Bamberg, E. & Clarke, R.J. Dephosphorylation kinetics of pig kidney Na+,K+-ATPase. *Biochemistry* **37**, 4581-4591 (1998).

107. Geibel, S.*, et al.* P(3)-[2-(4-hydroxyphenyl)-2-oxo]ethyl ATP for the rapid activation of the Na(+),K(+)-ATPase. *Biophysical journal* **79**, 1346-1357 (2000).

108. Babes, A. & Fendler, K. Na(+) transport, and the E(1)P-E(2)P conformational transition of the Na(+)/K(+)-ATPase. *Biophysical journal* **79**, 2557-2571 (2000).

109. Lu, C.C.*, et al.* Membrane transport mechanisms probed by capacitance measurements with megahertz voltage clamp. *Proceedings of the National Academy of Sciences of the United States of America* **92**, 11220-11224 (1995).

110. Steinberg, M. & Karlish, S.J. Studies on conformational changes in Na,K-ATPase labeled with 5-iodoacetamidofluorescein. *The Journal of biological chemistry* **264**, 2726-2734 (1989).

111. Pratap, P.R., Palit, A., Grassi-Nemeth, E. & Robinson, J.D. Kinetics of conformational changes associated with potassium binding to and release from Na+/K(+)-ATPase. *Biochimica et biophysica acta* **1285**, 203-211 (1996).

112. Lupfert, C.*, et al.* Rate limitation of the Na(+),K(+)-ATPase pump cycle. *Biophysical journal* **81**, 2069-2081 (2001).

113. Humphrey, P.A., Lupfert, C., Apell, H.J., Cornelius, F. & Clarke, R.J. Mechanism of the rate-determining step of the Na(+),K(+)-ATPase pump cycle. *Biochemistry* **41**, 9496-9507 (2002).

114. Pintschovius, J., Fendler, K. & Bamberg, E. Charge translocation by the Na+/K+-ATPase investigated on solid supported membranes: cytoplasmic cation binding and release. *Biophysical journal* **76**, 827-836 (1999).

115. Blanco, G. & Mercer, R.W. Isozymes of the Na-K-ATPase: heterogeneity in structure, diversity in function. *The American journal of physiology* **275**, F633-650 (1998).

116. Horisberger, J.D. & Kharoubi-Hess, S. Functional differences between alpha subunit isoforms of the rat Na,K-ATPase expressed in Xenopus oocytes. *The Journal of physiology* **539**, 669-680 (2002).

117. Apell, H.J. & Bersch, B. Na,K-ATPase in artificial lipid vesicles: potential dependent transport rates investigated by a fluorescence method. *Progress in clinical and biological research* **268A**, 469-476 (1988).

118. Segall, L., Javaid, Z.Z., Carl, S.L., Lane, L.K. & Blostein, R. Structural basis for alpha1 versus alpha2 isoform-distinct behavior of the Na,K-ATPase. *The Journal of biological chemistry* **278**, 9027-9034 (2003).

119. Bugnon, P., M. Doludda, E. Grell, and A. E. Merbach. High-pressure stopped-flow spectrometer for kinetic studies of fast bioinorganic reactions by

absorbance and fluorescence detection. in *High-Pressure Research in the Biosciences and Biotechnology.* (ed. Heremans, K.) 143-146. (Leuven University Press, Leuven, Belgium., 1997).

120. Domaszewicz, W. & Apell, H. Binding of the third Na+ ion to the cytoplasmic side of the Na,K-ATPase is electrogenic. *FEBS letters* **458**, 241-246 (1999).

121. Sachs, J.R. The order of addition of sodium and release of potassium at the inside of the sodium pump of the human red cell. *The Journal of physiology* **381**, 149-168 (1986).

122. Karlish, S.J. & Stein, W.D. Cation activation of the pig kidney sodium pump: transmembrane allosteric effects of sodium. *The Journal of physiology* **359**, 119-149 (1985).

123. Cornelius, F. & Skou, J.C. The sided action of Na+ on reconstituted shark Na+/K+-ATPase engaged in Na+-Na+ exchange accompanied by ATP hydrolysis. II. Transmembrane allosteric effects on Na+ affinity. *Biochimica et biophysica acta* **944**, 223-232 (1988).

124. van der Hijden, H.T. & de Pont, J.J. Cation sidedness in the phosphorylation step of Na+/K+-ATPase. *Biochimica et biophysica acta* **983**, 142-152 (1989).

125. Karlish, S.J. Characterization of conformational changes in (Na,K) ATPase labeled with fluorescein at the active site. *Journal of bioenergetics and biomembranes* **12**, 111-136 (1980).

126. Skou, J.C. & Esmann, M. The effects of Na+ and K+ on the conformational transitions of (Na+ + K+)-ATPase. *Biochimica et biophysica acta* **746**, 101-113 (1983).

127. Schuurmans Stekhoven, F.M., Swarts, H.G., de Pont, J.J. & Bonting, S.L. Na+-like effect of imidazole on the phosphorylation of (Na+ + K+)-ATPase. *Biochimica et biophysica acta* **815**, 16-24 (1985).

128. Schuurmans Stekhoven, F.M., Swarts, H.G., Lam, G.K., Zou, Y.S. & de Pont, J.J. Phosphorylation of (Na+ + K+)-ATPase. Stimulation and inhibition by substituted and unsubstituted amines. *Progress in clinical and biological research* **268A**, 355-362 (1988).

129. Mezele, M., Lewitzki, E., Ruf, H. & Grell, E. Cation Selectivity of Membrane Proteins. *Berichte der Bunsengesellschaft für physikalische Chemie* **92**, 998-1004 (1988).

130. Grell, E., R. Warmuth, E. Lewitzki, and H. Ruf. . Precision titrations to determine affinity and stoichiometry of alkali, alkaline earth, and buffer cation binding to Na,K-ATPase. in *The Sodium Pump: Recent Developments.* (ed. J. H. Kaplan, a.P.D.W.) 441-445 (Rockefeller University Press, New York, 1991).

131. Doludda, M., E. Lewitzki, H. Ruf, and E. Grell. Kinetics and mechanism of cation-binding to Na+,K+-ATPase. in *The Sodium Pump: Structure Mechanism, Hormonal Control and Its Role in Disease.* (ed. Schoner, E.B.a.W.) 629-632. (Steinkopff Verlag, Darmstadt, Germany., 1994).

132. Grell, E., E. Lewitzki, H. Ruf, and M. Doludda. Reassignment of cation-iduced population of main conformational states of FITC-Na+/K+-ATPase as detected by fluorescence spectroscopy and characterized by equilibrium binding studies. in *The Sodium Pump: Structure Mechanism, Hormonal Control and Its Role in Disease.* (ed. Schoner, E.B.a.W.) 617-620. (Steinkopff Verlag, Darmstadt, Germany., 1994).

133. Yatime, L.*, et al.* Structural insights into the high affinity binding of cardiotonic steroids to the Na+,K+-ATPase. *Journal of structural biology* **174**, 296-306 (2011).

134. Kanai, R., Ogawa, H., Vilsen, B., Cornelius, F. & Toyoshima, C. Crystal structure of a Na+-bound Na+,K+-ATPase preceding the E1P state. *Nature* **502**, 201-206 (2013).

135. Nyblom, M.*, et al.* Crystal structure of Na+, K(+)-ATPase in the Na(+)-bound state. *Science* **342**, 123-127 (2013).

136. Hool, L.C., Whalley, D.W., Doohan, M.M. & Rasmussen, H.H. Angiotensin-converting enzyme inhibition, intracellular Na^+, and Na^+-K^+ pumping in cardiac myocytes. *Am J Physiol* **268**, C366-375 (1995).

137. Hansen, P.S.*, et al.* Dependence of Na+-K+ pump current-voltage relationship on intracellular Na+, K+, and Cs+ in rabbit cardiac myocytes. *American journal of physiology. Cell physiology* **283**, C1511-1521 (2002).

138. Peluffo, R.D. Effect of ADP on Na(+)-Na(+) exchange reaction kinetics of Na,K-ATPase. *Biophysical journal* **87**, 883-898 (2004).

139. Schuurmans Stekhoven, F.M., Swarts, H.G., Lam, G.K., Zou, Y.S. & De Pont, J.J. Phosphorylation of (Na+ + K+)-ATPase; stimulation and inhibition by substituted and unsubstituted amines. *Biochimica et biophysica acta* **937**, 161-176 (1988).

140. Schneeberger, A. & Apell, H.J. Ion selectivity of the cytoplasmic binding sites of the Na,K-ATPase: II. Competition of various cations. *The Journal of membrane biology* **179**, 263-273 (2001).

141. Ekberg, K., *et al.* Structural identification of cation binding pockets in the plasma membrane proton pump. *Proceedings of the National Academy of Sciences of the United States of America* **107**, 21400-21405 (2010).

142. Clausen, J.D. & Andersen, J.P. Glutamate 90 at the luminal ion gate of sarcoplasmic reticulum Ca2+-ATPase is critical for Ca(2+) binding on both sides of the membrane. *The Journal of biological chemistry* **285**, 20780-20792 (2010).

143. Sheu, S.S. & Fozzard, H.A. Transmembrane Na+ and Ca2+ electrochemical gradients in cardiac muscle and their relationship to force development. *The Journal of general physiology* **80**, 325-351 (1982).

144. Barry, W.H. Na"Fuzzy space": does it exist, and is it important in ischemic injury? *Journal of cardiovascular electrophysiology* **17 Suppl 1**, S43-S46 (2006).

145. Grandi, E., Wang, F. & Bers, D.M. Na Diffusion Dependent Ca Handling in Rabbit Ventricular Myocytes. *Computers in Cardiology 2008, Vols 1 and 2*, 185-188 (2008).

146. O'Hara, T. & Rudy, Y. Quantitative comparison of cardiac ventricular myocyte electrophysiology and response to drugs in human and nonhuman species. *American journal of physiology. Heart and circulatory physiology* **302**, H1023-1030 (2012).

147. Shannon, T.R., Wang, F., Puglisi, J., Weber, C. & Bers, D.M. A mathematical treatment of integrated Ca dynamics within the ventricular myocyte. *Biophysical journal* **87**, 3351-3371 (2004).

148. Moreno, J.D.*, et al.* Ranolazine for congenital and acquired late INa-linked arrhythmias: in silico pharmacological screening. *Circulation research* **113**, e50-61 (2013).

149. Grandi, E., Pasqualini, F.S. & Bers, D.M. A novel computational model of the human ventricular action potential and Ca transient. *Journal of molecular and cellular cardiology* **48**, 112-121 (2010).

150. Despa, S. & Bers, D.M. Na/K pump current and [Na](i) in rabbit ventricular myocytes: local [Na](i) depletion and Na buffering. *Biophysical journal* **84**, 4157-4166 (2003).

151. Figtree, G.A.*, et al.* Reversible oxidative modification: a key mechanism of Na+-K+ pump regulation. *Circulation research* **105**, 185-193 (2009).

152. Brette, F. & Orchard, C. T-tubule function in mammalian cardiac myocytes. *Circulation research* **92**, 1182-1192 (2003).

153. Yao, A.*, et al.* The restriction of diffusion of cations at the external surface of cardiac myocytes varies between species. *Cell calcium* **22**, 431-438 (1997).

154. Jorgensen, P.L. Purification and characterization of (Na+ plus K+)-ATPase. IV. Estimation of the purity and of the molecular weight and polypeptide content per enzyme unit in preparations from the outer medulla of rabbit kidney. *Biochimica et biophysica acta* **356**, 53-67 (1974).

155. Bielen, F.V., Glitsch, H.G. & Verdonck, F. Na+ pump current-voltage relationships of rabbit cardiac Purkinje cells in Na(+)-free solution. *The Journal of physiology* **465**, 699-714 (1993).

156. Castillo, J.P.*, et al.* Energy landscape of the reactions governing the Na+ deeply occluded state of the Na+/K+-ATPase in the giant axon of the

Humboldt squid. *Proceedings of the National Academy of Sciences of the United States of America* **108**, 20556-20561 (2011).

157. Gallogly, M.M., Starke, D.W. & Mieyal, J.J. Mechanistic and kinetic details of catalysis of thiol-disulfide exchange by glutaredoxins and potential mechanisms of regulation. *Antioxidants & redox signaling* **11**, 1059-1081 (2009).

158. Lassegue, B., San Martin, A. & Griendling, K.K. Biochemistry, physiology, and pathophysiology of NADPH oxidases in the cardiovascular system. *Circulation research* **110**, 1364-1390 (2012).

159. Winterbourn, C.C. & Hampton, M.B. Thiol chemistry and specificity in redox signaling. *Free Radical Bio Med* **45**, 549-561 (2008).

160. Despa, S. & Bers, D.M. Na(+) transport in the normal and failing heart - remember the balance. *Journal of molecular and cellular cardiology* **61**, 2-10 (2013).

161. Semb, S.O. & Sejersted, O.M. Fuzzy space and control of Na+, K(+)-pump rate in heart and skeletal muscle. *Acta physiologica Scandinavica* **156**, 213-225 (1996).

162. Silverman, B., Warley, A., Miller, J.I., James, A.F. & Shattock, M.J. Is there a transient rise in sub-sarcolemmal Na and activation of Na/K pump current following activation of I(Na) in ventricular myocardium? *Cardiovascular research* **57**, 1025-1034 (2003).

163. Swift, F., Tovsrud, N., Enger, U.H., Sjaastad, I. & Sejersted, O.M. The Na+/K+-ATPase alpha2-isoform regulates cardiac contractility in rat cardiomyocytes. *Cardiovascular research* **75**, 109-117 (2007).

164. Swift, F.*, et al.* Altered Na+/Ca2+-exchanger activity due to downregulation of Na+/K+-ATPase alpha2-isoform in heart failure. *Cardiovascular research* **78**, 71-78 (2008).

165. Yamamoto, T.*, et al.* Relative abundance of alpha2 Na(+) pump isoform influences Na(+)-Ca(2+) exchanger currents and Ca(2+) transients in mouse ventricular myocytes. *Journal of molecular and cellular cardiology* **39**, 113-120 (2005).

166. Despa, S., Lingrel, J.B. & Bers, D.M. Na(+)/K)+)-ATPase alpha2-isoform preferentially modulates Ca2(+) transients and sarcoplasmic reticulum Ca2(+) release in cardiac myocytes. *Cardiovascular research* **95**, 480-486 (2012).

167. Thogersen, L. & Nissen, P. Flexible P-type ATPases interacting with the membrane. *Current opinion in structural biology* **22**, 491-499 (2012).

168. Oberg, B.P.*, et al.* Increased prevalence of oxidant stress and inflammation in patients with moderate to severe chronic kidney disease. *Kidney international* **65**, 1009-1016 (2004).

169. Cai, H. & Harrison, D.G. Endothelial dysfunction in cardiovascular diseases: the role of oxidant stress. *Circulation research* **87**, 840-844 (2000).

170. Repine, J.E., Bast, A. & Lankhorst, I. Oxidative stress in chronic obstructive pulmonary disease. Oxidative Stress Study Group. *American journal of respiratory and critical care medicine* **156**, 341-357 (1997).

171. Baynes, J.W. & Thorpe, S.R. Role of oxidative stress in diabetic complications: a new perspective on an old paradigm. *Diabetes* **48**, 1-9 (1999).

172. Dhalla, A.K., Hill, M.F. & Singal, P.K. Role of oxidative stress in transition of hypertrophy to heart failure. *Journal of the American College of Cardiology* **28**, 506-514 (1996).

173. Despa, S., Brette, F., Orchard, C.H. & Bers, D.M. Na/Ca exchange and Na/K-ATPase function are equally concentrated in transverse tubules of rat ventricular myocytes. *Biophysical journal* **85**, 3388-3396 (2003).